REPUBLIC OF CHILE

REPORT ON

GEOTHERMAL POWER DEVELOPMENT PROJECT

IN

PUCHULDIZA AREA

MARCH 1981

JAPAN INTERNATIONAL COOPERATION AGENCY

PREFACE

In response to a request of the Government of the Republic of Chile the Japanese Government decided to conduct a survey on the Puchuldiza Geothermal Development Project and entrusted the Japan International Cooperation Agency with the Survey. The J.I.C.A. sent to Chile a survey team headed by Mr. Yasunori Sakai for 56 days from October 24, 1979 and for 68 days from October 12, 1980.

The team exchanged views with the officials concerned of the Government of Chile and conducted a field survey in Puchuldiza area. After the team returned to Japan, further studies were made and the present report has been prepared.

I hope that this report will serve for the development of the Project and contribute to the promotion of friendly relations between our two countries.

I wish to express my deep appreciation to the officials concerned of the Government of Chile for their close cooperation extended to the team.

March, 1981

Keisuke Arita
President
Japan International Cooperation Agency

LETTER OF TRANSMITTAL

Mr. Keisuke Arita
President
Japan International Cooperation Agency

Dear Sir:

Submitted herewith is a report on the Puchuldiza Geothermal Development Projects, Republic of Chile.

This survey was a continuation of the previous survey made in 1978 and 1979. The survey was conducted at Puchuldiza area for 56 days from October 24 to December 18, 1979 and for 68 days from October 12 to December 18, 1980 with the kind cooperation of Corporacion de Formento de la Produccion (CORFO) of the Republic of Chile.

The objectives of the survey were to analyze and delineate the possible extent of the geothermal reservoir by conducting resistivity survey and to evaluate the characteristics of the geothermal reservoir from the results of physical logging and well tests.

The survey team, after returning to Japan, collated the various survey data and analyzed the information in conjunction with previous surveys done by "Comite Geotermico, CORFO" and JICA survey of Puchuldiza.

The result of the study indicated that Well No. 6 is promissing because of good temperature gradient recorded regardless of the fact that flushing was not good enough at this moment at the depth of 1,157 m. With deeper drilling the well has a good chance of being good.

Further study of well tests and swabbing are highly recommended in order to confirm the reservoir characteristics. It is also recommended to drill additional exploratory wells at the north of Well No. 6 to know the extent of the high potential geothermal reservoir.

In closing, I would like to express my heatfelt appreciation for the tremendous cooperation given by CORFO, Primero Region and other authorities and officials of the Japanese Embassy in Chile, the Ministry of Foreign Affairs, and Ministry of International Trade and Industry.

Sincerest best wishes and highest esteem, I remain

January 1981

Respectfully yours,

Y. Sakai

Yasunori Sakai, Leader
Japanese Survey Team for
Puchuldiza Geothermal
Development Project

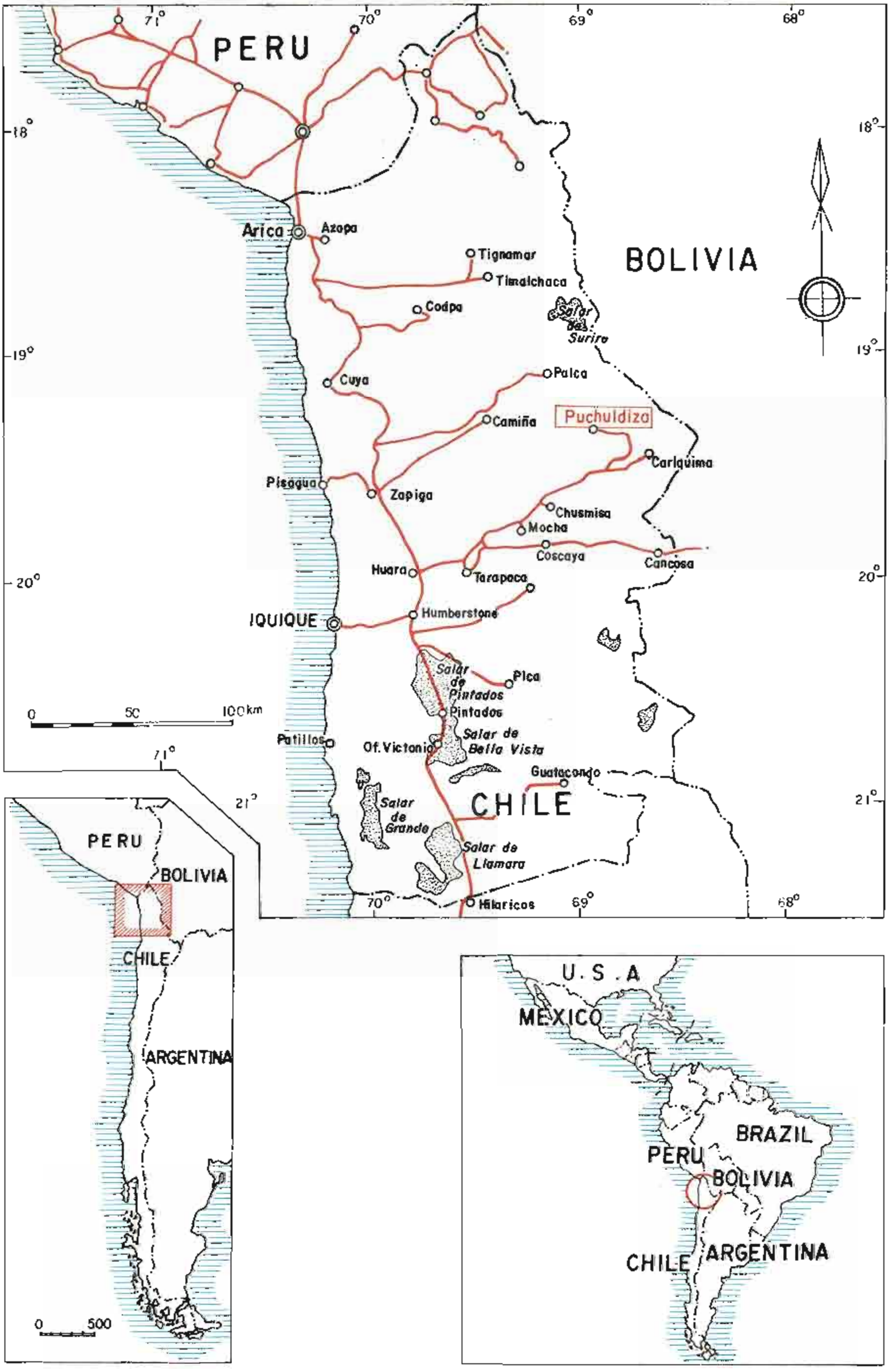

Fig I-1-1 LOCATION OF THE SURVEY AREA

Survey area from Co. Condoriri

Perspective view of the

exploration Well No.6

Production of Well No.6

CONCLUSION AND RECOMMENDATIONS

In order to evaluate the potential of the Puchuldiza geothermal field, the following steps were undertaken:

At the first stage geological, geochemical and geophysical explorations were carried out to select the drill site of Well No. 6 in 1978. Additional three resistivity survey lines of a total of 15 line-Km and the re-interpretation of 5 wells were conducted in 1979. And in 1980 evaluation of the exploratory drilling data of Well No. 6 up to 1,157 m depth was made.

The conclusion arrived at after an overall study that included well analysis as follows:

1. The result of continuous surveys for three years in the area indicated that the northern part of Well No. 6 is promissing for geothermal power generation because of over 200°C bottom temperature recorded with good temperature gradient at the deeper part of the well regardless of the fact that flushing was not good enough at this moment due to lack of permeable zone at the depth of 1,157 m.
2. However, the area of south and southeastern part of Mt. Tahipicollo, where were explored by CORFO prior to JICA Survey Mission would not be expected to be high temperature enough for the commercial power generation.
3. The reasons for the conclusion are:
   (1) Geological and gravity surveys brought that the area subjected to complicated block movement formed subsided basin structure to make a favorable condition for geothermal reservoir around Mt. Tahipicollo and its western vicinity.
   (2) The geology of the bottom hole of Well No. 6, the deepest well among six wells consists of Utayane or Churicollo Formation, which is favorable formation for the geothermal reservoir. This formation would be expected to continue further depth.
   (3) The aquifer temperature infered from the chemical compositions of hot water taken from the geysers and wells suggests to be over 200°C. And investigation of altered minerals using drill cores detected epidote at over 1,000 m depth of the well. It also suggests to be over 200°C in the depth around Well No. 6.
   (4) The maximum temperature of Well No. 1 to No. 4 located around Mt. Tahipicollo appeared at shallower depth and decreased it with depth. Resistivity sections in this area also showed that low resistivity anomaly zone did not continue to the depth. From these facts, the area mentioned above would not be expected to be high temperature reservoir.
4. The result of resistivity survey with total 30 km in length delineated the area for further exploration.
   (1) The low resistivity zone of less than 10 Ω-m was found in the basin structure (noted also by gravity survey of 1978), and was confirmed to spread in NW-SE direction. The anomaly zone shows an oval shape with 8 km major diameter and 4 km minor diameter length.
   (2) Especially, in lines D and E of the resistivity survey, the low anomaly of less than 5 Ω-m spreads at northern part of the lines. Accordingly, the location of high poten-

tial geothermal fluid concentration is inferred to be beneath the lower portion of Well No. 6 toward the north.

5. Well No. 6 was drilled up to 1,157 m depth which was the maximum capacity of the drilling rig used. The bottom temperature of the well was 201^{o}C indicating the highest temperature among six wells drilled. Furthermore, well temperature with a gradient of 0.9^{o}C/10 m toward depths was noted and this figure is different from the data of the other five wells. In order to reach the higher temperature zone, deeper drilling is therefore suggested.
6. During the drilling work, no mud circulation loss was observed. However, fractures were created at about 830 m depth by stimulation test. Injection index of fissure produced was quite good at 4 m^3/h/kg/cm^2. Around 40 t/h of steam and water mixture gushed out from the well, although the flow did not last long enough because the formation was not permeable enough as proven later by air lift test.
7. In view of the above-mentioned results, we recommend the followings:
   (1) We were able to gather many valuable data in conducting well drilling, however, due to insufficient flushing from the well and also due to lack of drilling rig capacity, detailed information on the reservoir characteristics could not be obtained. Accordingly it is recommended to conduct further temperature logging and stimulation test in order to reopen the cracks by repeating the pressure test using bigger pump.

   (2) To confirm higher temperature at depth it is considered to continue further exploratory well in the northern area of Well No. 6, because the temperature gradient of the well is still increasing. Especially, all data gathered such as geological, geochemical and geophysical informations indicate favorable condition for high temperature geothermal reservoir. Proposed site for the exploratory well is as follows:

   Near 859N, 501E

   (3) In addition to the exploratory well, additional electrical survey with at least three 6 km (AB/2 = 2,000 m) lines of E-W trend at southern slope of Mt. Natividad is recommended.

   (4) Italian Electro Consul also recommended to continue further exploration endorsing the JICA's first phase investigation. It is very important to confirm the potential extent of geothermal reservoir in the area.

   (5) In most geothermal field of the world, the depth of the well for geothermal generation is more than 2,000 m deep. Accordingly, it is important to prepare a bigger capacity drilling rig for this purpose.

   (6) In conducting well drilling, the seepage of waters at shallow depth should be controlled and sealed off. In order to do this properly, enough length of production casing must be programmed.

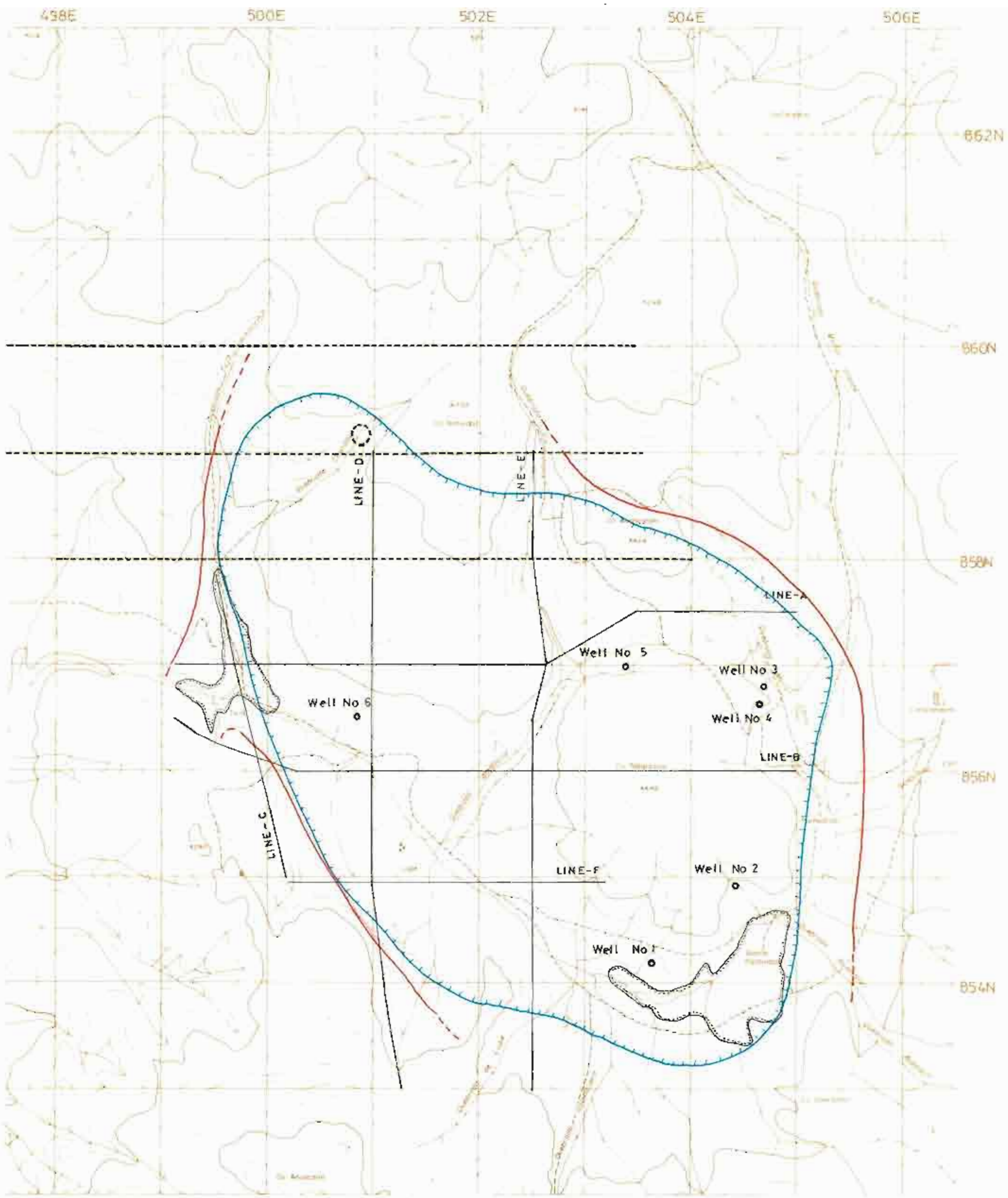

PROPOSED SITE

LEGEND

- Low Gravity anomaly
- Low Resistivity anomaly
- Sinter deposition area
- Drilled Exploratory wells
- Surveyed line
- Proposed Survey line
- Proposed Drilling site

CONTENTS

MAP LIST

TABLE LIST

PART I

STUDY ON WELL NO. 1 TO NO. 5
AND
ADDITIONAL ELECTRICAL SURVEY

CHAPTER I INTRODUCTION

PART – I

Chapter 1. Introduction

I – 1 Objectives of the Survey

The Government of Japan in response to the request of the Government of the Republic of Chile has conducted the detailed survey by means of the electrical, geological and geochemical survey and geophysical logging of the exploratory well No. 6 in the Puchuldiza geothermal field, northern Chile. This field had been surveyed by CORFO of the republic of Chile in the first phase, and after that the Government of Japan in response to the request of Chile has assigned the survey team 1978, which has been reported, 1979 and 1980, in order to verify the geothermal reservoir for the development.

The Republic of Chile being a similar volcanic country to Japan locating in the Circum Pacific Fire Belt, there is a high potentiality of geothermal development in many field.

CORFO has organized "Comite para el Aprovechamiento de la Energia Geotermica" in 1968, which has selected El Tatio and Puchuldiza geothermal field as the promising area.

In El Tatio area, geothermal explorations have been carried out from 1968 to 1974 under the economical and technical help of UNDP and has succeeded in geothermal development.

In Puchuldiza area, Comite Geotermio has conducted their own explorations to arrive at the conclusion that the possibility of development is high. Fig. I–1–1 shows the location of Puchuldiza area.

Due to the world wide energy resources problems and the industrialization policy of the Government of Chile, the geothermal electrical power development in Primero Region is considered to require top priority for development.

Regarding the geothermal power generation project, the government of the Republic of Chile has requested the Government of Japan for the technical assistance, 1978.

Whereas, the Government of Japan in response to the request of Chile has assigned the project to JICA (Japan International Corporation Agency) to be carried out.

1 – 2 MEMBERS OF II PHASE SURVEY TEAM

Team Leader	Mr. Yasunori Sakai Mitsubishi Metal Corporation	Geologist
Coordinator	Mr. Masaru Tateishi Japan International Cooperation Agency	
Geophysical Survey	Mr. Asahi Hattori Bishimetal Exploration Co., Ltd.	Geophysicist
Electrical Survey	Mr. Masashi Kurosawa Bishimetal Exploration Co., Ltd.	Geophysicist
do	Mr. Saburo Tachikawa Nikko Exploration and Development Co., Ltd.	Geophysicist

Counterpart (Comité Geotermico – CORFO)

Project Manager	Mr. Claudio Cádiz Chavarria	Industrial Engineer
Assistant Project Manager	Mr. Raul Bravo Espinoza	Geochemist
Camp Manager		
	Mr. Turides Solar Venegas	Chemical Engineer
	Mr. Ricardo Sandoval Salas	Geologist

1–3 Itinerary

ITINERARY OF II PHASE JAPANESE SURVEY TEAM

No.	Date			Day	Schedule	
1	1979.	Oct.	24		Tokyo Lv. → Los Angels Ar.	
2			25		Los Angels Lv.	
3			26		Santiago Ar.	
4			27		A courtesy call on the Japanese Embassy, CORFO etc.	
5			28	Sun.	Arrange for the survey	
6			29		Customs procedure	
7			30		Santiago → Iquique	
8			31		A courtesy call on the relative facilities in TARAPACA	
9		Nov.	1		Iquique → Chusmiza (3,500 m elevation)	
10			2		Chusmiza → Puchuldiza	
11			3			
12			4	Sun.	Beginning of the survey	
13			5		”	
14			6		”	
15			7		”	
16			8		”	
17			9		”	
18			10		”	
19			11	Sun.	”	
20			12		”	
21			13		”	
22			14		”	
23			15		”	
24			16		”	
25			17		”	
26			18	Sun.	Team Leader	Tokyo Lv. → New York Ar.
27			19			New York Lv.
28			20			Santiago Ar.
29			21			A courtesy call on the Japanese Embassy, CORFO
30			22			
31			23			Arrange for the survey
32			24			Santiago → Iquique → Chusmiza
33			25	Sun.	Survey	
34			26		”	Chusmiza → Puchuldiza
35			27		”	
36			28		”	
37			29		”	
38			30		”	
39		Dec.	1		”	
40			2	Sun.		
41			3		Finish the survey	
42			4		Puchuldiza → Iquique	
43			5		Arrange the survey data	
44			6		Pack and transport the equi.	
45			7		”	
46			8	Sun.		
47			9		Iquique → Santiago	
48			10		Calculate the data	
49			11		Write up the interim report	
50			12		”	
51			13		Report the interim report and Export the equi.	
52			14		Santiago Lv. → Miami	
53			15		San Francisco Ar.	
54			16	Sun.	San Francisco Lv.	
55			17		Tokyo Ar.	

CHAPTER 2

STUDY ON WELL NO. 1 TO NO. 5

Chapter 2. Study on Well No. 1 to No. 5

2–1 Outline of the Exploratory Wells Drilled by CORFO

Prior to the field survey conducted by JICA Mission in 1978, five (5) exploratory wells with total 3,774 m in length were already drilled by CORFO at the sites surrounding Mt. Tahipicollo hill in the Puchuldiza geothermal field.

The thermal logging and flush test of these wells were repeatedly carried out and their results were reported.

As shown Fig. I–2–1, the maximum temperature among five wells is recorded to be 166.2°C at 280 m depth of Well No. 2, and the other wells show the maximum temperature of 130°C – 140°C, which are thought to be comparatively low temperature as geothermal well. Especially, the temperature gradient curve shows that the maximum temperature zone in the well is not always at the bottom hole, but shallow part, that is, temperature gradient profile of the wells shows reverse curve near the bottom of the wells.

The production zones of each well are sited to be shallow part of the wells as confirmed by reinjection tests and their geologic formations are thought to be lower than Condoriri formation.

The flush tests of the wells were carried out often and geochemical investigation of the effluent water from the wells was also reported.

Well No. 1 was not flush out in the trial of flush test due to low temperature of the well, although water level near the well is higher than that of the wellhead.

Well No. 2 to No. 4 were successfully able to flush out conducting stimulation test by compressed air.

Well No. 5, however, was not flow out by sending high pressure air and also air lift due to the deeper water level than those of the others. Swabbing method, therefore, was recommended and was successfully urged flushing of the well.

Being low temperature of geothermal reservoir near Mt. Tahipicollo area, the effluent steam was low enthalpy. Quantity of the fluid gushed out from the wells was visually measured to be 20 to 30 tons per hour and the ratio of steam and water was 1 : 10.

The flushing of the wells, however, was not last long enough after a month continuous flushing because of scaling in the casing pipes of the wells. The natural cease of flushing, according to CORFO's explanation, was often happened during the tests in the past, and recleaning of the wells using drilling rig caused the next flush.

2–2 Analysis of the Exploratory Wells

As stated before, five (5) exploratory wells were sunk in the area. These holes distributed around 1.2 km^2 are located in the north of Puchuldiza manifestation surrounding Mt. Tahipicollo. All of wells are sited on andesite of Puchuldiza formation and drilled through lower formations.

The five locations for the drilling were selected in the low resistivity anomaly zone, which indicate 3 – 5 Ω-m in the AB/2 = 500 map. These drilling sites are also topographically situated at lower elevation considering the mobilization of rig and water supply. As stated in the first survey mission's report, the most active geothermal manifestations distributed on the surface have occurred at the intersection of different faults of N-S, NW-SE and NE-SW trend system.

The sites selected for the drilling are located near the fractured zone and are covered with thin andesite lava which no longer plays a role of cap rock of geothermal reservoir. Fracture zone near the surface would be not only good conduits of geothermal fluid from the depth, but also pass way down of cold water from the surface. Therefore, if the production zone occurs at shallow part of the well, mixture of high temperature fluid from the depth and cold water from the surface would be provided into the well. Moreover, the installation of production casing pipes is not deep enough in the well, seeping water at shallow depth would be acceralated. It causes the drop of reservoir temperature and pressure.

On the study of thermal logging charts conducted by CORFO, the thermal gradient curves show that the maximum temperature of Well No. 2 to No. 4 comes out at the shallow part of the wells, and Well No. 5 of which is revealed at the bottom hole. In the arrangement of well location, the wells sited at the southeastern part surrounding Mt. Tahipicollo like Well No. 2 to No. 4 indicate that the maximum temperature in the wells is revealed at the upper part of the well and temperature decreases with depth. On the other hand, Well No. 5 which located at the northwestern part of the well arrangement shows that temperature increases with depth.

On study of the resistivity section maps reported by the First JICA Mission in 1978, the low resistivity anomaly less than 5 Ω-m in the south-eastern sloop of Mt. Tahipicollo, where Well No. 2 to No. 4 located was found near the surface and was not continued to the depths. In contrast, the low resistivity zone near Well No. 5 sited at the northwestern part of Mt. Tahipicollo continued to the depth. There might be some arguments to discuss with the relation between temperature gradient curve and values of resistivity profile map in order to estimate the geothermal potential in the depth. In fact, there is good coincidence between them in the survey area. Accordingly, to conduct more detailed resistivity survey in the area would suggest us valuable information for the further exploration work.

To indicate the maximum temperature at shallow part in the wells and to show reverse curve of temperature gradient at the depth suggests that geothermal fluid around Mt. Tahipicollo would be flowing from west or northwest direction through the permeable formation and also be mixing with infiltrated cold water from the surface near Puchuldiza river.

On the cause of decline and natural cease of flushing from the production well, many reasons would be considered such as, excessive production from the limited area, mutual interference between wells, cave in or blocking of production casing, choking of fissures or cracks in the productive formation and temperature pressure drop of geothermal reservoir etc.

In this case as stated above, the natural cease of flushing in each well happened in the past is reportedly to be caused by the chemical precipitation of carbonate materials included in the fluid. During the flushing, it would be considered from the fact stated above that the mixture of high temperature fluid from the depth and the infiltrated cold water from the shallow depth were provided into the well. Besides, the vaporization of geothermal fluid caused prompt temperature drop to be a favorable condition for the chemical deposition inside the production pipes.

CHAPTER 3 ELECTRICAL SURVEY

Chapter 3. Electrical Survey

3–1 Details and Purpose of Survey

In Puchuldiza area, Risk (1970) and Hostein (1971) et al. have roughly conducted the geoelectrical studies and confirmed wide zone of low resistivity corresponding with geothermal fluid.

This low resistivity anomaly less than 10 Ω-m has about 3 km width in E-W direction with Tahipicollo as its center and more than 4 km length in N-S direction opened towards north and has been considered as thick stratum with abundunt hot geothermal fluid, the exploratory Well No. 1 to No. 5 have been dug in this area.

The results of those wells, however, showed the comparatively shallow geothermal fluid which has turned out to be not good enough for geothermal power generation and the need of conducting survey for more promissing area has been felt.

In 1978 Japan International Cooperation Agency (JICA) conducted the preliminary survey such as geological, geochemical, gravity, magnetic and electric survey to study the geological structure of this area.

In addition to horizontal electric survey which has been formarly carried out, vertical electrical sounding was adopted, which measures the change of apparent resistivity with the continuous change of electrode spacing, and geo-electrical structure was interpreted in the area from Tahipicollo to Tuja with the concept of geothermal reservoir and low resistivity.

As a results of general interpretation several points are selected as the drilling sites where there is thick andesite overburden of high resistivity which forms the caprock and where low resistivity zone are seen in the depths with the assumption of geological structural zone.

The site of Well No. 6 was selected by those explorations. But in the first-phase survey in 1978 only 2 E-W lines of each 6 km length were surveyed, it is recommended that in parallel with the drilling work of No. 6 another two N-S lines of each 6 km should be conducted in order to know the scale of geothermal reservoir in detail.

In the electrical survey conducted in Oct. – Dec., 1979, three lines, line-D almost same as 501E passing the site of Well No. 6, line-E along Q. Chiguanane and 502.5E each 6 km and line-F along 855N of 3 km length were surveyed to confirm the N-S extension of low resistivity zone.

3–2 Method of Survey

In order to compile the past data and make the plan map of distribution of low resistivity the same method was adopted with the 2nd phase.

Method:	Vertical Electric Sounding by Schlumberger Configuration
Electrode Spacing:	Current Electrode AB/2 : 10 – 1,500 m
	Potential Electrode MN/2 : 2 – 100 m
Current Supply:	0.1 Hz Constant current square wave
	0.1 – 2.0 A
	A current supplied was read from out put A-meter of transmitter and

the shape of the current was monitored by a pen recorder.

Voltage Difference: Recorded on a penrecorder after the compensation of self potential and chose the low S/N record.

The combination of current electrode and potential electrode spacing adopted in this survey are as follows.

Measurering electrode spacing

No.	AB/2(m)	MN/2(m)	K	No.	AB/2(m)	MN/2(m)	K
1	10	2	75.4	12	200	40	1508
2	15	2	173.6	13	250	40	2392
3	20	2	311	14	375	40	5459
4	30	2	703.7	15	500	40	9755
5	40	2	1253	16	500	100	3770
6	50	2	1960	17	625	100	5979
7	50	10	377	18	750	100	8679
8	75	10	867.9	19	1000	100	15550
9	100	10	1555	20	1250	100	24390
10	150	10	3519	21	1500	100	31590
11	200	40	6267				

K: Geometrical factor

Except the end of the survey line maximum electrode spacing is AB/2 = 1,500 m, with 21 measurements of each station to make a VES curve.

3–3 Method of Analysis

Apparent resistivity values of each station are put into the computer so that the VES curves are displayed on the CRT. Once assumed geo-electric model structure such as depths and resistivity are given, the theoretical VES curves appeared instantaneously and when there is the difference with the observed value, the input data are modified to determine the satisfatory geo-electric structure.

In conducting this simulation, geo-electric structure of line A, B and C conducted in 1978 were reffered.

1) Upper layer (high-resistivity)

ⓐ-layer (1,000 – 3,000 Ω-m)

This layer is distributed between No. 60 and No. 100 and near No. 180 on Line A, having the thickness of 0 to 200 m. It corresponds to the Quaternary andesite.

ⓑ-layer (100 – 600 Ω-m)

The layer is between No. 4 and No. 110, near No. 140 and No. 40, between No. 90 and No. 190 on Line B, its thickness is about 100 m, and corresponds to the Quaternary andesite and Tertiary pyroxene andesite or the altered ⓐ-layer.

ⓒ-layer (20 – 80 Ω-m)

The distribution of ⓒ-layer is in Tuja altered zone between No. 20 and No. 40 of Line A, and on the east side of No. 140 of Line A, and between No. 20 and No. 150 of Line B and on the east side of No. 200 of Line B. Its thickness range from about 100 to 400 m, and corresponds to andesitic welded tuff of upper Puchuldiza formation.

2) Middle layer (low-resistivity) 2 – 6 Ω-m

It distributes thickly under both survey lines. In Tuja and Puchuldiza, near the end of survey lines, the resistivity is lowest between No. 90 and No. 100 in Line B. Its thickness is about 500 to 700 m and corresponds to andesitic welded tuff of Puchuldiza formation, dacitic welded tuff of Condoriri formation, and green sand stone of Chojña Chaya formation.

According to the calculated effective porosity as shown in the Table II–4–4, the resistivity of Condoriri formation is presumed to be the lowest with the tendency to gradually increase, proportional to the high depth increment.

3) Lower layer (high-resistivity) 15 Ω-m <

The basement layer is detected from the rising of the VES curve. Here, the resistivity is higher than upper layer, but the resistivity values could not be determined exactly.

In both survey lines, it grows shallow on the east side and deep on the west, and not detectable at the west ends of these lines. This seems to correspond to rhyolitic welded tuff of Utayane formation, but the thickness is not calculated.

The presumed resistivity values from the cores of well No. 4 and No. 5 are also a little high. The drainage of wells in the Puchuldiza area occur mainly in this layer.

On Line D and Line E which run parpendicular with Line A and Line B almost the same change of resistivity are seen so that the same classification of resistivity can be used.

3–4 Results of Interpretation

3–4–1 Apparent Resistivity Section (Fig. I–3–1)

VES curves are plotted by the observed apparent resistivity corresponding to each and by curve matching method resistivity and depth of each stratum are determined.

It is important to make an apparent resistivity section prior to make interpretation of geo-electric structure to know the outline of resistivity change.

Generally by looking an apparent resistivity section the parallel contour of resistivity with the surface shows the stratified geo-electrical structure and the distortional contour of resistivity corresponds to the boundary of geology, fault and the change of shallow resistivity change.

· General geo-electrical structure was assumed by this apparent resistivity section when the field survey finished at the site.

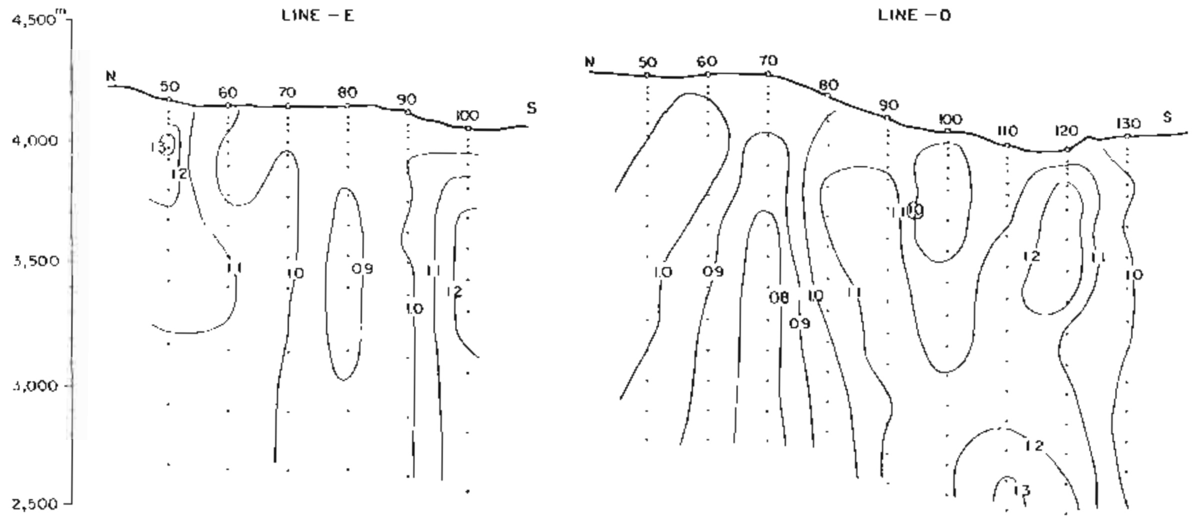

Fig I-3-3 DISTRIBUTION OF APPARENT RESISTIVITY ON CONDUCTIVE PAPER

Line D

Judging from the pattern of the apparent resistivity contours the geoelectrical structure seems to be stratigraphically different with the overburden by high resistivity readings of around 2,000 Ω-m.

Over the Natividad hill north of No. 110 the high resistivity overburden covers the surface while in the southern half of the line comparatively low resistivity zone is recognized from the surface.

The high resistivity zone seems to corresponds with hornblende andesite of Holocene and Puchuldiza andesite of Miocene distributed over Natividad hill, north of Puchuldiza river.

Some faults are supposed to exist at the depths around No. 100, No. 120, No. 135, No. 155, and No. 175 judging from the curved flow of the contour.

The low resistivity contours are seen at the depth around No. 40, No. 80 and No. 90 and so Well No. 6 was sited around No. 100.

Line E

The pattern of the contours is almost the same as Line D with the high resistivity overburden in the north and comparatively low resistivity readings in the south.

The thickness of the overburden is, however, thinner and the resistivity reading is lower than those of Line D.

Around No. 60 low resistivity readings less than 5 Ω-m are detected in the shallow zone. which is supposed to be due to the warm saline water of Chiguanane river.

Discontinuity of resistivity readings are recognized around No. 45, 65, 115, 145 and No. 185.

Line F

This line was planned complementary to the sourthern part of Line D and Line E in order to know the southern extent of the low resistivity zone. The topography is generally gentle with the Puchuldiza river as its center.

The pattern of resistivity readings is monotonously decreasing toward depths and is generally low. The lowest resistivity zone less than 7.5 Ωm is noted between two faults near No. 45 and No. 70. This zone is very thick and is assumed to be due to hot saline water.

3–4–2 Resistivity Section (Fig. I–3–4)

Line D

High resistivity layer corresponding with Quaternary andesitic rocks with thickness of 100 – 200 m covers the whole line and especially in the northern part of No. 94 where Well No. 6 was dug ⓐ-layer of more than 2,000 Ω-m with thickness of 50 – 70 m covers the surface. This high resistivity overburden is considered to be the whethered andesitic lava but not seen at No. 30.

Among the upper high resistive layers and ⓒ-layer of comparatively low resistivity (20 – 30 Ω-m) distribute over, about 1 km in North-South with No. 120 as its center, where Line-D intersects with Line-B, and the thickness is about 200 m forming the graben structure by the faults near No. 95 and No. 135.

Here along the Puchuldiza River it shows wide low resistivity zone due to the abundant surface saline water.

The same ⓒ-layer are seen near No. 160, where Line-D intersects with Line-F, and near No. 220, which is probably due to the weak geothermal phenomena in the depths.

Middle low resistivity layer shows comparatively low resistivity (3.5 – 5 Ω-m) in the northern part of resistivity-discontinuity around No. 130 – No. 140 and 5 – 7 Ω-m in the southern part of the discontinuity.

Especially in the area of south-western slope of Co. Natividad between No. 30 – 60 comparatively low resistivity suggests the deep geothermal fluid.

Besides in the depth of about 1,000 m near No. 140 comparatively high resistivity of 30 Ω-m are detected but no detection of the same resistivity around No. 140 does not suggest the presence of basement in the depths.

CLASSIFICATION OF VES CURVES LINE-D

unit : Ω–m

STATION	TYPE	UPPER LAYER			MIDDLE LAYER	LOWER LAYER	REMARKS
		a	b				
10	2*	3,300	820		5.0		2* : two layer
20	Q	2,900	720		5.0		––– : Fault
30	2*		500		3.5		. . . : Boundary
40	Q	2,000	300		3.5		
50	Q	2,800	500		3.5		
60	Q	3,000	800		3.5		
70	Q	4,800	500		4.0		
80	Q	2,350	200		4.0		
90	Q	2,000	115		4.8		
100	Q	b	130	c 25	4.5		
110	Q		55	22	4.9		
120	Q		70	30	4.8		
130	Q		90	25	4.8		
140	H	b	70		5.0	30	
150	Q		66		6.6		
160	2*	c		25	7.0		
170	Q	b	50	20	6.0		
180	2*	b	33		6.5		
190	2*		52		6.5		
200	2*		45		5.0		
210	2*		42		7.3		
220	2*	b	90	c 17			
230	2*		45	20			

Resistivity classification		Resistivity (Ω–m)	Thickness (m)
I.	Upper L.	a. 2,000 ~ 4,800	50 ~ 70
		b. 33 ~ 820	30 ~ 250
		c. 17 ~ 30	150 ~ 300
II.	Middle L.	3.5 ~ 7.3	800±
III.	Lower L.	30<	

CLASSIFICATION OF VES CURVES LINE–E

unit : Ω–m

STATION	TYPE	UPPER LAYER			MIDDLE LAYER	LOWER LAYER	REMARKS
10	2*			c 55	9.0		2* : two layer
20	Q		b 160	c 30	4.8		
30	Q	a 2,000	600		3.5		——— : Fault
40	2*	2,000			4.0		. . . : Boundary
50	QH	2,000		c 13	3.0	25	
60	H			55	3.5	20	
70	QH		b 120	60	3.0	20	
80	H		250		3.2	20	
90	Q	a 550	100		4.0		
100	H		60		5.0	20	
110	QH		b 85	c 30	3.8	20	
120	Q		200	33	5.0		
130	QH		70	30	3.5	15	
140	Q		250	45	4.0		
150	Q		b 80	c 30	4.8		
160	Q		55	25	5.5		
170	Q		85	30	5.5		
180	Q		110	30	7.5		
190	Q		65	12	4.5		
200	2*			c 13	4.5		
210	2*			c 25	8.0		
220	2*		b 95	c 15			
230	2*		70	16			

Resistivity classification		Resistivity (Ω–m)	Thickness (m)
I.	Upper L.	a. 200 ~ 2,000	30 ~ 60
		b. 55 ~ 600	40 ~ 130
		c. 12 ~ 55	60 ~ 480
II.	Middle L.	3 ~ 9	500+
III.	Lower L.	15<	

CLASSIFICATION OF VES CURVES LINE–F

unit : Ω–m

STATION	TYPE	UPPER LAYER		MIDDLE LAYER	LOWER LAYER	REMARKS
10	2*	c	100	15		2* : two layer
20	2*		75	13		——— : Fault
30	Q	b 100	55	10		. . . : Boundary
40	2*		50	10		
50	2*	c	60	7.5		
60	Q	b 100	33	4.5		
70	2*		25	4.5		
80	Q	b 120	25	4.3		
90	2*	c	22	5.0		
100	2*		55	10		
110	2*	b 150		20		

Resistivity classification		Resistivity (Ω–m)	Thickness (m)
I.	Upper L.	b. 100 ~ 150	20 ~ 65
		c. 22 ~ 100	200 ~ 260
II.	Middle L.	4.3 ~ 15	500+
III.	Lower L.	–	

Line E

High resistiveⓐ-layer are not found except on the top of the hill of No. 40 and No. 90.

The area between No. 90 and No. 110 along the Ancocollo Creek seems to cross the faults and the resistivity discontinuity are seen there as thickⓒ-layer distribute in the south of No. 110.

Depth of middle low resistivity zone are very shallow in the north of No. 65 along Chiguanane Creek and the deep layer of 15 – 40 Ω-m are not seen in the north of No. 40. In this zone hot saline water seems to flow towards south and this area is selected as one of the drilling sites by the first phase survey.

In around No. 80, where Line-E intersects with Line-A, the middle low resistivity shows almost 3 Ω-m which is comparatively lower than that of No. 140 of Line-A. It may be due to the development of N-S cracks and path judging from the parallel faults of generally N-S direction.

Lahsen (1970, 73) reffered to this tendency of anisotropy that ρN-S is lower than ρE-W in this area and this has become one of the evidence of supply of geothermal fluid from the North.

Both between No. 140 – No. 150 and No. 180 – No. 190, where Line-E crosses the Puchuldiza river, there is the resistivity discontinuity, and the area between No. 190 – No. 200 show the graben structure with lower resistivity than the surrounding area.

Line F

A complementary survey (3 km) along 855N in the south of Lupe was conducted to know the southern extension of low resistivity zone.

The thickness ofⓒ-layer is generally thick devided into several blocks by some N-S faults, and it becomes thinner towards east in the east of Puchuldiza river, and in the east end of this lineⓑ-layer caused by the Puchudiza andesite are confirmed.

An syncline or a fault is assumed around No. 70 and the low resistivity of 4 – 5 Ω-m are confirmed in the depth of more than 300 m.

Besides the lower layer is shallow around No. 40 forming the up-lift structure which coincides with the results of the gravity survey very well.

3–4–3 Apparent Resistivity Plan Map (Fig. I–3–5)

Survey results of Phase II in 1979 and the existing data were compiled on the apparent resistivity plan map. Two maps were made for electrode distance of AB/2 = 500 m and 1,000 m, indicating the general resistivity change and delineating the promissing productive area.

AB/2 = 500 Map

Significant low resistivity zones are seen around Tahipicollo hill through Puchuldiza and also around Tuja both in N-S directions along the creek covered by Tertiary dacite and Quaternary sediments.

On the other hand, high resistivity zone are seen over Natividad hill and west to Tuja creek, showing N-S distribution just like the low resistivity zones corresponding to Holocene hornblende-biotite andesite.

Resistivity readings along Puchuldiza river are generally 10 – 15 Ω-m with little change.

A zone of dense contours of resistivity lines or with the disturbed contours of resistivity lines nearly corresponds with faults or boundary of geologic formations confirmed by surface geological and geophysical surveys.

AB/2 = 1,000 m Map

Low resistivity zones separated into Tuja and Puchuldiza on AB/2 = 500 m map become one wide zone less than 750 m in depths and located north of Puchuldiza river covering Tahipicollo hill in N-W direction.

The area is assumed to be about 8 km by 4 km.

PART Ⅱ
EXPLORATORY WELL NO. 6

CHAPTER I INTRODUCTION

PART II

Chapter 1. Introduction

1–1 Objective of the Survey

Prior to the field investigation conducted by JICA survey mission in 1978, five (5) exploratory wells were already drilled by CORFO at sites surrounding Mt. Tahipicollo hill in the Puchuldiza geothermal field. However, the results of temperature logging of these wells indicated that they were not high enough for commercial power generation.

After an integrated evaluation of geological, geochemical and geophysical surveys in the area, JICA survey mission concluded that the most promising area in the field might be at the area of about one (1) km east of Tuja manifestation. Consequently, exploratory Well No. 6 was sited and recommended in order to have more detailed information on the reservoir characteristics necessary for the evaluation of high temperature geothermal fluid.

Drilling exploratory wells, in general, have the following objectives; to confirm geological stratigraphy and structure, to get the geochemical and the geophysical properties of the formation, and also to examine the effluent materials from the well and to gather other important data which could not be obtained by the surface investigation. Finally, all these informations collected from the well would be used for the scientific evaluation of the geothermal reservoir in the area if there is any.

Well No. 6, in fact, had been designed by CORFO engineers following the recommendation of JICA mission to drill at least 1,000 m depth well. It was also suggested that seepage of cold water from shallow part should be sealed off.

1–2 Members of the Survey Team

Team Leader	Mr. Yasunori Sakai Mitsubishi Metal Corporation	Geologist
Coordinator	Mr. Masaru Tateishi Japan International Cooperation Agency	
Reservoir survey	Mr. Yasuhiro Kubota Mitsubishi Metal Corporation	Production engineer
Logging survey	Mr. Masashi Kurosawa Bishimetal Exploration Co., Ltd.	Geophysicist

Counterpart (Comite Geotermico – CORFO)

Project Manager	Mr. Claudio Cadiz Chavarria	Industrial Engineer
Camp Manager	Mr. Turides Solar Venegas	Chemical Engineer
	Mr. Ricardo Sandoval Salas	Geologist
	Mr. Renan Argandoña Ramos	do
	Miss. Margarita Letelier Parga	do
	Mr. Jaime Caviedes Dupra	do

1−3 Itinerary

ITINERARY OF III PHASE JAPANESE SURVEY TEAM

No.	Date		Day	Schedule	
1	1980. Oct.	12	Sun.	A member KUROSAWA, Tokyo Lv. → Los Angels Lv.	
2		13		Santiago Ar.	
3		14		A courtesy call on the Japanese Embassy, CORFO	
4		15		Make arrangements with CORFO	
5		16		Santiago → Iquique	
6		17		Make arrangements with CORFO	
7		18		Iquique → Chusmiza (3,500 m elevation)	
8		19	Sun.	Chusmiza → Puchuldiza (4,300 m elevation)	
9		20			
10		21		Temperature logging	
11		22		Calculation of logged data	
12		23		"	
13		24		Temperature logging of Well No. 2	
14		25		Calculation of logged data	
15		26	Sun.	"	A member KUBOTA, Tokyo Lv.
16		27		"	Santiago Ar.
17		28		Adjustment	A courtesy call on the Japanese Embassy and CORFO
18		29		"	Santiago → Iquique
19		30		"	Iquique → Chusmiza
20		31			Chusmiza → Puchuldiza
21	Nov.	1			Around inspection at the area
22		2	Sun.	Temperature logging	
23		3		Cementation of anchar casing pipe	
24		4		Calculation of logged data	
25		5		"	
26		6		Logged data calculation	
27		7		"	
28		8		Geothermal survey	
29		9	Sun.	"	
30		10		"	
31		11		"	
32		12		"	
33		13		"	

No.	Date		Day	Schedule
34	1980. Nov.	14		Logging preparation
35		15		Temperature logging
36		16	Sun.	Temperature logging
37		17		Logging data Calculation, Cementation of production casing pipe
38		18		Puchuldiza → Iquique
39		19		
40		20		Iquique → Puchuldiza
41		21		Logged data calculation and geological survey
42		22		”
43		23	Sun.	”
44		24		”
45		25		”
46		26		Logging preparation
47		27		Temperature logging
48		28		”
49		29		”
50	Dec.	30	Sun.	”
51		1		Injection test
52		2		Calculate the data
53		3		Production test
54		4		Temperature logging
55		5		Pack the equipment
56		6		Puchuldiza → Iquique
57		7	Sun.	Calculate the data
58		8		Write up the interim report
59		9		”
60		10		”
61		11		A member KUBOTA, Iquique → Puchuldiza
62		12		A member KUROSAWA, Iquique → Chusmiza
63		13		Mr. KISHIDA of JICA make of field inspection
64		14	Sun.	Iquique → Santiago
65		15		Report the interim report
66		16		Santiago Lv.
67		17		Los Angels Ar. and Lv.
68		18		Tokyo Ar.

CHAPTER 2.

EXPLORATORY WELL DRILLING

Chapter 2. Exploratory Well Drilling

2–1 Drilling Rig and Drilling Method

The specifications of the Drilling Rig used at Well No. 6 is shown below:

Drilling Rig	:	Portable Water Well Drilling Rig Model 2500, Made by Gardner Denver U.S.A.
Engine	:	Cat 3306-66D, 250 HP
Drums	:	Single Line Pull 18,000 lbs
Mast	:	Height 65 feet Recommended working load capacity on six lines 60,000 lbs
Pump	:	N.S. Co. Ideal C-250 N.S. Co. Ideal C-150

Maximum drilling capacity of the rig is 1,372 meter using a 2 & 7/8 inches pipe diameter under ordinary condition. However, since the site is located 4,200 meter above sea level, the capacity of rig would be reduced to about 10 – 20 percent.

Drilling method employed at the site was the ordinary use of bentonite mud and circulation of water. Conditions relating to the drilling work are shown below:

P.H. Value of controlled mud water	:	9 to 10
Specific gravity of controlled mud water	:	1.04 to 1.09 (up to 650 m depth)
" "	:	1.01 to 1.08 (deeper than 650 m)
Viscosity velocity of Mud	:	37 to 45 sec
Bit load	:	about 1,000 lbs
R.P.M.	:	70 to 80
Bit type used	:	OWN, W7R
Drilling rate	:	15 to 45 min per meter

In the course of the drilling work, the nature of circulating mud water and bit load were controlled effectively. Regardless of the request to recover drilling cores every 30 m, the drilling rate was maintained at 15 to 45 minutes per meter.

2–2 Drilling Procedure and Well Completion

Fig. II–2–2 shows the drilling record and casing design installed. Well No. 6 was drilled to a depth of 55 m in 1979 and 17 & 1/2 inches surface casing pipe was used to support the well wall in unconsolidated formation so as to shut off surface water and shallow water aquifer of low temperature.

Below 55 m depth, drilling work was resumed on Sept. 1st, 1980. From 55 to 312 m depth, the well was cased by 12 & 1/4 inches diameter pipe and was anchored by a 9 & 5/8 inches of casing pipe. In the course of drilling, 400 liter of mud circulation loss was observed instantaneously at the depth of 154 m.

From 312 to 653 m, 8 & 3/4 inches bit was used and 7 inches production casing pipe was installed in the well after the first temperature logging. During the drilling, no mud circulation loss was observed. The cementing of the production casing was carried out by filling the annular space between the casing pipe and well with ordinary portland cement milk mixed with four percent bentonite.

In the course of the cementation using Ideal C-150 pump, the cementing of the production casing was considered effective on the basis of the observed circulation of cement milk.

In general, production casing must be used when the elevated temperature reservoir is confirmed, say over 200°C. In this case, however, temperature was 122°C at 650 m depth (Table II–4–2, Fig. II–4–2), not high enough to set the casing. But judging from the capacity of the drilling machine used and total length of casing pipes prepared at site, it was unavoidable not to place the casing at this temperature and depth.

After the cementation, well head equipments were installed before starting deeper drilling work again. The well was smoothly drilled down to 1,000 m depth as planned initially. Therefore, the drilling plan was revised in order to drill deeper because the reservoir temperature at the depth was not high enough and the well did not have any mud circulation loss.

On November 27, when the well reached the 1,157 m depth, the drilling work was stopped because the drilling rig has reached its maximum capacity. Mud circulation loss of 1.9 kl lasting for three hours took place at 1,090 m depth. Between 650 m and bottom hole, 5 inches slotted pipe was used.

2–3 Flush Test

After the slotted pipe was set at deeper part of the well, cleaning of well wall was made by pumping water to the well. After cleaning the well, temperature logging was conducted in order to know the well characteristics. Although the result of well measurements will be discussed later in detail, the maximum temperature of 180°C at the bottom hole and 4 $m^3/h/kg/cm^2$ injection index were confirmed in spite of no mud circulation loss encounter during the drilling work.

Reservoir temperature was not high enough than what was expected, however, the injection index was quite good. Water level in the well was assumed to be about 4,200 m A.S.L., higher than the height of well head. Accordingly, the geothermal fluid would flow out automatically when the main valve of well head was opened.

On December 3 and 4, flush tests were carried out opening the main valve. Low temperature fluid gushed out from the well head for about 20 minutes after the valve was opened. As the effluent temperature exceeded over 85°C, which is boiling point of water in the area, mixture ratio of geothermal steam and water from the well gradually increased and thus intensified flushing was observed.

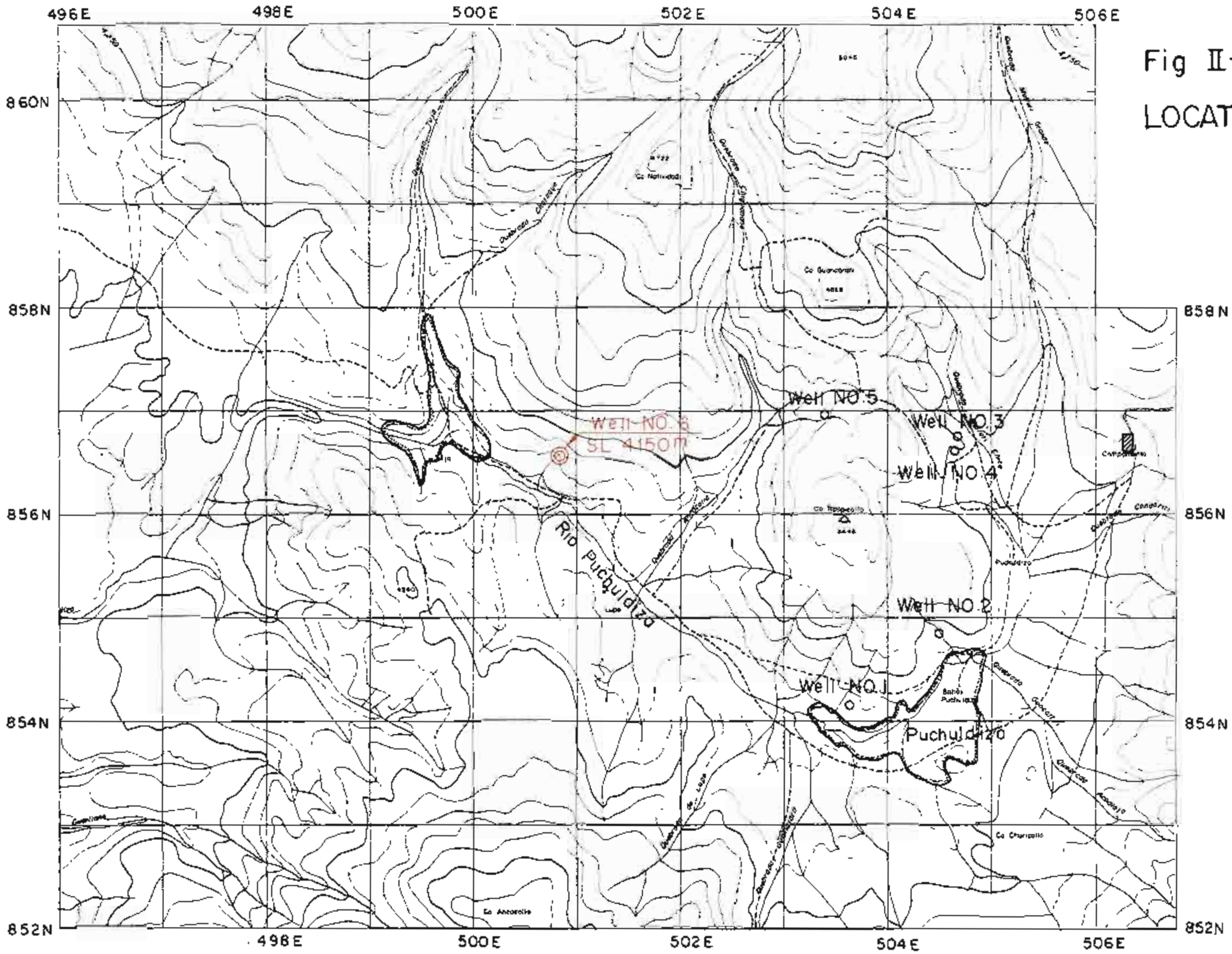

Fig II-2-1

LOCATION OF WEll NO.6

Scale 1:50,000

LEGEND

o Well NO.

Sinter deposition area

After one hour of flushing, gushing of geothermal fluid was no longer continuous but intermittent because of lack of enough supply of hot effluent from the reservoir. In order to accelerate temperature recovery of the well water, compressed air was tightly enclosed in the well shutting the main valve. When the main valve was opened on December 12, no flow was observed from the well, although the shut in pressure indicated 10 atg.

The probable reasons why no geothermal fluid gushed out from the well are as follows:

(1) As shown in temperature logging map in Fig. I–4–1, cold water that concentrated at upper part of the well prevented the flow of geothermal fluid up from the depth.

(2) Fine cracks and fissures which are the sources of fluid were clogged by mud and other debris.

In order to remove the cold water from upper part of the well, air lift test was conducted for two days and the result is shown in the following table.

Date	Hours conducted	Drawnout water	Water Level before trial	Water Level after trial
Dec. 12	$2{:}^{h}20^{m}$	3 m^3	– 7 m	ND
Dec. 13	$3{:}^{h}00^{m}$	7 m^3	–24 m	–58 m

The table showed that the water level in the well has not recovered sufficiently to the previous water level after the air lift test.

It means that cracks or fissures which are the conduit of the fluid are still clogged unexpectedly. For example, residual mud used in drilling had solidified under high temperature condition or effluent impurities like calcium carbonate had scaled in the well.

CHAPTER 3

GEOLOGY, THERMAL ALTERATION AND GEOCHEMISTRY

Chapter 3. Geology, Thermal Alteration and Geochemistry

3–1 Method of the Investigation

In the course of drilling, core and well cuttings were sampled every 30 m and 5 m respectively, as recommended by the JICA Mission.

These samples taken from the well were observed macroscopically in detail at the well site and were stratigraphically correlated with geological formations of the field survey made previously. Some representative samples of the geological formation in the area were studied by microscopic examination in order to know their components, texture, and assemblage of constituent minerals of the rocks.

X-ray diffraction analysis was also made in order to determine the alteration minerals produced by thermal activities.

In addition, hot water effluent from the Well No. 6, river waters, and hotspring waters around the area were brought back to Japan for analysis.

The equipment used and measurement parameters are as follows:

(1) Microscopic Observation

1) Equipment

Orto plan, Vol (Ernst Leiz) POH (Nippon Kogaku) Rutomat (Photography, Ernst Leiz)

2) Observation Method

Mineral assemblages, paragenesis and texture were examined by polarizing microscope for each thin section.

Microscopic picture of typical samples were taken with both parallel and cross Nicol prisms.

(2) X-Ray Diffraction Analyses

1) Instruments used

Philips X-ray diffractometer

2) Test Procedure

The collected samples were ground between 50 – 100 mesh in a stainless steel mortar. Furthermore, the samples were ground in the agate mortar until no grit is felt by the finger tip to produce non-oriented particles. Some special samples were treated to produce oriented particles and were analyzed after treatment of HC1 and ethylene glycol.

3) X-ray diffraction conditions

Target	Cu Kα
Filter	Craphite monocrometer
Voltage	30 KV
Current	20 mA
Divergence slit	1^{o}
Receiving slit	0.2 mm

Scanning slit	2^{o}/min and 1^{o}/min
Chart speed	2 cm/min and 1 cm/min

(3) Chemical Analysis of Hotwater

Geothermal fluid gushing out from the Well No. 6, hot spring water, and river water in the area were collected and were brought back to Japan for chemical analysis.

3–2 Geology

Stratigraphy of Well No. 6 consists of Churicollo formation of middle to upper Cretaceous, and Utayane, Chojna-Chaya, Condoriri and Puchuldiza formation of Tertiary, and the overlaying Quaternary volcanics given in ascending order. Andesite dyke with unknown age were noted at 660 m to 750 m depth.

The geological classification, stratigraphy and thickness of each formation in the well coincided with those of surface field investigation conducted by JICA survey mission in 1978.

The following descriptions show the result of macroscopic and microscopic observations of the cores taken from the well. Fig. II–3–1 shows a geological column chart of Well No. 6.

○Quaternary Volcanics

Quaternary Volcanics appears from surface down to 75 m depth. The rock consists of andesite lava and pyroclastics. Under microscopic observation, the andesite is characterized by large phenocrysts of plagioclass and hornblende with porphyritic texture. The andesite in the well is the same as those that prevails at northern area of the drilling site. No geothermal alteration was observed.

○Puchuldiza Formation

Puchuldiza formation occurs from 75 m to 415 m depth. This formation is subdivided into three (3) groups from its rock facies, that is, andesite lava flow (I), pyroclastic rock, and andesite lava flow (II). Upper andesite lava flow appears from 75 m to 215 m depth and is characterized by massive, compact and black groundmess. Phenocrysts of plagioclase and pyroxene were observed. Under the microscope, augite and hypersthene of pyroxene minerals are recognized. Groundmass is composed of very fine grains of plagioclase, augite, and opaque minerals. Alternation of the rock is generally weak.

Pyroclastic rock from 215 m to 315 m depth consists of lapilli tuff and tuff breccia. The former predominate at the upper part of the well and the latter at the deeper part. Plagioclase, pyroxene, and opaque minerals are the main constituent phenocrysts with small amount of quartz, K-feldspar and biotite. Fragments included in the pyroclastic rock are mainly pyroxene andesite, the essential material of the formation and rarely rhyolitic rock thought to be derived from Utayane formation. Montmorillonite, as alteration mineral, occurs mainly replacing glass, groundmass, and along the rim of cavities.

Andesite lava flow (II) which is essentially the same as the upper andesite lava flow (I) appears from 315 m to 415 m depth and is characterized by flow structure showing the oriented feldspar in the groundmass. Montmorillonite of the lower andesite flow is more severely altered compared with upper andesite flow. The alteration is mainly in groundmass, rim of phenocrysts and along cracks of the phenocrysts. Montmorillonite, sometimes, shows fiine vein structure.

Andesite which occurs at 370 m depth is reddish brown in color. Under microscopic observation, it consists of irregular aggregated hematite.

∘Condoriri Formation

This formation occurs from 415 m to 530 m depth and is characterized by large amount of pumice, consisting of dacitic tuff and lapilli tuff. Under the microscope, the rock consists of mixture of glass and phenocrysts. Breccia included in the formation is of dacitic rock only and the crystal flakes are plagioclase, biotite and opaque minerals. Alteration of the formation is more intense than that of Puchuldiza formation because the pumices completely altered to montmorillonite.

∘Chojña Chaya Formation

The formation appears from 530 to 662 m depth and is composed of lapilli tuff breccia. Although this formation was gradually derived from Condoriri formation, it can be distinguished from Condoriri by the lack or very small presence of pumice in the formation. Breccia included in the formation are mainly dacitic rock and rarely pyroxene andesite. Matrix of the rock is strongly altered to montmorillonite. Under microscopic observation, montmorillonite develops along the cleavages and cracks of plagioclase phenocrysts. All mafic and opaque minerals are also altered to montmorillonite.

Chojña-Chaya formation in the surface is composed of well-bedded, dark green to dark brown medium-grained sandstone intercalated by thin conglomerate beds. This formation however, shows different rock facies from the surface. Difference between Chojña-Chaya and Condoriri is that the former does not contain pumice. Accordingly, the writer has correlated this formation to Chojña-Chaya formation. Pyroclastic sediment possibily change to normal sediment toward East part in the area.

∘Utayane Formation

Utayane formation occurs from 750 to 930 m depth and is characterized by striped structure with light shade of purple, brownish gray of dacitic welded tuff. In some cases, this rock looks like andesite. The strongly welded tuff occurs at upper part of the well and is in direct contact with andesite dyke. Phenocrysts of the rock are plagioclase, biotite, hornblende and opaque minerals, and its groundmass is made of plagioclase, quartz, small amount of K-feldspar and secondary clay minerals. Core sample T27 is welded tuff, occuring at the deeper part of the well. Constituent minerals of the sample are the same as those of welded tuff of the upper part. The formation, as a whole, is strongly altered, especially the groundmass and mafic minerals. Altered minerals are mainly composed of montmorillonite, fine grained secondary quartz, and sericite.

∘Churicollo Formation

Churicollo formation appears at deeper than 930 m depth and subdivided into three (3) rock facies, namely, coarse grained tuff, tuff breccia and andesite lava in descending order. Coarse grained tuff occuring from 930 m to 1,060 m depth consists of plagioclase with small amount of quartz crystal and fragments of mafic minerals. Rock facies gradually change from coarse grain to tuff breccia in the lower part of the well. Sorting of coarse tuff is somewhat good but graded structure is not clearly recognized.

Pyroxene andesite appears at deeper than 1,060 m depth and consists of phenocrysts of plagioclase, augite and opaque minerals and its groundmass is composed of plagioclase, secondary formed quartz, clay minerals and opaque minerals. Since the phenocrysts present are oriented, the rock might be a weled tuff.

This formation is classified into three (3) groups at the surface, namely, andesitic or dacitic welded tuff, intercalation of rhyolitic tuff and welded tuff, and greenish sandstone or conglomerate in ascending order. In core investigation, greenish sandstone or conglomerate could not be found. However, these rocks in surface geology are tuffaceous, and not well rounded. Breccia included in the tuff consists mainly of andesite. Taking into consideration the above, this pyroclastic rock would be correlated with Churicollo formation.

This formation is generally altered strongly compared to other upper formation, especially its groundmass and mafic minerals. Altered minerals consist mainly of chlorite and occasionally sericite, chlorite-montmorillonite mixed layer, carbonate and quartz. To make special mention of altered minerals, epidote has developed in crystal of plagioclase and in the groundmass at the lower part of 1,040 m depth. Most of mafic minerals were altered to opacite or chlorite.

∘ Andesite dyke

Andesite occuring from 662 to 750 m depth are considered dyke because of the following reasons even though this rock was not identified in surface geology:

a) Dip of flow structure of the rock is very steep (approx 70°), that is discordant with the structure of upper and lower formations.
b) Breccia of this rock is not found in the upper formations. It means that there is a possibility that the andesite would be younger than the upper formation.
c) Alteration is somewhat weak with the upper and lower formations. And sometimes montmorillonite prevailing in each formation is not recognized even by X-ray diffraction analysis.

This rock is characterized by very find grain andesite with few minerals showing distinct flow structure. At the boundary of the lower formation, the rock shows cataclastic structure and no accidental breccia. Only plagioclase was recognized as phenocryst in microscopic observation while all other mafic minerals are altered. Groundmass consists of plagioclase, secondary formed quartz, clay minerals and opaque minerals. Mafic minerals and groundmass have been replaced by montmorillonite. A small amount of calcite was noted along cracks of plagioclase. Fine grain secondary quartz was also observed in the groundmass. In some occasions, fine veins of chalcedony silica, quartz, clay minerals and rarely limonite were seen along stripes of flow structure.

Well No. 6 has been drilled at the eastern wing of anticlinal structure passing through the Tuja manifestation as shown in geology portion of the report of First Stage JICA survey mission.

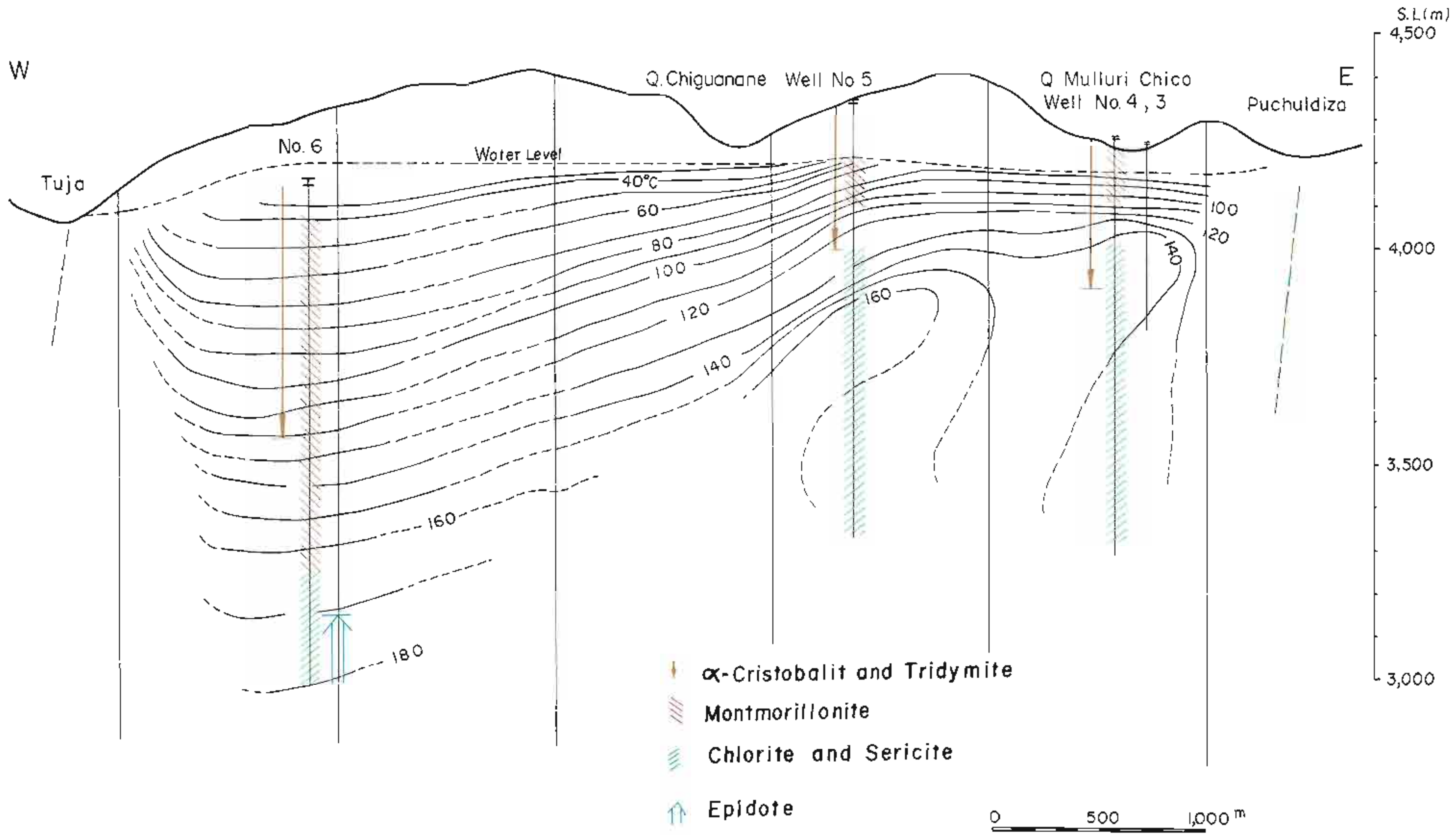

Fig. II-3-2 DISTRIBUTION OF ALTERED MINERAL AND LOGGING TEMPERATURE SECTION W-E (857N)

The relation between geological stratigraphy and structure in the surface survey and geological feature of the well is similar in most parts, except that the Churicollo formation which occurs at 200 m depth is shallower and the thickness of Utayane formation is 200 m thinner than what was expected.

3–3 Geothermal Alteration

Altered minerals detected by X-ray diffraction and microscopic observations of the samples taken from Well No. 6 consist of montmorillonite, sericite-montmorillonite mixed layer, sericite, chlorite, epidote and small amount of calcite. Zeolite mineral however, was not detected. Some of the altered minerals like α-crystobalite and trydimite were used as geothermometer.

α-cristobalite and trydimite were detected by X-ray analysis from surface samples down to 580 m depth. These minerals are not clearly recognized in microscopic observation.

Montmorillonite is present from shallow part down to 905 m depth altering the phenocryst of primary minerals and groundmass. Andesite dyke which occurs from 662 to 750 m depth was weakly altered compared with that of surrounding formations. This suggest that the dyke was of later period intrusion.

Sericite and chlorite occur at deeper than 935 m depth of the well. The occurrence of sercite is the same as that of montmorillonite, replacing the phenocryst and groundmass and sometimes appears as veinlets.

Chlorite is considered to belong to the less Fe content type by its optical characteristics.

Epidote was noted in microscopic observation at places deeper than 1,040 m. The occurrence of epidote is evidenced by spots and veins replacing plagioclase phenocrysts.

Calcite is only detected by X-ray analysis from drill core T-9. Table II–3–1 shows the altered minerals detected by X-ray analysis. All X-ray charts and photographs of thin sections are also attached in the report.

In order to know the subserface temperature of geologic time in geothermal field, a study on the stable domain of alteration minerals produced under high temperature condition was done and the result can be used as a tool of geothermometry.

It was said that α-cristobalite and tridimite would be transformed to quartz at about 100°C when temperature goes up. (Tomasson et al, 1972, Kimbara 1977)

α-cristobalite was detected from the surface of the well up to about 600 m deep indicating a 100°C temperature in the past.

Basing on the results of actual temperature measurements and the distribution of altered minerals, the highest temperature for which montomorillonite can exist at highest stable condition was between 230° ~ 240°C. (Brown et al. 1970, Tomasson et al, 1972). Therefore, about 930 m of the well was presumed to have a higher temperature (230° ~ 240°C) in the past compared to the present. On the other hand, the lowest limit of stable domain of chlorite and sericite in the high temperature condition is about 200° ~ 210°C.

As stated above, epidote was detected at 1000 m depth. The upper limit temperature of epidote is about 230° ~ 260°C. Accordingly, Puchuldiza Geothermal field was at a

Table II–3–1 X-ray Diffraction Analysis

No.	Sample No. and its depth (-m)		Silica			Feldspar		Clay					Zeolite		Others			
			α-Qz	Tri	α-Cr	Pl	K-Fel	Mon	S-M	Ser	Chl	Kao	Mor	Lau	Cc	Hm	Bi	Epi
1	T–3	186–192		•	○	○	•	•										
2	T–4	215–221				○		•										
3	T–5	243–247				○		○										
4	T–5′	* O.S				•		◎										
4′	″	* E.G						◎										
5	T–7	315–320	•			•		◎										
6′	T–7′	O.S						◎										
6	″	E.G						◎										
7	T 9	368–373	•				•	◎							•	•		
8	T 9′	O.S					•	◎								•		
8′	″	E.G						◎										
9	T–10	402–404				○	•	•										
10	T–13	489–492	•	•		◎	•	◎										
11	T–15	550–552	•			○		◎										
12	T–16	580–583			•	○	•	•	•									
13	T–17	611–614				•		◎										
14	T–17′	O.S				•		◎										
14′	″	E.G						◎										
15	T–18	641–643	•			○		◎										
16	T–20	702–704	○			○	•	•										
17	T–21	733–735	○			○	•											
18	T–22	763–765	○			○		◎									○	
19	T–24	812–814	◎			◎		○									○	
20	T–27	904–908	○			○	•	◎										
21	T–28	935–937	○			◎				○								
22	T–30	996–996.3	○			○				○								
23	T–30′	O.S	•			•			◎		○							
23′	″	E.G							◎		○							
24	T–31	1039–1041	○			○				○	○							•
25	T 34	1154–1157	○			○				○	○							•

Qz : Quartz
Tri : Tridymite
α-Cr : α-Cristobalite
Pl : Plagioclase
K-fel : K-feldspar
S-M : Sericite-Montmorillonite Mixed-Layer

Mon : Montmorillonite
Ser : Sericite
Chl : Chlorite
Kao : Kaoline
Mor : Mordenite

Lau : Laumontite
Cc : Calcite
Hm : Hematite
Bi : Biotite
Epi : Epidote

• : rare
○ : common
◎ : abundant

* O.S (Oriented Sample) * E.G (Ethylene Glycol)

higher temperature condition in the geologic age.

However, the geologic formation wherein the altered minerals was detected belong to Tertiary and Cretaceous formations. If the altered minerals were produced prior to the thermal activity in the area, the said minerals can not be used for geothermometry.

From this point of view, altered mineral geothermometry was reviewed based on the distribution of the altered minerals.

The lowest depth for which montmorillonite occurs and the upper depth for which sericite and chlorite occur at 930 m depth of the well. This depth coincide with the boundary of Tertiary and Cretaceous formations.

At the boundary of montmorillonite and sericite, sericite-montmorillonite mixed layer was found. From this data, altered minerals such as montmorillonite, sericite and chlorite could be considered as product of hydrothermal alteration due to geothermal activity.

Fig. II–3–2 shows the measured isothermal temperature profile map from Well No. 4 passing through Well No. 5 and Well No. 6. From the map, the upper limit of chlorite appearance in the well is approximately found along the 140°C isothermal line and also, the boundary of geologic formation is disconcordant from the isothermal lines. The map also shows that the depth of sericite appearance tends to be deeper toward the west and the temperature near the surface is higher in the east and lower around Well No. 6.

3–4 Geochemistry of Geothermal Solution

In order to recheck the result of the First Stage exploration work conducted by JICA mission and to evaluate the geothermal reservoir in the area, the following samples were collected:

(1) Effluent water from Well No. 6
(2) Surface water near Well No. 6
(3) Hot spring water arround manifestations
(4) Hot spring water in the area
(5) Hot water from Suriri geothermal field

In addition to the above samples, hot water from Suriri, located about 40 km north of Puchuldiza was also sampled.

These samples were brought back to Japan and analyzed. Fig. II–3–3 shows the sample localities and Table II–3–2, 3 the chemical composition of water sample.

(1) Chemical Composition of Hot Water from Well No. 6

As stated above, when the main valve was opened after the pump test, geothermal fluid automatically gushed out from the wellhead. Samples were taken from the wellhead after one hour and after two hours right respectively after flushing started.

Judging from the chemical composition of the samples, the samples taken from Well No. 6 are considered typical geothermal fluid because of high silica, sodium, and chlorides contents although these samples were taken one and two hours after the flushing started. However, the elements present are less compared with the waters taken from Well No. 1 to Well No. 5 and hot spring waters around the area. This simply means that the water used for the

Table II–3–2 LIST OF WATER SAMPLES

Nos. and its location		Temp. °C	Flow Rate ℓ/min	Remarks
(Well No. 6)				
1	Well No. 6 1	86	700	
2	Well No. 6 2	86	700	
(Meteoric Water)				
3	Near Well No. 6	13	1	Cold spring water for potable water
4	Tuja Al Fondo	13	0.5	River water
5	Charaque Al Fondo	13	1	River water
6	Near Well No. 5	10	5	River water
(Manifestation of Tuja and Puchuldiza)				
7	Tuja No. 112	85	0.5	Hot spring water
8	Tuja No. 115	86	5	"
9	Tuja No. 124	85	0	"
10	Puchuldiza No. 2	85	0	"
11	Puchuldiza No. 4	85	10	"
12	Puchuldiza No. 5	85	10	"
13	Puchuldiza No. 58	85	3	"
14	Puchuldiza No. 76	86	1	"
(Manifestation surround Volcan Co. Blanco)				
15	Quitariri	86	10	Hot spring water
16	Uscana	32	15	Hot spring water with CO_2 gas in salt lake
17	Pingalluri 1	25	2	Hot spring water
18	Pingalluri 2	30	4	"
19	Laguna Parinacota	25	5	Cold spring water near salt lake
20	Laguna Parinacota	20	5	
21	Suriri No. 1	55	0.5	Hot spring water
22	" 2	62	0	"
23	" 3	50	2	"
24	" 4	85	10	"
25	" 5	85	1700	Most large hot spring water

Table II–3–3 CHEMICAL COMPOSITION OF HOT WATER

Sample No. and its location	Chemical Composition					(unit in ppm)		
	PH	Na	K	Ca	Mg	Cℓ	SO_4	HCO_3
(Well No. 6)								
1. Well No. 6 1	6.50	1060	61	61.5	1.6	1512	205	118
2. Well No. 6 2	7.98	1200	81	80.2	0.8	1860	336	142
(Meteoric Water)								
3. Near Well No. 6	6.52	39	22	26.3	8.9	62.8	83	36.7
4. Tuja al Fondo	6.46	26	10.8	67.5	17.4	4.5	280	23.3
5. Charaque al Fondo	4.66	25	12	44.1	7.1	4.5	119	Tr
6. Near Well No. 5	4.02	42	31	53.2	13.7	7.9	291	Tr
(Manifestations of Tuja and Puchuldiza)								
7. Tuja No. 112	6.72	2010	243	41.3	3.9	3376	114	111.5
8. Tuja No. 115	7.46	1775	169	64.5	2.3	3081	107	96.8
9. Tuja No. 124	6.42	2790	140	78.6	2.1	2866	114	86.9
10. Puchuldiza No. 2	7.46	1570	210	24.1	3.7	2673	122	213
11. Puchuldiza No. 4	7.72	1600	206	26.7	2.3	2226	121	216
12. Puchuldiza No. 15	7.94	1620	222	31.1	2.4	2484	124	218
13. Puchuldiza No. 58	6.50	1670	222	44.4	3.7	2661	131	288
14. Puchuldiza No. 76	7.58	1610	201	23.4	1.5	2494	117	202
(Manifestation surround Volcan Co. Blanco)								
15. Quitariri	8.80	1340	84	0.6	2.5	1549	282	637
16. Uscana	6.50	222	34	78.5	16.9	264	332	115
17. Pingalluri 1	6.46	268	54	51.1	7.0	453	90	154
18. Pingalluri 2	6.54	149	64	23.2	9.1	185	90	138
19. Laguna Parinacota	6.18	11	21	15.7	7.0	7.5	64	36.7
20. Laguna Parinacota	6.22	11	18	10.7	5.9	7.5	45	36.7
(Suriri)								
21. Suriri No. 1	6.42	1690	223	115.1	8.0	2722	240	140
22. " 2	6.54	1190	180	150.7	19.0	1880	317	265
23. " 3	6.58	1160	186	100.2	11.7	1852	283	247
24. " 4	6.60	1100	179	143.5	25.7	1890	359	260
25. " 5	6.54	1210	217	227.7	39.5	1707	1036	279

pump test is still admixed with the guised water.

It is understandable that these chemical contents cannot be used for geothermometry.

(2) Chemical Composition of River Water near Well No. 6

It contains relatively much Ca, Mg, and HCO_3 and less salt than normal geothermal fluid. The water taken from the place therefore is a typical river water around the area.

(3) Hot spring water arround manifestations

In order to recheck the chemical composition of hotspring waters from Tuja and Puchuldiza manifestations, several water samples were taken. The result of chemical analysis indicates that it was the same as that reported by the First Stage survey mission.

(4) Hot spring water in the area

Besides the two manifestations stated above, there are several geothermal indications surrounding Volcano Mt. Blanco. In order to make comparison with Puchuldiza geothermal field, hot spring waters were collected from several places.

Quitariri: Silica sinter deposits as big as Tuja geothermal field spreads widely in the area. Chemical composition of hot water shown high content of salt.

Uscana: It is located at the margin of Uscana salt lake. Hot water flow out to the surface with some gases. This hot spring is classified as HCO_3 type because of high content of carbonate, in spite of high salt content.

Pingalluri: It is located at river bank of western part of Tuja manifestation. Small amount of hot water is flowing out with some chemicals. The temperature of water is about 35°C. It has high HCO_3 salt suggesting the contamination of surface water with NaCl type geothermal fluid.

Laguna Parinacota: It is located at northern slope of Mt. Blanco. Spring water flow out naturally into the salt lake. Salt concentration is comparatively low. It seems this water is derived from a shallow surface water.

Considering the chemical analysis of hotspring water around the area, the same geothermal system or different units of system with similar geothermal fluid as that of Puchuldiza might exist at depth of the southwestern slope of Mt. Macurquina.

Judging from the flow out condition of hotwater, to estimate the aquifer temperature based on the chemical composition of hotspring water around the area could be a mistake. However, a geothermal reservoir of about 200°C or over would be present at the north-west of Tuja manifestation.

(5) Hot water from Suriri Geothermal Field

The field belongs to NaCl type and its geochemical temperature derived from the chemical composition is expected to be 200°C or over.

CHAPTER 4 PHYSICAL LOGGING

Chapter 4. Physical Logging

4–1 Objectives and Method of Logging

In order to make qualitative evaluation of the geothermal reservoir, physical logging such as resistivity, thermal, sonic, radioactive, and electromagentic logging and transmissibility test are generally conducted. In this phase, thermal logging and transmissibility tests were carried out as two of the most important tests.

Thermal logging especially is the most important for the reservoir evaluation for the detection of the permeable zone or the fractured zone, the analysis of thermal change and the estimation of the productive steam quantity of the reservoir.

By conducting thermal logging during the drilling of well and evaluating the results, accidents can be avoided and the probable depth of production casing pipe can be planned and determined.

Furthermore by compiling the geothermal data of several survey wells, the potential size of the reservoir and the distribution of the dominant geothermal resources can be studied.

To interpret the productivity of the reservoir and to estimate the flow rate of geothermal fluid, a transmissibility test was carried out.

The instruments used for the logging is called "Kuster" with Amerada type thermometer and pressure gauge. In this thermometer certain solution is enclosed in a thermosensor whose expansive power proportional with temperature change is automatically recorded on a chart.

Thermometer	:	KTB Temperature Element No. 10004 (KUSTER COMPANY, U.S.A.)
Manometer	:	KPG Pressure Element No. 10201 (KUSTER COMPANY, U.S.A.)
Winch	:	Oil pressure type C.A. Mathey F.H. 1210/12 (MACHINE WORKS INC., U.S.A.)
Cable	:	Stainless Wire ϕ 2.08 mm
Chart Reader	:	Type S.G. 250-1 (HILGER WATTS, ENGLAND)

Amerada type thermometer of KUSTER is originally designed for intermittent measurement at a certain depth. But the temperature gradient of the well was continuously measured by moving down a probe at a velocity of less than 10 m/min.

4–2 Thermal Logging

Thermal logging was carried out four times at depths of 400 m, 600 m, 800 m and 1,150 m respectively.

In the first three loggings, circulating fluid was mud. In the last logging the hole was cleaned by river water after installation of slotted pipes. The temperatures of recovery were measured for five days after the circulation has ceased.

Table II-4-1 Logged Temperature of Well No. 6

Logging No.	I	II – 1	II – 2	III – 1	III – 2	III – 3
Logging Curve No.	①	②	③	④	⑤	⑥
Date	21/Oct/1980	1/Nov/1980	2/Nov/1980	15/Nov/1980	15/Nov/1980	16/Nov/1980
Drilling Depth (m)	463.0	653.0	653.0	814.5	814.5	814.5
Standing Time (hour)	144:05	4:30	23:40	7:30	16:30	31:00
Circulation Water	Bentonite Mud	Bentonite Mud	Bentonite Mud	Bentonite Mud	Bentonite Mud	Bentonite Mud
Water Level (m)	73.0	0	7.0	0	0	0
Water Level Temp. (°C)	No data	No data	No data	No data	18.0	25.0

Depth / Temp.	(°C)	(°C)	(°C)	(°C)	(°C)	(°C)
0 m	No data	No data	–	No data	No data	No data
50 m	No data	44.9	–	No data	No data	No data
100 m	43.9	48.0	44.7	44.4	45.5	43.9
150 m	48.2	48.9	48.8	46.8	50.9	49.8
200 m	51.7	50.7	51.1	51.9	54.6	53.5
250 m	53.2	51.1	53.3	53.5	56.9	56.0
300 m	60.3	51.8	56.3	57.3	60.3	59.1
350 m		53.1	57.0	61.4	64.8	65.2
400 m		54.4	59.7	64.3	69.3	71.0
450 m		55.6	70.5	65.4	73.3	76.1
500 m		57.8	77.2	72.1	78.1	82.7
550 m		58.5	83.9	76.2	85.1	88.3
600 m		59.8	93.9	77.7	88.0	93.4
650 m		60.3	111.2	84.1	93.3	103.2
700 m				90.5	103.2	109.4
750 m				95.8	113.4	116.3
800 m				114.5	132.8	142.6
Remark						

Table II–4–1 Logged Temperature of Well No. 6

Logging No.	IV – 1	IV – 2	IV – 3	IV – 4	IV – 5	V – 1
Logging Curve No.	⑦	⑧	⑨	⑩	⑪	⑫
Date	27/Nov/1980	28/Nov/1980	29/Nov/1980	30/Nov/1980	1/Dec/1980	4/Dec/1980
Drilling Depth (m)	1,157.0	1,157.0	1,157.0	1,157.0	1,157.0	1,157.0
Standing Time (hour)	10:20	23:00	48:00	72:00	96:00	–
Circulation Water	Cool water	Cool water	Cool water	Cool water	Cool water	Cool water
Water Level (m)	0	0	0.5	1.5	2.0	–
Water Level Temp. (°C)	14.0	19.0	19.0	20.0	22.0	–

Depth / Temp.	(°C)	(°C)	(°C)	(°C)	(°C)	(°C)
0 m	No data	No data	No data	No data	No data	–
50 m	43.8	No data	No data	No data	43.8	–
100 m	49.2	44.3	43.8	44.0	46.6	–
150 m	54.4	45.6	52.1	54.3	52.4	–
200 m	57.3	57.6	56.3	57.0	56.9	–
250 m	60.1	62.4	60.2	61.5	61.0	–
300 m	65.4	67.9	64.8	66.4	66.9	–
350 m	71.3	72.5	71.1	72.7	74.7	–
400 m	77.1	78.3	77.7	79.8	81.8	–
450 m	81.3	83.5	83.7	86.9	87.5	–
500 m	86.9	89.1	90.8	93.3	94.8	–
550 m	90.4	94.5	96.5	99.8	99.9	–
600 m	94.9	99.6	102.3	106.3	108.3	–
650 m	99.7	107.9	111.4	113.1	117.8	72.2
700 m	105.1	117.7	117.2	120.6	124.4	93.5
750 m	109.5	116.6	121.7	126.4	129.3	104.8
800 m	112.6	121.4	127.7	131.7	136.6	109.1
850 m	117.3	125.3	131.8	136.5	141.0	110.7
900 m	120.7	130.7	138.5	143.2	146.3	117.7
950 m	123.7	135.2	142.2	147.3	151.0	122.1
1,000 m	127.9	139.5	147.1	152.1	155.8	132.9
1,050 m	132.9	145.7	152.2	157.4	162.4	142.5
1,100 m	138.6	151.5	159.2	163.2	167.2	155.8
1,150 m	146.1	158.9	165.5	169.3	171.5	166.8
Remark						

Table II–4–2 Analized Reservoir Temperature

Measures / Depth (m)	I	II	III	IV
100	44	39	40	45
200	52	53	53	57
300	60	67	64	70
400		70	90	90
500		100	106	105
600		122	127	121
700			139	140
800			161	155
900				165
1000				170
1100				176
1150				179

* I	Depth of Drilling		463.0 m
II	"		653.0 m
III	"		814.5 m
IV	"		1,157.0 m

Fig. II-4-1 LOGGED TEMPERATURE OF WELL NO. 6

Dec 1980

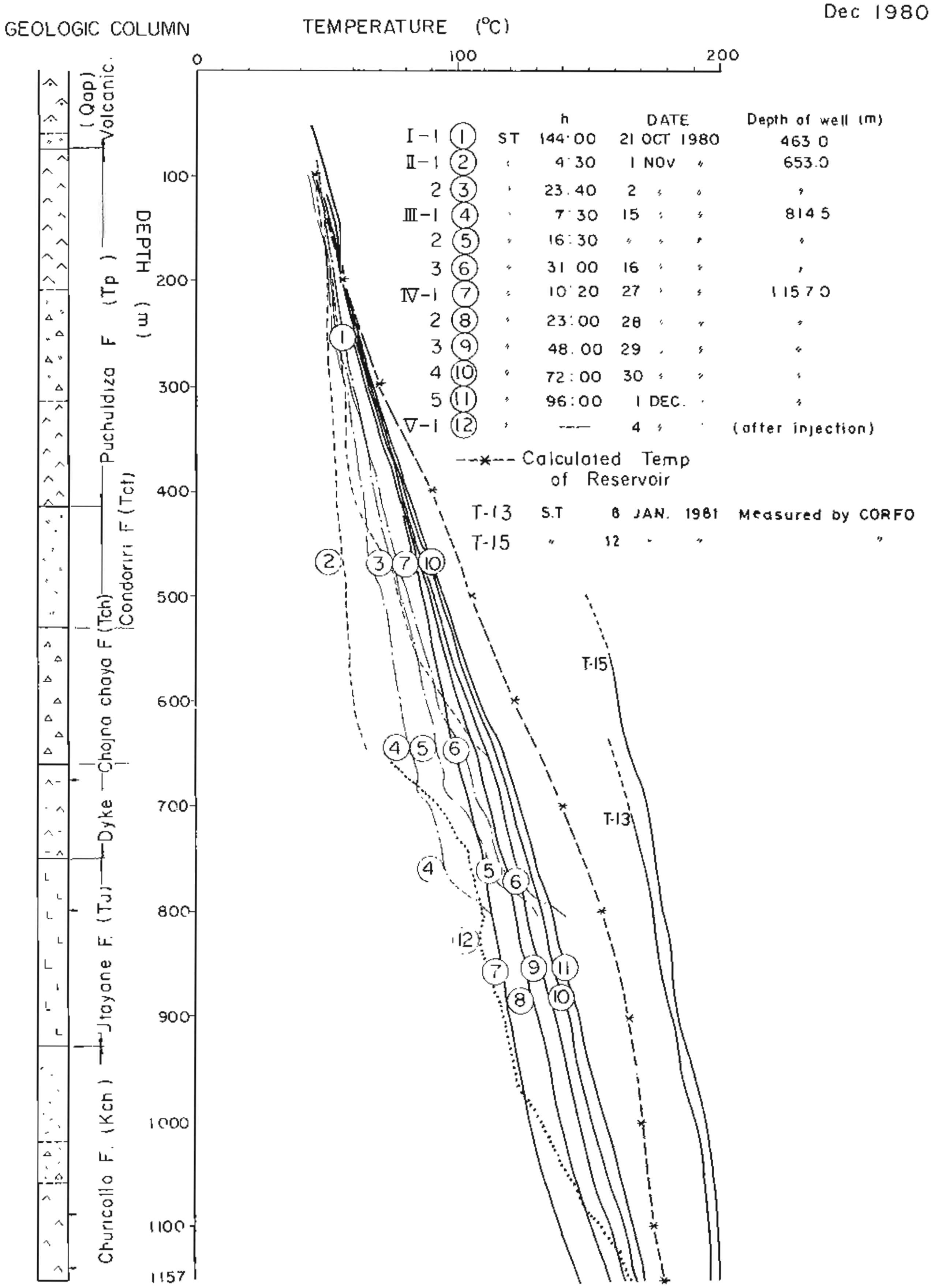

Fig. II-4-2 CALCULATED RESERVOIR TEMPERATURE

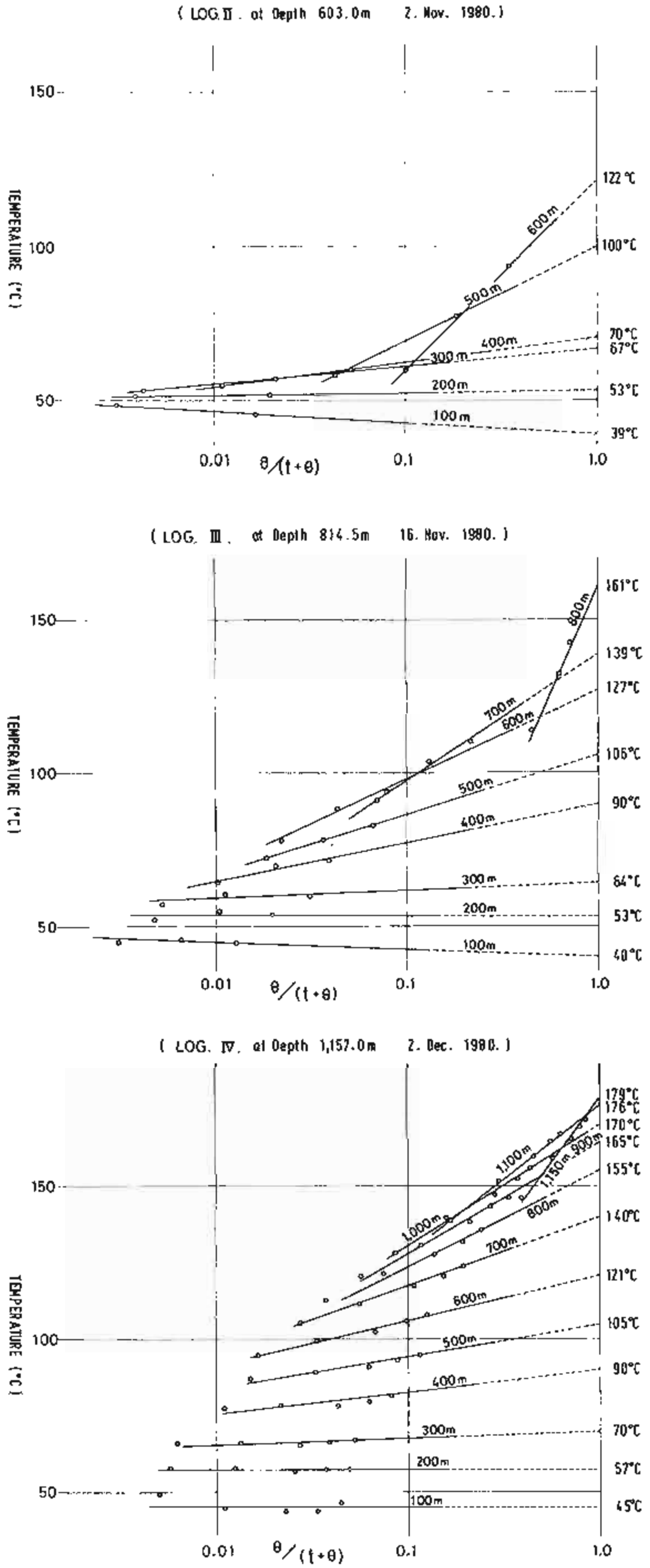

The measured conditions and the results are shown in Tables II–4–1 and Figure II–4–1.⑦ ~ ⑪

Theoretical reservoir temperature of each depth were calculated from those data by using equations.

The basic data and the calculated reservoir temperature for each depth are shown in Table II–4–2 and Fig. II–4–2 respectively.

The reservoir temperatures produced by this calculation are about 130°C at 650 m after installation of production casing and about 180°C bottom hole temperature at 1,150 m depth.

The temperature suggests the flushing of the geothermal fluid with sufficient fracture or permeable zone under enough pressure difference.

Measured thermal gradient shows almost linear from the surface to the bottom of the well indicating no mud loss during drilling. The thermal gradient shallower than 800 m is about 1.5°C/10 m and deeper than 800 m is about 0.7°C/10 m, which is slightly less than the shallower zone as in normal case.

Thermal logging results conducted after transmissibility test are shown in Fig. II–4–1,⑫. The thermal curve shows comparatively low temperature between depths of 800 and 850 m. It is due to the cold water admixture into the zone as logging was conducted after only 5 hours of pumping cold water under high pressure.

Same low temperature changes although not as marked as the abovementioned zone are seen around 730 m and 950 m depths indicating also the admixture of cold water into the zone.

After the survey team returned to Japan, however, CORFO repeatedly conducted temperature logging using their own apparatus, as shown in Fig. II–4–1 (T–13, T–15.). Result of measurement showed that the bottom temperature of the well confirmed to be 201°C after one month drill work ceased.

The temperature gradient between 550 m depth and bottom hole was also calculated to be 0.9°C/10 m.

4–3 Transmissibility Test

During drilling, mud circulation loss which suggest the conduit of geothermal fluid into the well was not observed. There is a possibility, however, that mud water must have clogged the fine cracks and fissures located near the well. Expecting the fracture effect, cold water was pumped into the well under high pressure condition. The pump used for the test was NSCO, IDEAL, C-250.

The transmissibility test was carried out twice, on December 1st and December 4th. TAble II–4–3 and Fig. II–4–3, 4 show the result of the test. The maximum load pressure at well head was 22.6 kg/cm^2. The apparent injection index was determined to average 4.1 m^3/h/kg/cm^2, ranging from maximum of 5.7 to minimum of 2.1. From the Drawdown curve, the permeability of the fissure was calculated.

Table II–4–3 Wellhead Pressure and Injection Rate

No.	Date	Time		* Wellhead pressure	Injection volume	** Injection Rate
V–1 P–1	1/Dec	16:10 – 16:40		18.0 Kg/cm^2	19.25 m^3	38.5 m^3/h
V–1 P–2		16:40 – 17:10		22.5	44.95	89.9
V–1 P–3		17:10 – 17:25		7.5	4.50	18.0
		17:25 – 17:40	*** D.D. No. 1			
V–2 P–4		17:40 – 18:05		18.0	48.71	83.5
V–2 P–5		18:05 – 18:25		7.5	5.57	16.7
V–2 P–6		18:25 – 18:45		22.6	29.97	89.9
		18:45 – 19:40	*** D.D. No. 2			
V–3 P–7	4/Dec	10:50 – 11:40		14.3	67.75	81.3
		11:40 – 14:00	*** D.D. No. 3			

* Wellhead pressure is measured by pressure gauge

** Injection rate is measured by stroke number of the Pump

*** D.D. is Drow Down Curve measurement

Fig. II-4-3 INJECTION RATE OF WELL NO. 6

Dec. 1980

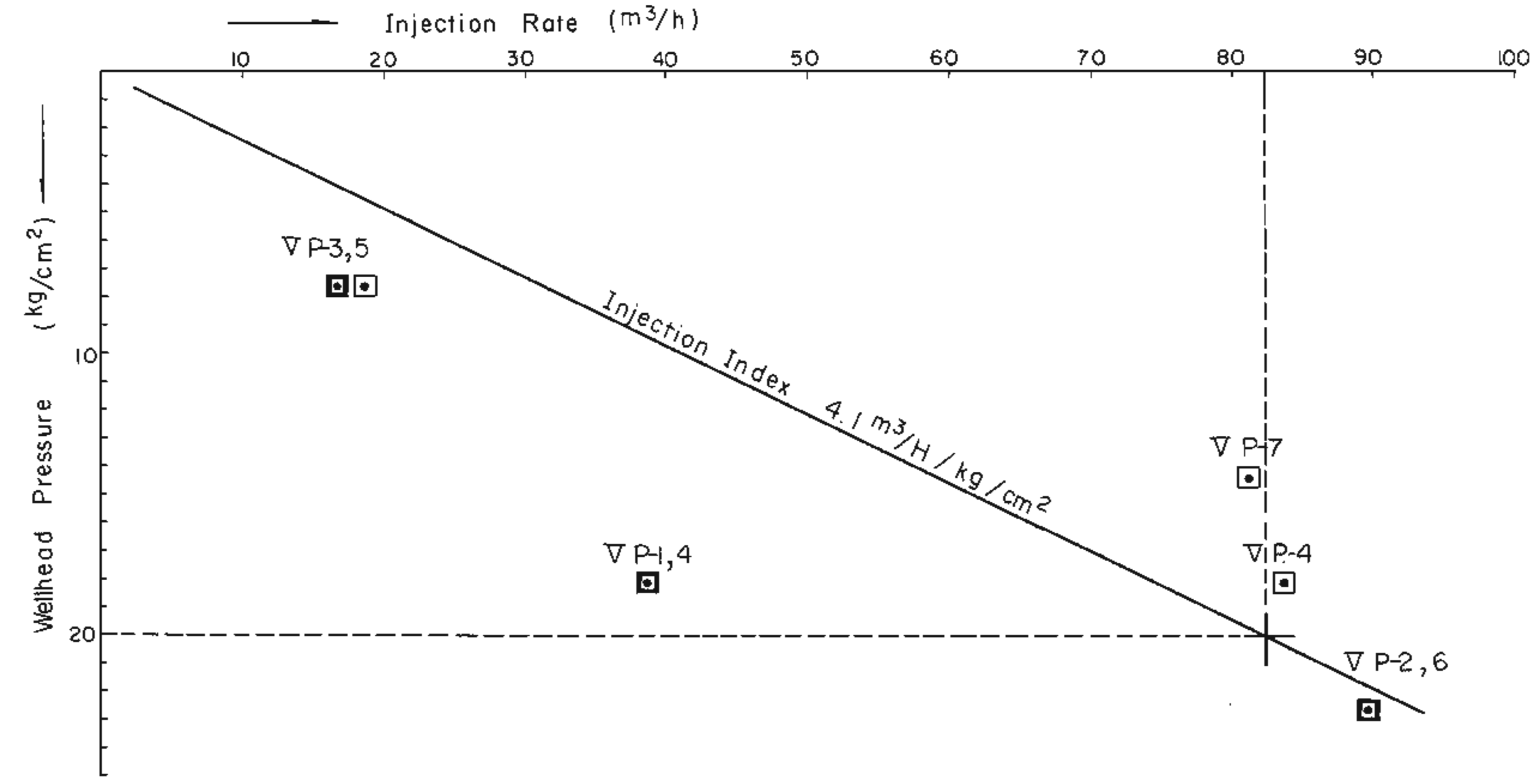

Fig. II-4-4 DROW DOWN CURVE

(V－DD NO 1,2) Dec 1980

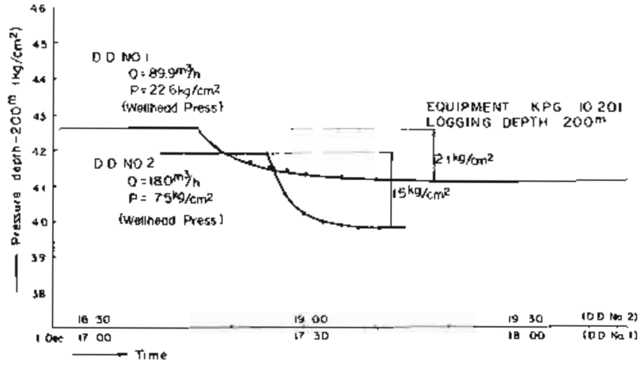

DROW DOWN CURVE

Dec 1980

V－DD NO 3

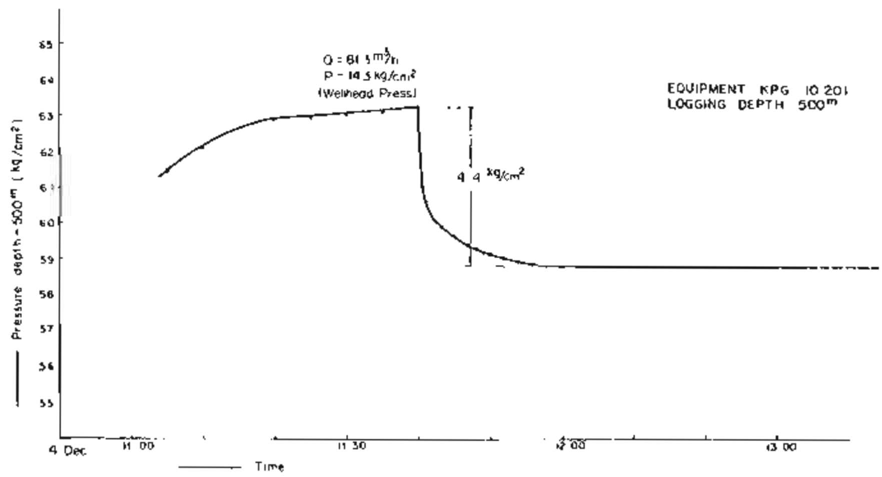

DROW DOWN CURVE

Dec 1980

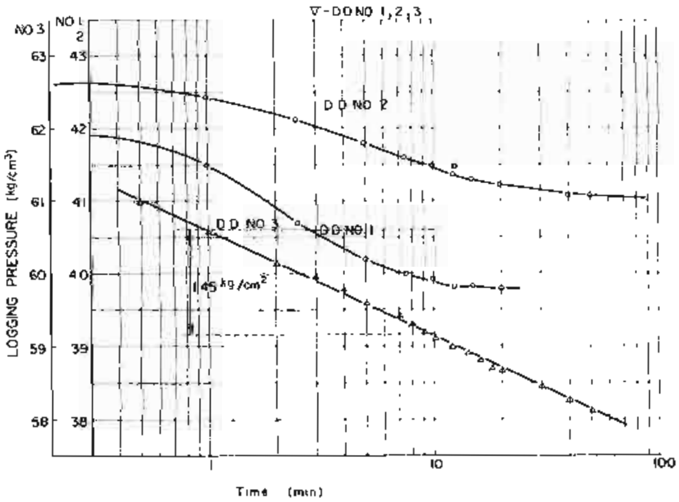

Fig. II-4-5 ISO-TEMPERATURE CURVE

N-S (SECTION 504E)

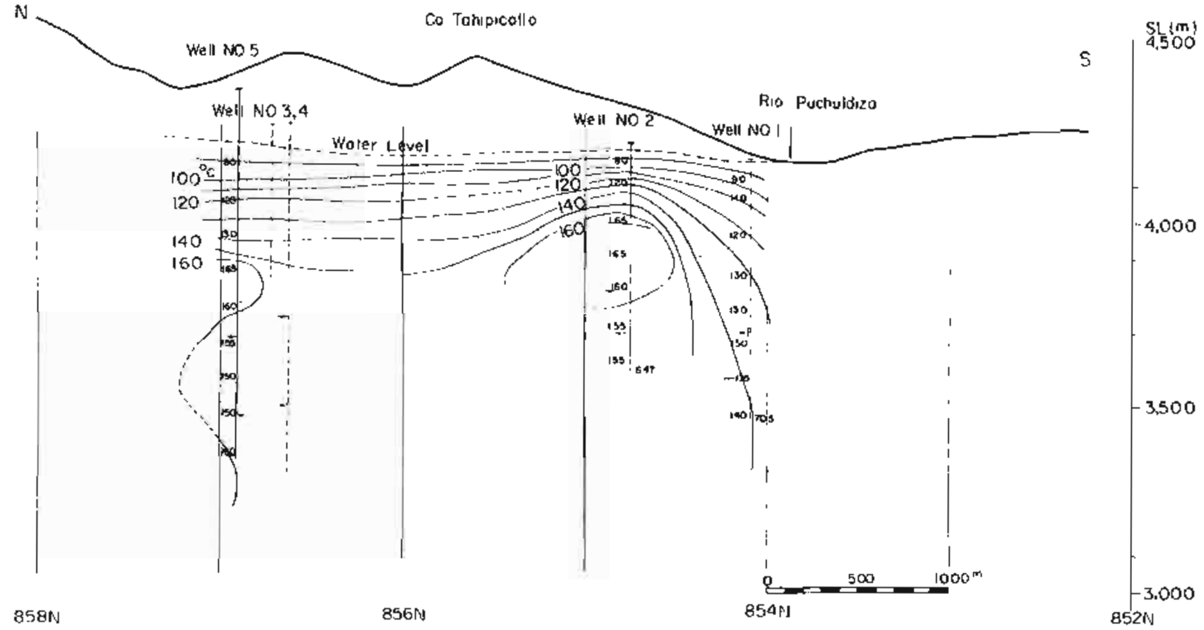

W-E (SECTION 857 N)

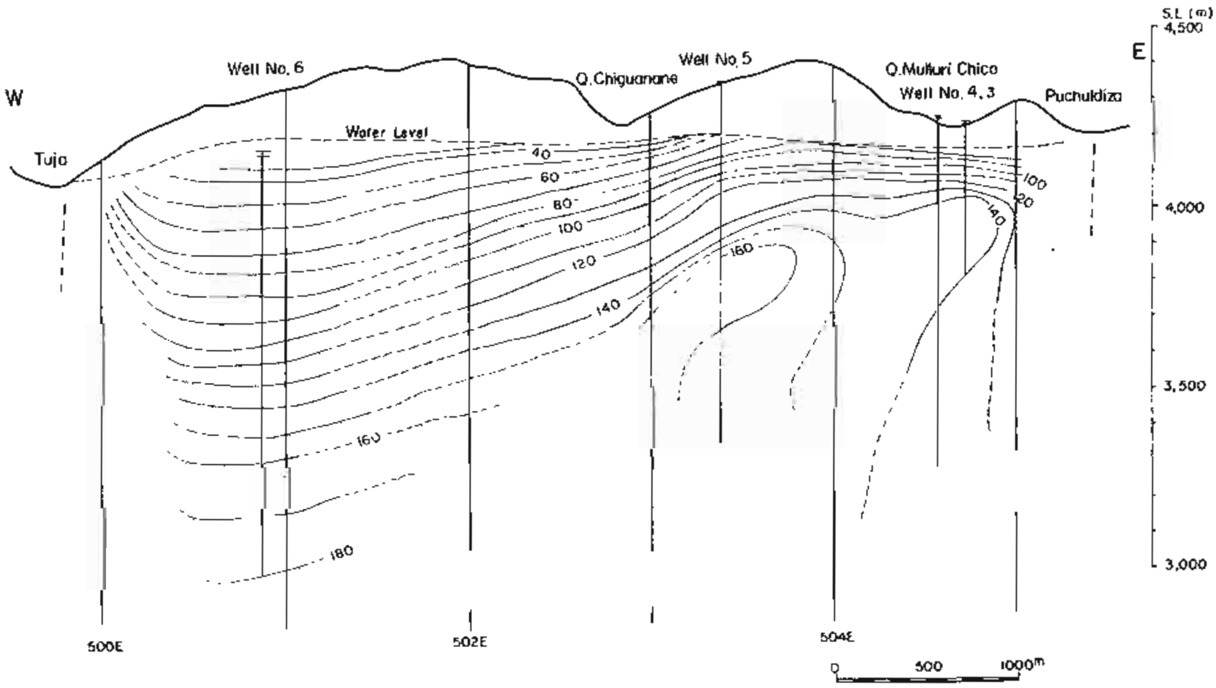

Test	Transmissibility m^2/h
I	1.46
II	1.00
III	1.03

The water table of the aquifer stabilized 20 minutes after the termination of water pumping into the well. No pressure change was observed by pressure gauge even after 2 hours.

The water level therefore of the aquifer is considered to be over about 100 m higher than the height of the well head as shown below:

Test	Depth of the Pressure gauge	Theoretical Pressure	Stable Pressure after compression	Estimated water level (above the well head)
I	−200 m	20 kg/cm^2	39.8 kg/cm^2	198 m
II	−200 m	20 kg/cm^2	41.1 kg/cm^2	211 m
III	−494	47.1 kg/cm^2	58.8 kg/cm^2	117 m

Although the injection index of the crack is quite good and water level of the aquifer is higher than the well head, there was no mud circulation loss and no flow of geothermal fluid from the well. The reasons for this phenomena are:

Mud water healed the cracks of the reservoir. Specific gravity of mud water used for the drilling was 1.06 to 1.09. Pressure of mud water pillar pressure is balanced with reservoir pressure.

Assumed water level at the site of Well No. 6 is the same or little bit higher than that of Well No. 1 to No. 5 as confirmed previously. This indicates that the geothermal fluid near Well No.6 is under the geopressured condition. Accordingly, geothermal fluid automatically flowed out from the well as stated in Chapter 2–3.

After survey team returned to Japan, the injection test was also carried out by CARFO. According to their information on the transmissibility test, pumping water was initially swallowed into the formation through the fissures, with same figure as stated. However, injection rate decreased with time.

When the main valve was opened, geothermal fluid flowed out instantaneously from the wellhead. Flushing of geothermal fluid was no longer continuous after injected water flowed out.

From the fact, it was confirmed that the fissures created by stimulation test was not permeable.

4–4 Physical Characteristics

Density, porosity and resistivity of core samples from well No. 6 have been measured, as shown in Table II–4–4.

Range of the density is 1.96 to 2.59, and generally the density of tuff breccia is lower that of lava and dyke. The porosity take a range 2.29% to 30.12%. The resistivity of andesite and andesitic welded tuff is about 1×10^3 Ωm, and that of dacitic welded tuff, tuff and tuff breccia is about 1×10^2 Ω-m.

Rock samples were collected in 1978 and 1980 each and Resistivity, density and porosity of the rock samples are as follows.

PHYSICAL PROPERTIES

Rock Type	Resistivity (Ω – m)	Density (g/cm^3)	Porosity (%)
Andesite (Quaternary)	$(1.2 \pm 0.2) \times 10^3$	2.50±0.10	6.56±1.5
Andesite (Tertiary)	$(3.2 \pm 0.8) \times 10^3$	2.54±0.1	6.46±2.0
Andesitic Welded Tuff (Quaternary)	$(0.4 \pm 0.2) \times 10^3$	2.40±0.1	6.70±1.0
Dacitic Ignimbrite (Tertiary)	$(1.5 \pm 0.8) \times 10^2$	2.25±0.15	16.1 ±2.5
Dacitic Tuff (Quaternary)	$(0.8 \pm 0.3) \times 10^2$	2.12±0.1	24.4 ±5.0
Andesitic Tuff (Cretaceous)	$(1.3 \pm 0.5) \times 10^2$	2.39±0.05	14.2 ±3.0

Compiled data of geologic column, geophysical characteristics of core samples and geo-electrical column of Line A and D shows as follows:

(1) Upper electrical layer corresponds to the Quaternary andesite lava.

(2) Middle electrical layer corresponds to the Tertiary pyroclastic formation, containing geothermal fluid with high temperature and salinity.

(3) Lower electrical layer corresponds to the andesite lava of Churicollo formation.
Electrical survey analysis, above mentioned before, is supported by this result.

Table II–4–4 Resistivity of Rock Sample of Well No. 6

Geologic Column & Formation	Sample No	depth (m)	Resistivity (Ω·m)/20°C	Density (g/cm³)	Porosity (%)
Q (Qap): Hornblende Andesite lava its Pyroclastics (0–~110 m)					
Puchuldiza Formation (Tpl): Pyroxene Andesite Lava intercalated with its Pyroclastics	1	152			
	2	166			
	3	190	1,360	2.59	2.29
	4	220			
	5	245	26.5		
	6	280	685		
	7	317			
	8	350	160		
	9	370			
	10	403	182.5		
Condoriri F. (Tct): Dacitic Pumiceous Tuff to lapilli tuff	11	430			
	12	460	29.5	1.96	30.12
	13	490			
	14	520	32		
Chojña chaya F. (Tch): Tuff breccia	15	551	154		
	16	582	32		
	17	612	40		
	18	642			
Dyke: Basic Andesite	19	672	540		
	20	703	570	2.53	6.65
	21	734	565		
Utayane F. (Tu): Dacitic Ignimbrite	22	764	124		
	23	783	33.5		
	24	813	44.5	2.39	16.81
	25	844	71.5		
	26	875	79		
	27	905	26.5		
	28	936	97.5		
Churicollo F (kch): Pyroxene Andesite Lava and its Pyroclastics	29	966	60	2.43	16.14
	30	996			
	31	1,041	73		
	32	1,075	82		
	33	1,125	43.5		
	34	1,155	65.5		

Depth (m): 0 – 1,157

Resistivity Column (Ω·m)

Line A No.70: 80 m, 100 m (300, 2500); 40 to 1,075 m; 20 below 1,075 m

Line D No.90: 40 m (2700); 115 to 170 m; 48 below 170 m

CHAPTER 5 SUMMARY

Chapter 5. Summary

The summary of the investigation on Well No. 6 is as follows:

1. The age of geologic formation of the geothermal reservoir in the area is Tertiary and Cretaceous.
2. The well was drilled down to 1,157 m deep.
   The bottom temperature of the well is 180°C, however, temperature gradient of the hole is still increasing at 1,157 m.
3. Water level of the aquifer around the drill site is about 100 m higher than the elevation of the wellhead.
4. Production casing was set down to 650 m deep. The temperature at 650 m depth was 130°C but this was not high enough for the installation of casing pipes.
5. During the drilling work, no mud circulation loss was observed, however, cracks or fissures were created by pumping high pressure water at 825 m depth.
6. Injection index of the fissure created by the pump test was 4 $m^3/h/kg/cm^2$.
7. Geothermal fluid flowed out instantaneously from the wellhead when the main valve was opened. Quantity of steam and water was visually measured to be 5 tons and 40 m^3 per hour respectively.
   PH value of the hot effluent was neutral.
8. Gushing of geothermal fluid, however, was no longer continuous but intermittent after one hour flushing because of insufficiency of geothermal fluid.
9. In order to accelerate flushing, air lift test was conducted but unfortunately, no thermal fluid flowed out. The water level of the well did not recover fast enough to the previous level one day after the test.
10. Presumably fine cracks and fissures, the sources of geothermal fluid, were clogged by solidified mud or some other reason after subjected under high temperature condition.
11. Compared with the wells No. 1 to No. 5, the temperature of Well No. 6 has the highest bottom hole temperature. The temperature gradient profiles of Well No. 1 to No. 5 all showed reverse curves near the bottom of the wells. In contrast, Well No. 6 did not have a temperature reversal and therefore, the well seems to be a good one. The well should be drilled deeper for further investigation.
12. According to the information from CORFO, temperature logging and stimulation test were conducted after survey team left for Japan. They confirmed that bottom hole temperature rose over 200°C, with good temperature gradient and production zone was actually impermiable.

Considering the above, the high temperature reservoir in the area for the power generation would be sited deeper than 1000 m depth. The production zone in Well No. 6 seemed to be about 800 m deep and its temperature was measured to be 160°C. The ratio of steam and water was 1 : 8. The high temperature zone over 200°C would be around 1500 m deep or over on the basis of the thermal gradient profile of Well No. 6. And in order to prevent cold water seepage from the shallower depths, more production casing must be programmed.

The siting of drill-hole with a view of getting permeable zones is perhaps the most difficult problem posed for the geothermal scientists as failures can indeed be very costly. Even less than 2 mm cracks or fissures can give generous flows of effluent for production wells and hence great care must be taken when drilling in order to avoid the loss of rock permeability.

REFERENCES

References

((Unpublished report of Comite Geotermico-CORFO))

Healy, J., 1968, Geological Reconnaissance of Hot Spring Localities in Tarapaca and Antofagasta Province.

Healy, J., 1969, Geological Reconnaissance of Hot Spring Localities in Tarapaca and Antofagasta Province. (Second Interim Report)

A. Lahsen, 1969, Exploracion Geotermica en la Provincias de Tarapaca de Puchuldiza.

P. Trujillo, 1970, Manifestaciones Termales de Puchuldiza.

A. Lahsen, 1970, Informe Preliminar Sobre la Geologia de Puchuldiza.

A. Lahsen, 1973, Geologia de Puchuldiza.

A. Lahsen, 1975, Evaluacion del Sistema Geotermico de Puchuldiza.

P. Trujillo, 1977, The Puchuldiza Geothermal Field.

A. Lahsen, 1978, Evaluacion de los Resultados de la Exploracion del Campo Geotermico de Puchuldiza, Region Tarapaca.

((Published Report))

Cristi, J., Hand Book of South American Geology p. 189–214.

Vicente, C., 1970, Liminary and Geosynclinal Andes Major Orogenic Phases and Synchronical Evolutions of the Central Andes, Buenos Aires Solid Earth Problem Conference, p. 451–470.

Bhattachaya, P.K. and H.P. Patra, 1968, Direct Current Geoelectric Sounding, Method in Geochemistry and Geophysics 9, Elsevier.

Onodera, S., 1975, An Evaluation of Geothermal Potential by Resistivity Sounding Curves, Second United Nations Symposium, p. 1167–1174.

Ward, S.H. el al, 1978, A summary of the Geology, Geochemistry, and Geophysics of the Roosevelt Hot Springs Thermal Area, Utah, Geophysics, v. 43, no. 7, p. 1515--1542.

Onodera, S., 1971, Geophysical Exploration for Geothermal Field, Kyushu University.

Tomasson, J. and Kristmannsdottir, 1972, High temperature alteration minerals and thermal brines Reyhijanes, Iceland. Contr. Mineral and Petrol., 36, p. 123–134.

Kinbara, K. and Okubo, T., 1978, Hydrothermal attend rock found in an exploration borehole (No. SA-1), Satsunan geothermal area, Japan, J. Japan. Assoc. Min. Petr. Econ. Geol. 73, p. 125–136.

Brown, P.R.L. and A.J. Ellis (1970): The Ohaki-Broadlands hydrothermal area, New Zealand, A. Jous. Sci., 29, p. 97–131.

Ellis A.J. and W.A. Mason (1977): Chemistry and Geothermal system. Academic Press, N.Y.

Kinbara, K. (1977): Some Cristalites and Tridymites in Geothermal Area (in Japanese) Jour. Japan. Geothermal Energy Asso. 14, p. 13–20.

Kristmansdttir, H. (1975): Hydrothermal alteration of basaltic rocks in Icelandic geothermal areas, Proc. 2nd. U.N. Geothermal Symp. 1, p. 441–445.
Kubota, Y. (1979): Hydrothermal rock alteration in the northern HACHIMANTAI Geothermal field. Jour. Japan. Geother. Ener. Asoc., 16, p. 15–31 (in Japanese)
Lochenbruch, A.H and Brewer, M.C. (1959): Dissipation of the temperature effect of drilling a well in Ardic Alaska.
Geological Survey Bulltein p. 1083

VES CURVES

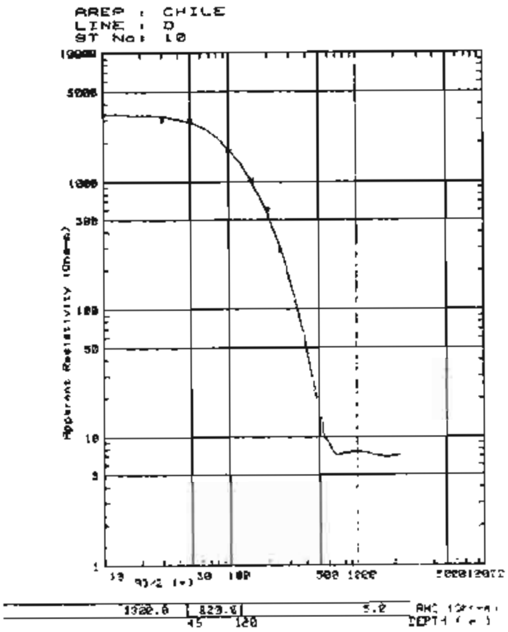
AREA : CHILE
LINE : D
ST No: 10
Apparent Resistivity (Ohm-m)
AB/2 (m)
1320.0
829.0
5.2
RHO (Ohm-m)
45
120
DEPTH (m)

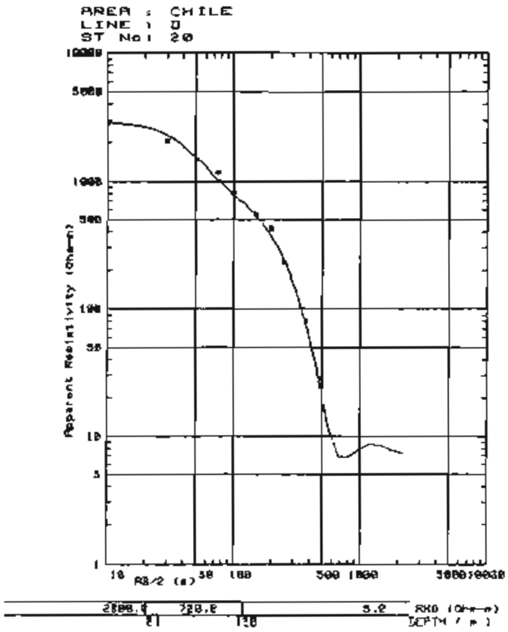
AREA : CHILE
LINE : D
ST No: 20
Apparent Resistivity (Ohm-m)
AB/2 (m)
2800.0
720.0
5.2
RHO (Ohm-m)
81
130
DEPTH (m)

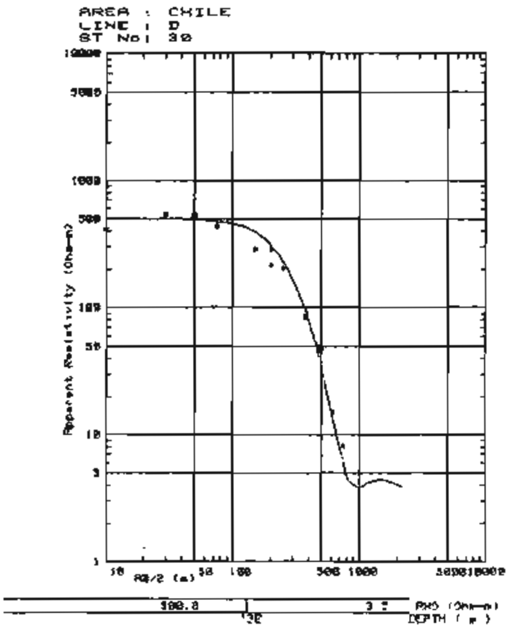
AREA : CHILE
LINE : D
ST No: 30
Apparent Resistivity (Ohm-m)
AB/2 (m)
500.0
RHO (Ohm-m)
130
DEPTH (m)

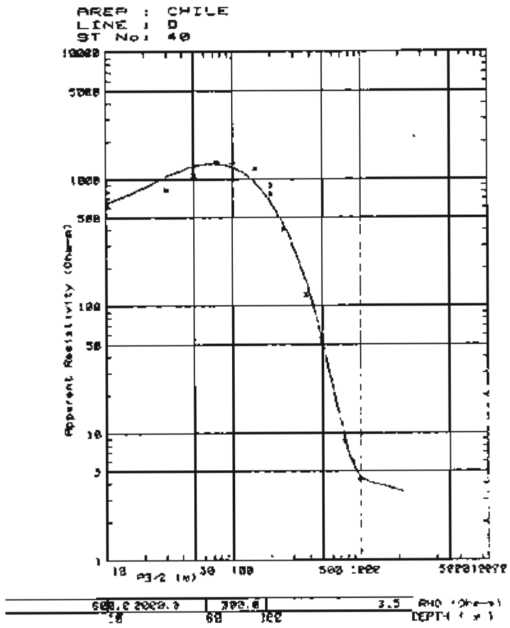
AREA : CHILE
LINE : D
ST No: 40
Apparent Resistivity (Ohm-m)
AB/2 (m)
600.0
2000.0
300.0
3.5
RHO (Ohm-m)
60
DEPTH (m)

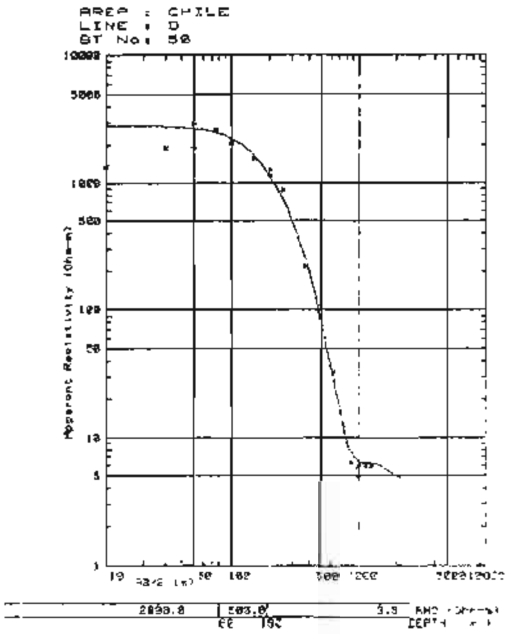
AREA : CHILE
LINE : D
ST No: 50
Apparent Resistivity (Ohm-m)
AB/2 (m)
2000.0
500.0
3.5
RHO (Ohm-m)
DEPTH (m)

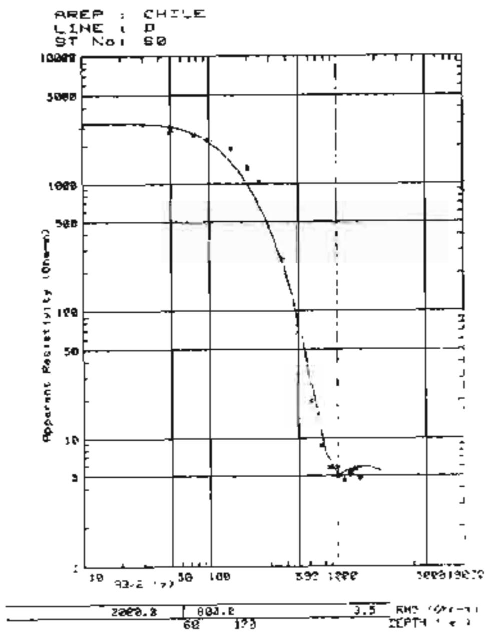
AREA : CHILE
LINE : D
ST No: 60
Apparent Resistivity (Ohm-m)
AB/2 (m)
2000.0
800.0
3.5
RHO (Ohm-m)
DEPTH (m)

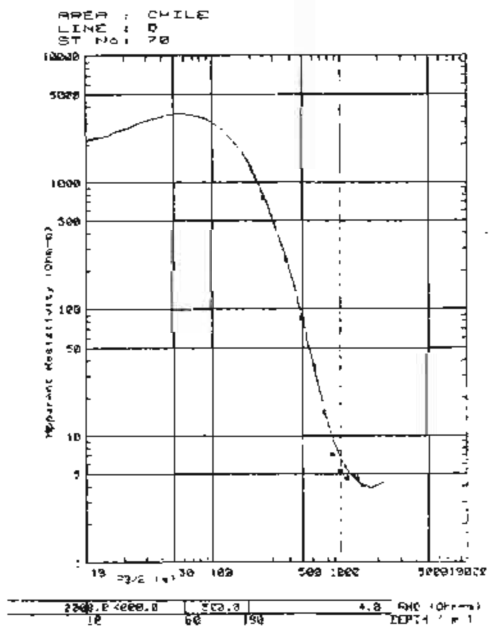
AREA : CHILE
LINE : D
ST No: 70
Apparent Resistivity (Ohm-m)
AB/2 (m)
2200.0
4000.0
500.0
4.0
RHO (Ohm-m)
DEPTH (m)

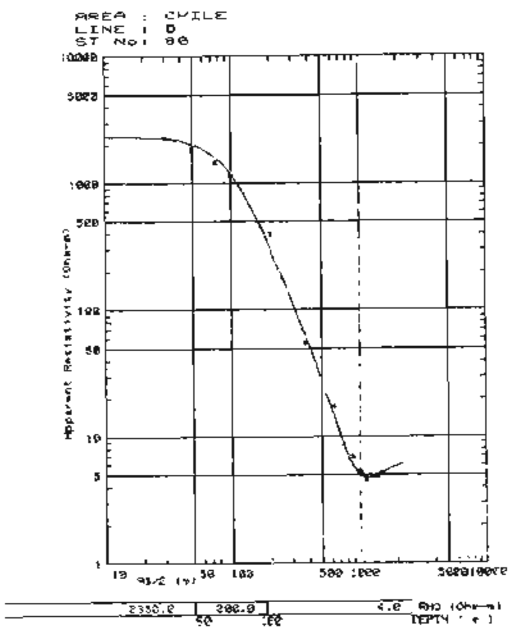
AREA : CHILE
LINE : D
ST No: 80
Apparent Resistivity (Ohm-m)
AB/2 (m)
2330.0
200.0
4.0
RHO (Ohm-m)
DEPTH (m)

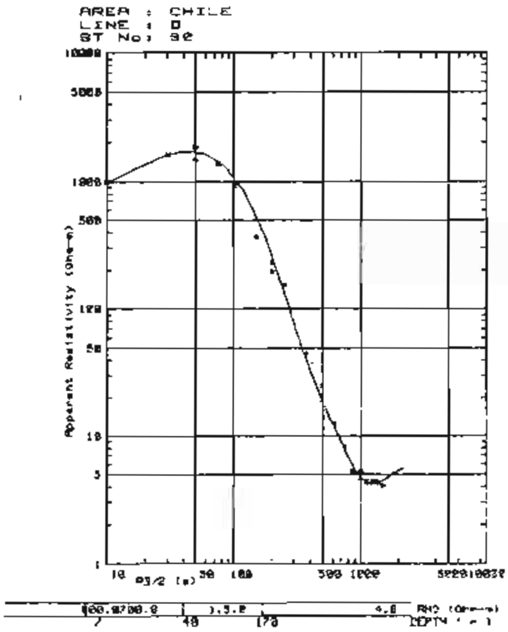
AREA : CHILE
LINE : D
ST No: 90
Apparent Resistivity (Ohm-m)
AB/2 (m)
RHO (Ohm-m)
DEPTH (m)

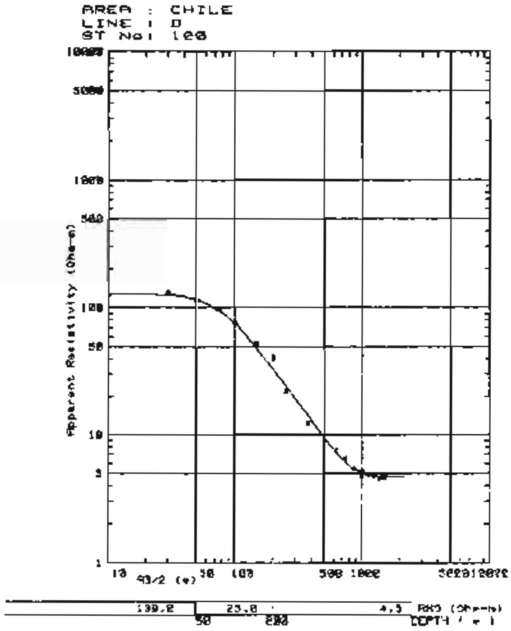
AREA : CHILE
LINE : D
ST No: 100
Apparent Resistivity (Ohm-m)
AB/2 (m)
RHO (Ohm-m)
DEPTH (m)

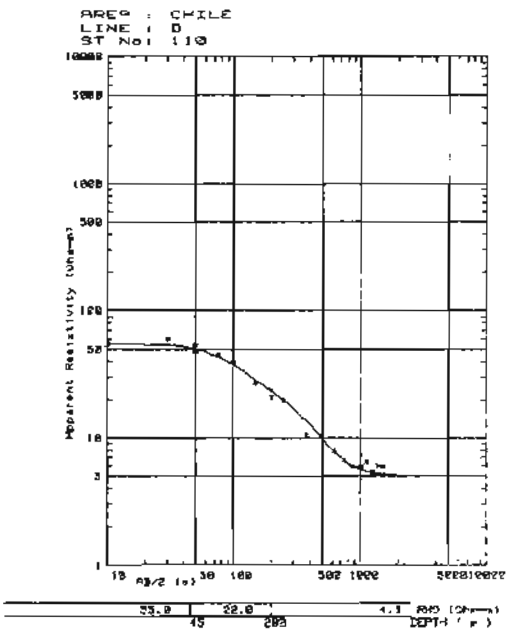
AREA : CHILE
LINE : D
ST No: 110
Apparent Resistivity (Ohm-m)
AB/2 (m)
RHO (Ohm-m)
DEPTH (m)

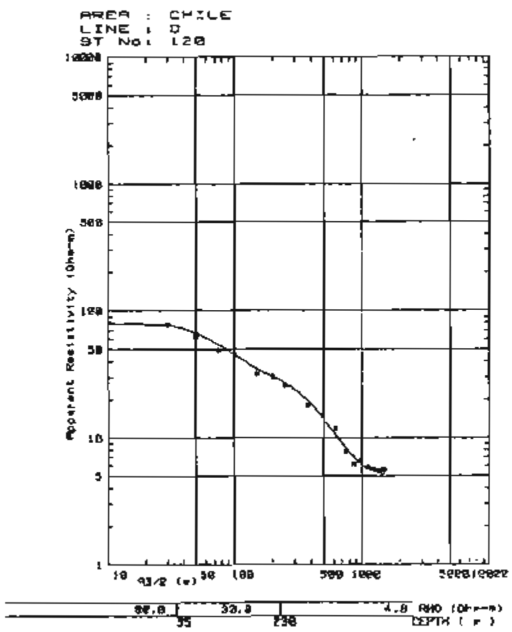
AREA : CHILE
LINE : D
ST No: 120
Apparent Resistivity (Ohm-m)
AB/2 (m)
RHO (Ohm-m)
DEPTH (m)

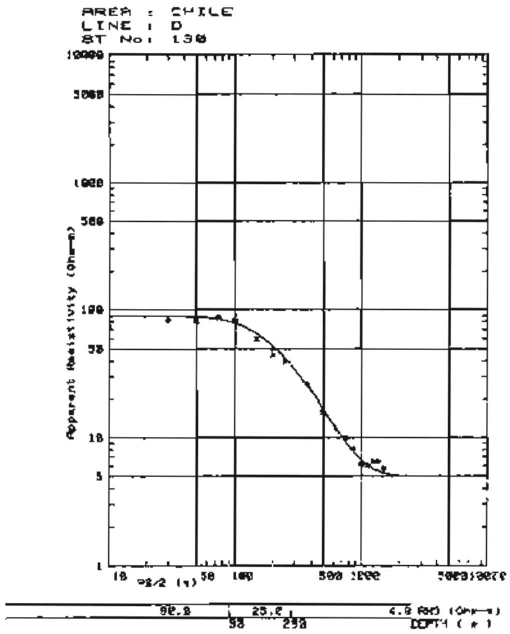
AREA : CHILE
LINE : D
ST No: 130
Apparent Resistivity (Ohm-m)
AB/2 (m)
90.0
25.2
4.9 RHO (Ohm-m)
50
250
DEPTH (m)

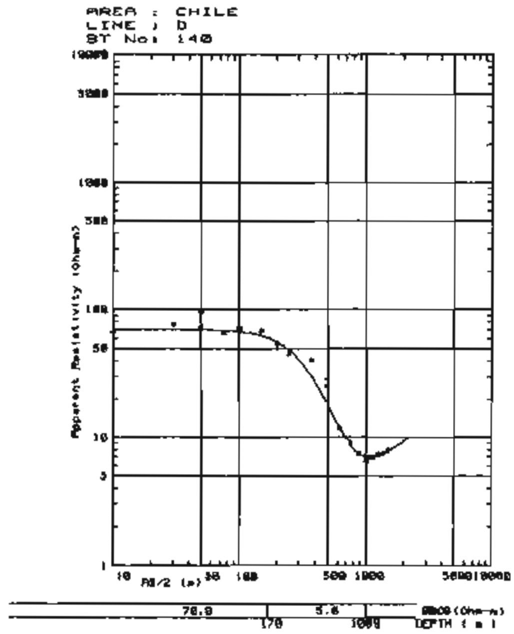
AREA : CHILE
LINE : D
ST No: 140
Apparent Resistivity (Ohm-m)
AB/2 (m)
70.0
5.6
RHO (Ohm-m)
170
1000
DEPTH (m)

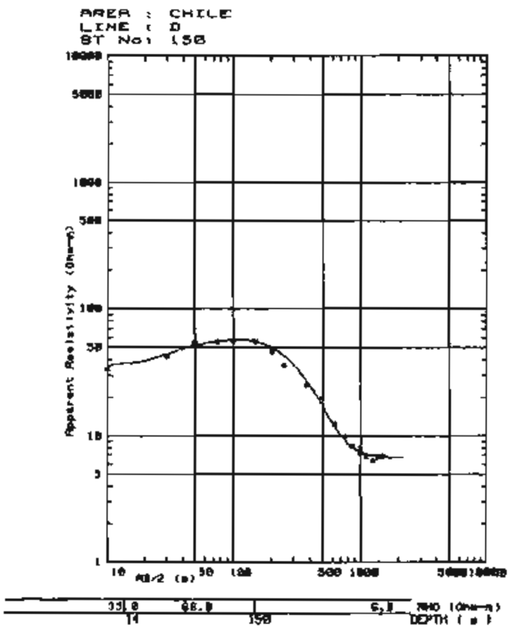
AREA : CHILE
LINE : D
ST No: 150
Apparent Resistivity (Ohm-m)
AB/2 (m)
RHO (Ohm-m)
14
150
DEPTH (m)

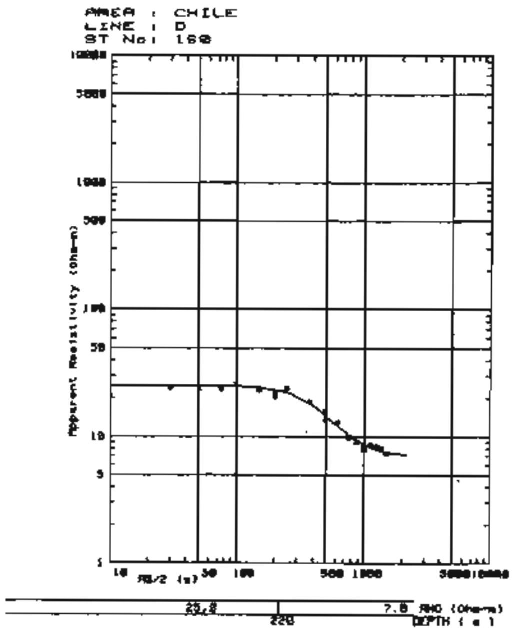
AREA : CHILE
LINE : D
ST No: 160
Apparent Resistivity (Ohm-m)
AB/2 (m)
7.8 RHO (Ohm-m)
220
DEPTH (m)

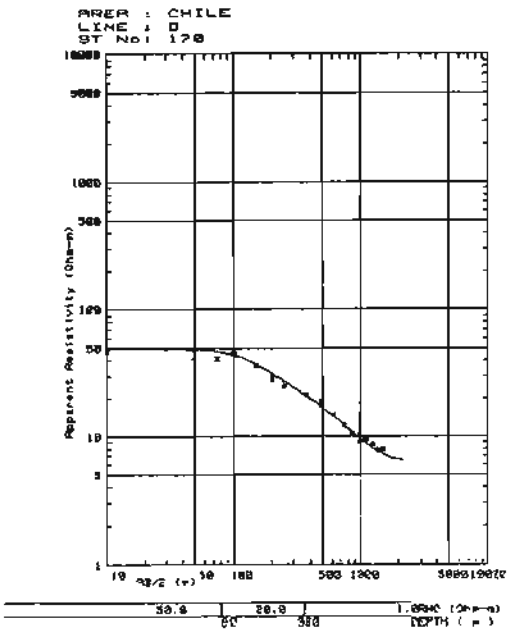
AREA : CHILE
LINE : D
ST No: 170
Apparent Resistivity (Ohm-m)
AB/2 (m)
50.0
20.0
1.0 RHO (Ohm-m)
60
300
DEPTH (m)

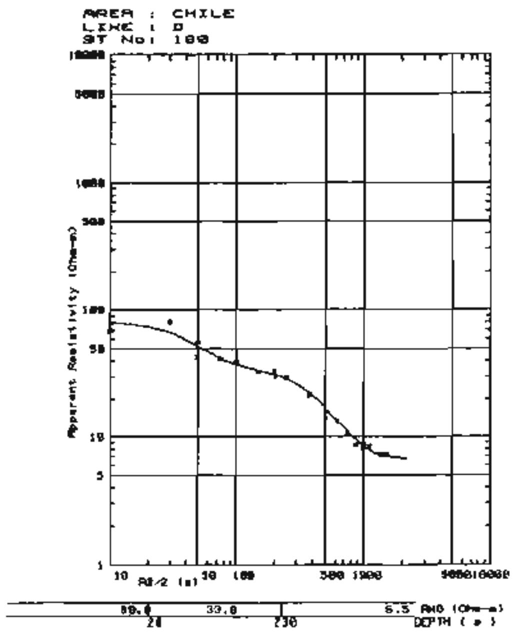
AREA : CHILE
LINE : D
ST No: 180
Apparent Resistivity (Ohm-m)
AB/2 (m)
80.0
33.0
6.5 RHO (Ohm-m)
20
230
DEPTH (m)

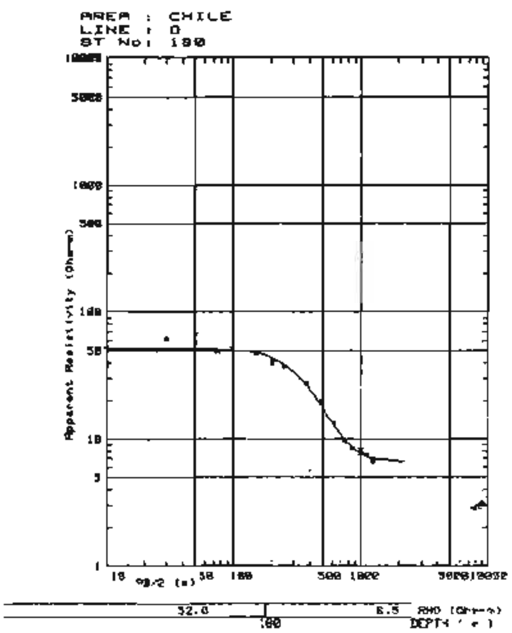
AREA : CHILE
LINE : D
ST No: 190
Apparent Resistivity (Ohm-m)
AB/2 (m)
52.0
6.5 RHO (Ohm-m)
100
DEPTH (m)

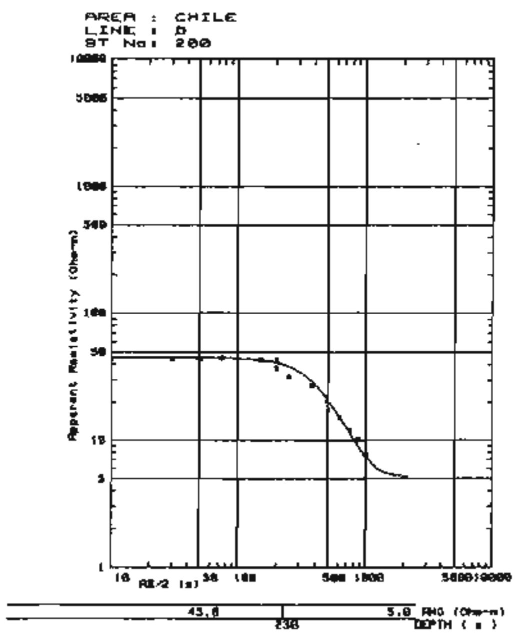
AREA : CHILE
LINE : D
ST No: 200
Apparent Resistivity (Ohm-m)
AB/2 (m)
43.0
5.0 RHO (Ohm-m)
230
DEPTH (m)

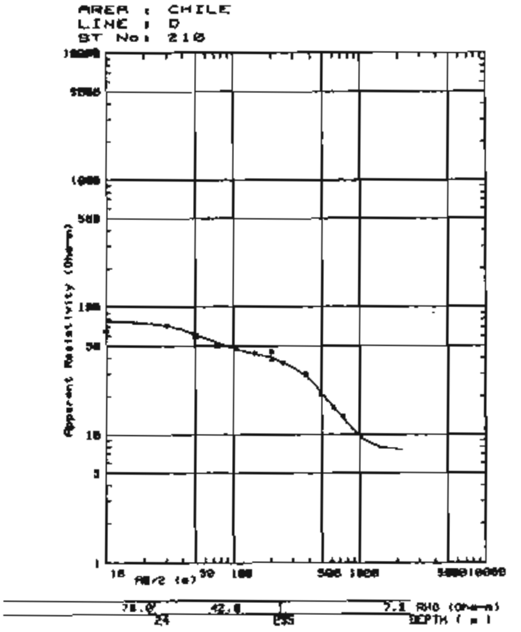
AREA : CHILE
LINE : D
ST No: 210
Apparent Resistivity (Ohm-m)
AB/2 (m)
RHO (Ohm-m)
DEPTH (m)

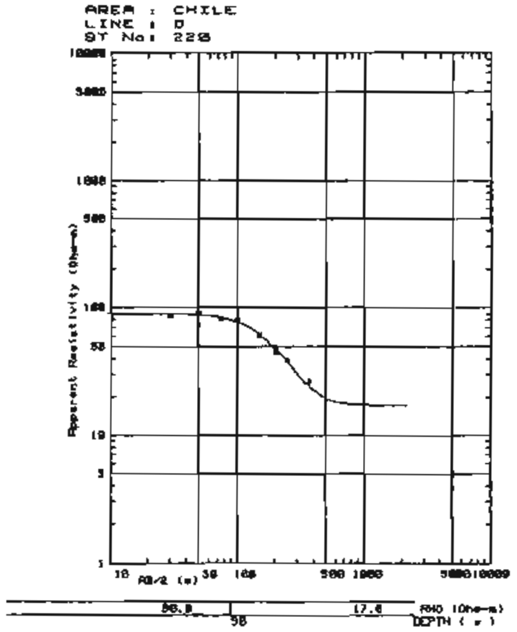
AREA : CHILE
LINE : D
ST No: 220
Apparent Resistivity (Ohm-m)
AB/2 (m)
RHO (Ohm-m)
DEPTH (m)

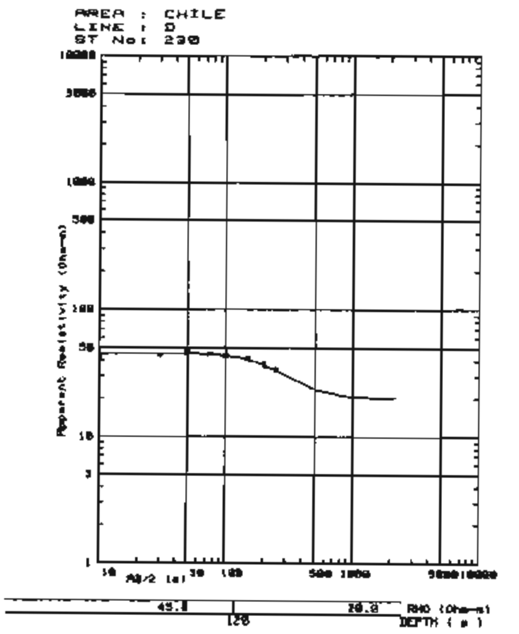
AREA : CHILE
LINE : D
ST No: 230
Apparent Resistivity (Ohm-m)
AB/2 (m)
RHO (Ohm-m)
DEPTH (m)

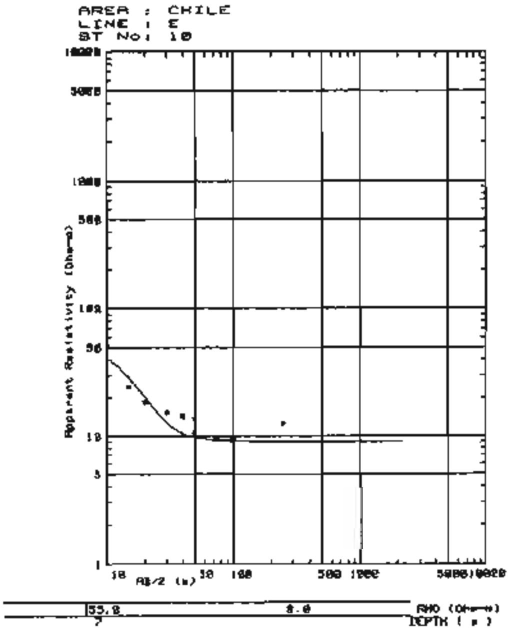
AREA : CHILE
LINE : E
ST No: 10
55.0
8.0
RHO (Ohm-m)
7
DEPTH (m)

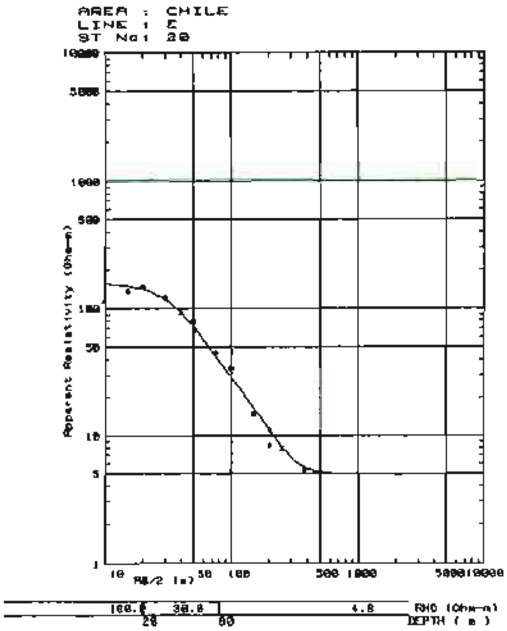
AREA : CHILE
LINE : E
ST No: 20
160.0
30.0
4.8
RHO (Ohm-m)
28
80
DEPTH (m)

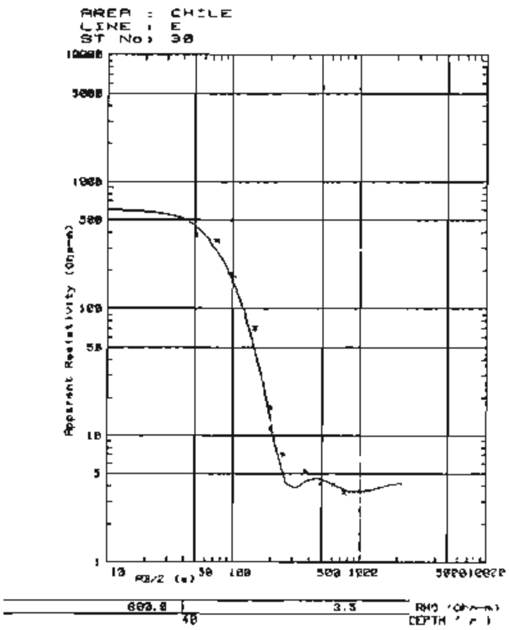
AREA : CHILE
LINE : E
ST No: 30
600.0
3.5
RHO (Ohm-m)
40
DEPTH (m)

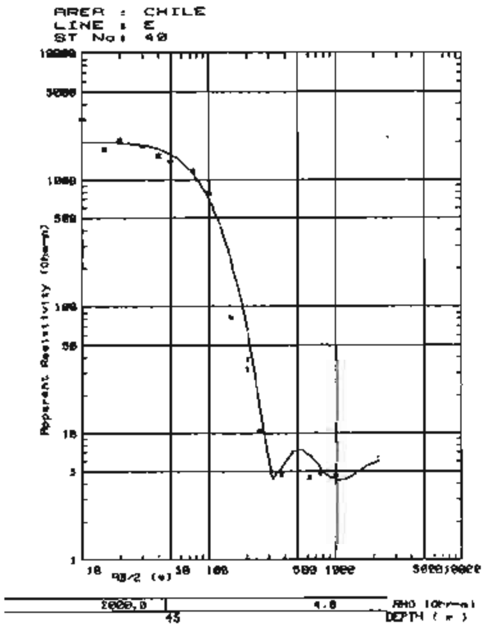
AREA : CHILE
LINE : E
ST No: 40
2000.0
4.8
RHO (Ohm-m)
45
DEPTH (m)

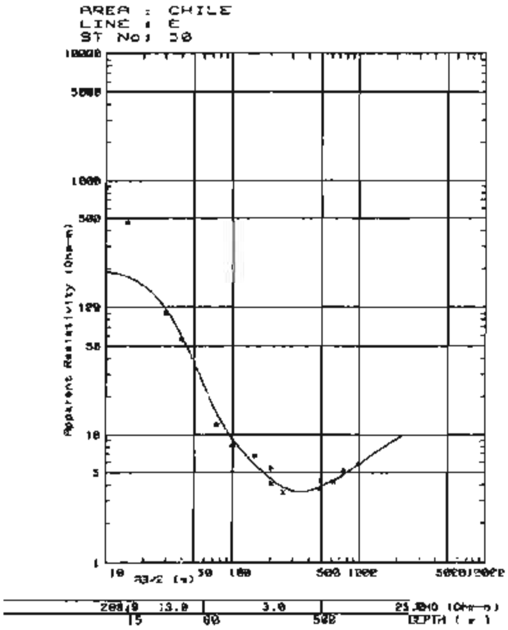
AREA : CHILE
LINE : E
ST No: 50
Apparent Resistivity (Ohm-m)
AB/2 (m)
DEPTH (m)

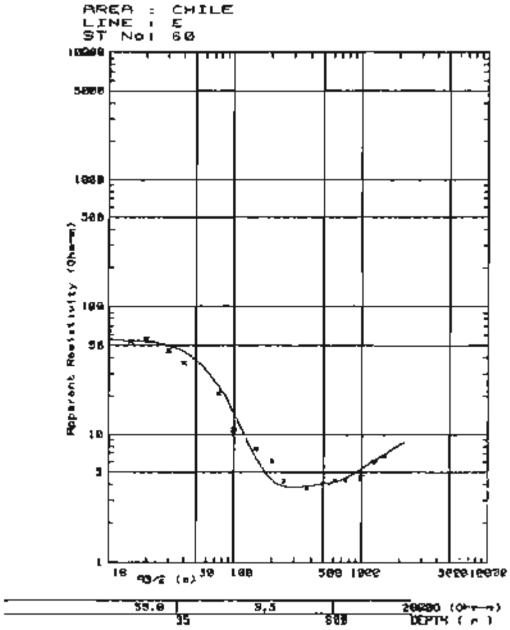
AREA : CHILE
LINE : E
ST No: 60
Apparent Resistivity (Ohm-m)
AB/2 (m)
DEPTH (m)

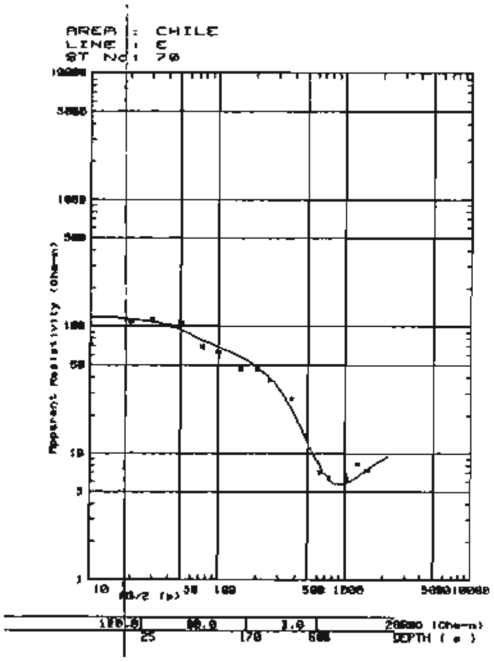
AREA : CHILE
LINE : E
ST No: 70
Apparent Resistivity (Ohm-m)
AB/2 (m)
DEPTH (m)

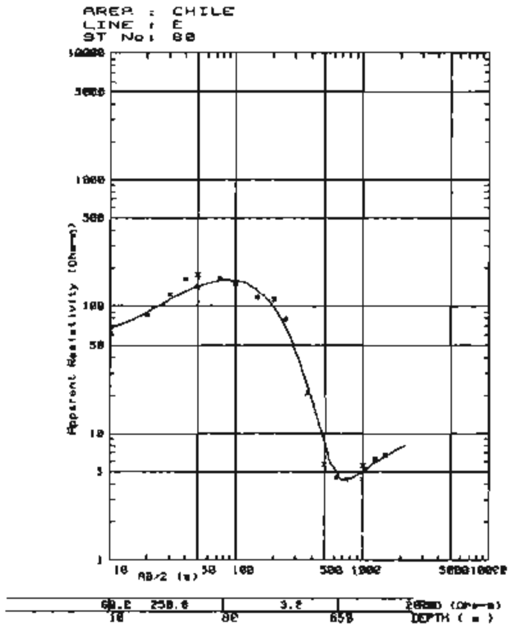
AREA : CHILE
LINE : E
ST No: 80
Apparent Resistivity (Ohm-m)
AB/2 (m)
DEPTH (m)

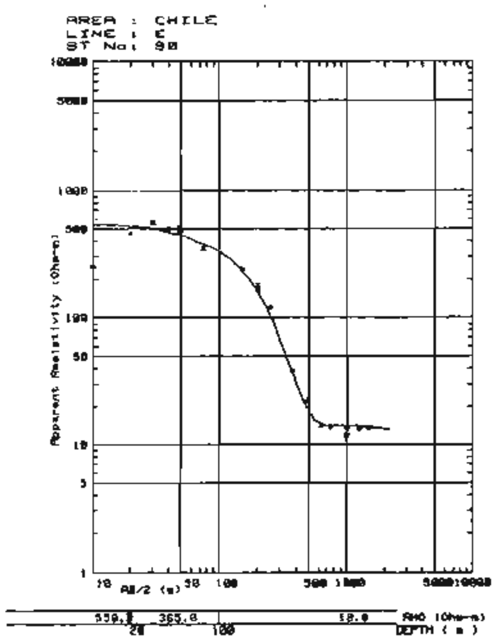
AREA : CHILE
LINE : E
ST No: 90
Apparent Resistivity (Ohm-m)
AB/2 (m)
365.0
RHO (Ohm-m)
DEPTH (m)

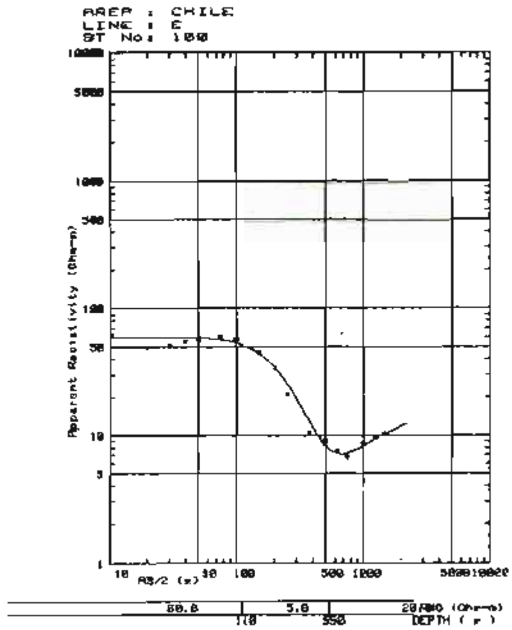
AREA : CHILE
LINE : E
ST No: 100
Apparent Resistivity (Ohm-m)
AB/2 (m)
60.0
5.0
RHO (Ohm-m)
550
DEPTH (m)

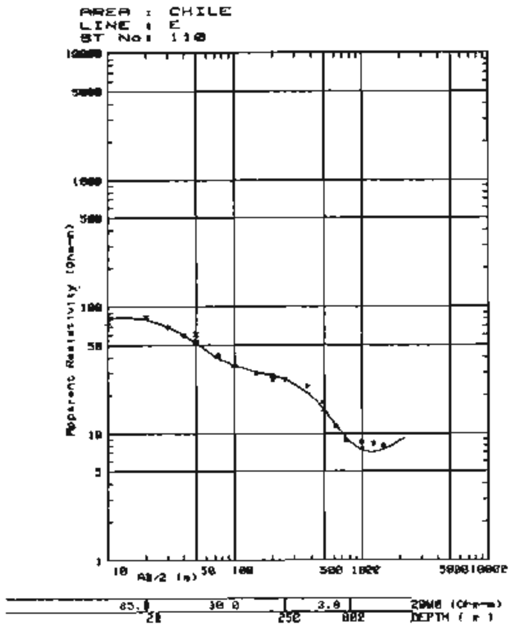
AREA : CHILE
LINE : E
ST No: 110
Apparent Resistivity (Ohm-m)
AB/2 (m)
RHO (Ohm-m)
DEPTH (m)

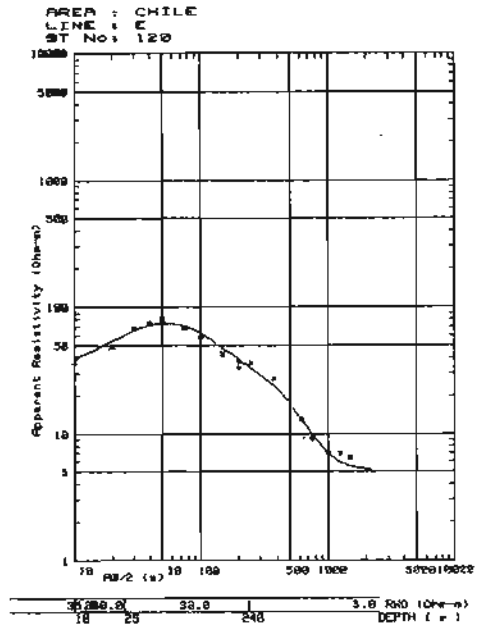
AREA : CHILE
LINE : E
ST No: 120
Apparent Resistivity (Ohm-m)
AB/2 (m)
RHO (Ohm-m)
DEPTH (m)

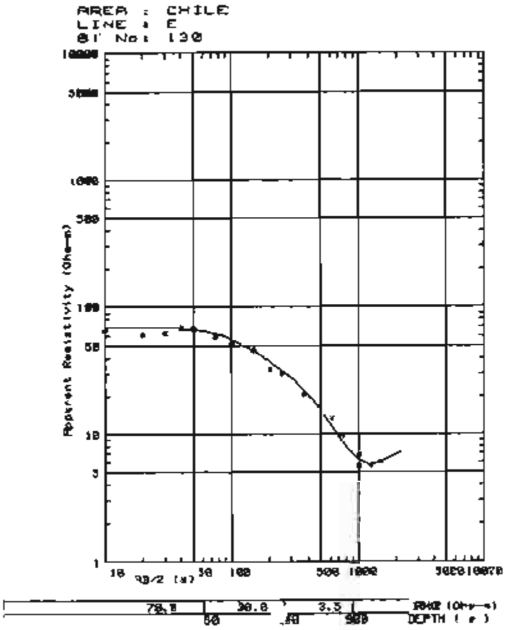
AREA : CHILE
LINE : E
ST No: 130
Apparent Resistivity (Ohm-m)
AB/2 (m)
70.0 30.0 3.5 RHO (Ohm-m)
50 900 DEPTH (m)

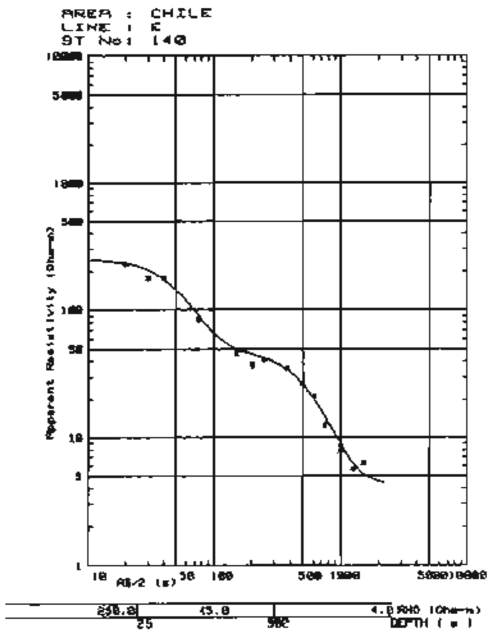
AREA : CHILE
LINE : E
ST No: 140
Apparent Resistivity (Ohm-m)
AB/2 (m)
250.0 45.0 4.0 RHO (Ohm-m)
25 500 DEPTH (m)

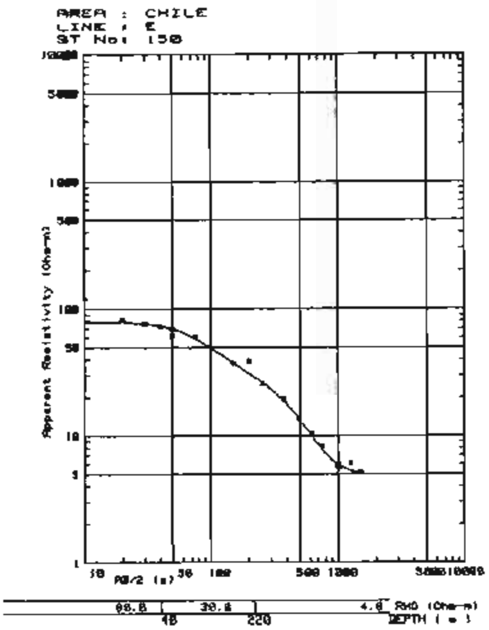
AREA : CHILE
LINE : E
ST No: 150
Apparent Resistivity (Ohm-m)
AB/2 (m)
80.0 30.0 4.0 RHO (Ohm-m)
40 220 DEPTH (m)

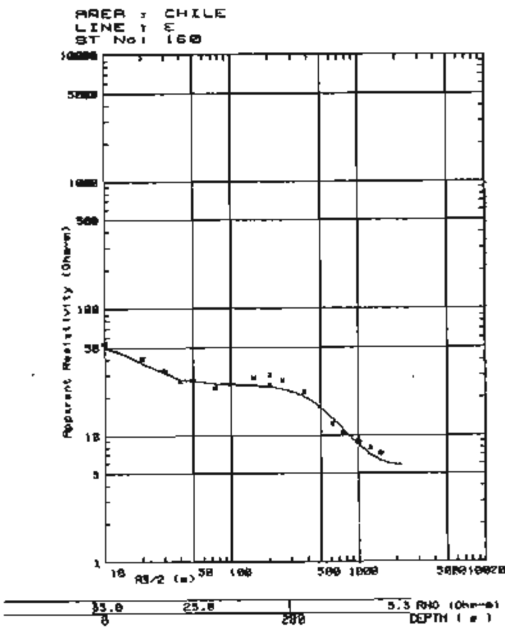
AREA : CHILE
LINE : E
ST No: 160
Apparent Resistivity (Ohm-m)
AB/2 (m)
55.0 25.0 5.5 RHO (Ohm-m)
8 280 DEPTH (m)

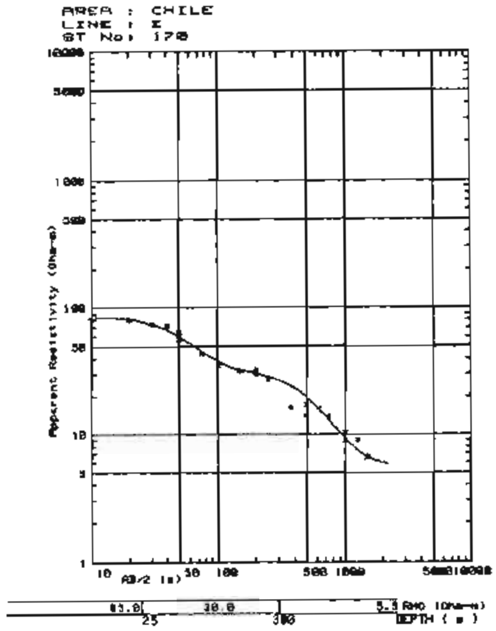
AREA : CHILE
LINE : E
ST No: 170
Apparent Resistivity (Ohm-m)
AB/2 (m)
83.0
30.0
5.5
RHO (Ohm-m)
25
300
DEPTH (m)

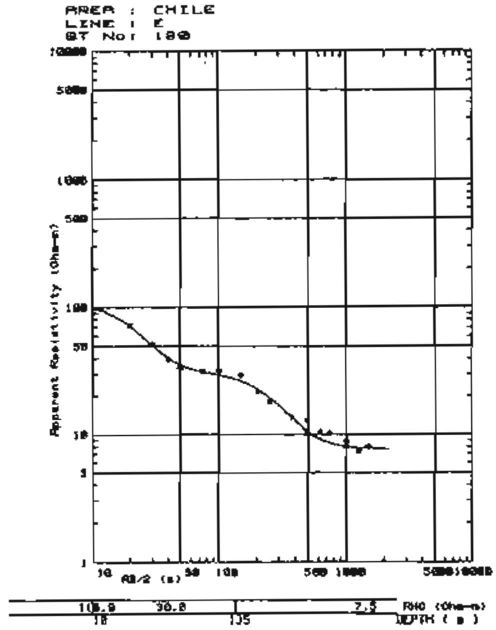
AREA : CHILE
LINE : E
ST No: 180
Apparent Resistivity (Ohm-m)
AB/2 (m)
106.9
30.0
7.5
RHO (Ohm-m)
18
135
DEPTH (m)

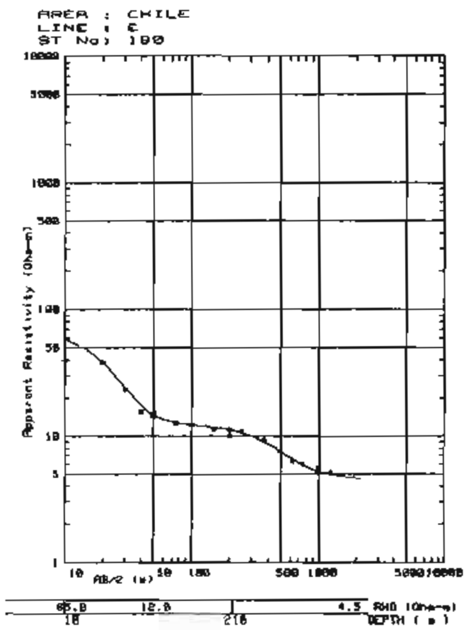
AREA : CHILE
LINE : E
ST No: 190
Apparent Resistivity (Ohm-m)
AB/2 (m)
65.0
12.0
4.5
RHO (Ohm-m)
18
210
DEPTH (m)

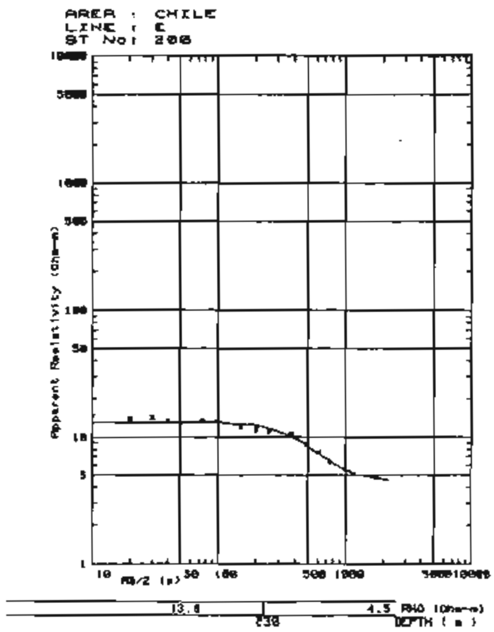
AREA : CHILE
LINE : E
ST No: 200
Apparent Resistivity (Ohm-m)
AB/2 (m)
13.6
4.5
RHO (Ohm-m)
230
DEPTH (m)

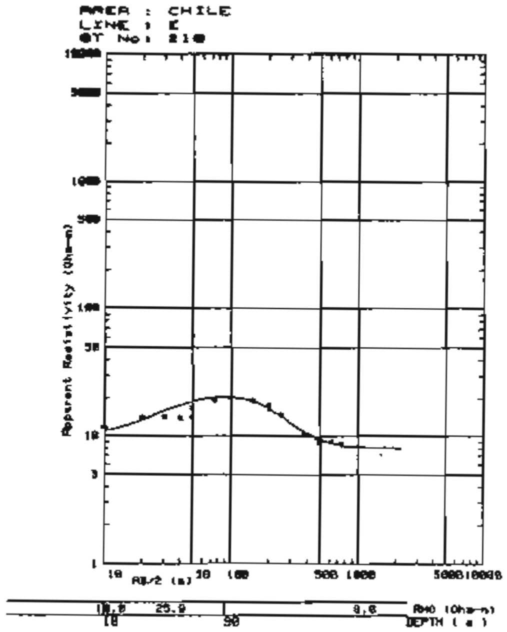
AREA : CHILE
LINE : E
ST No: 210
Apparent Resistivity (Ohm-m)
AB/2 (m)
RHO (Ohm-m)
10.0 25.9 8.0
DEPTH (m)
10 50

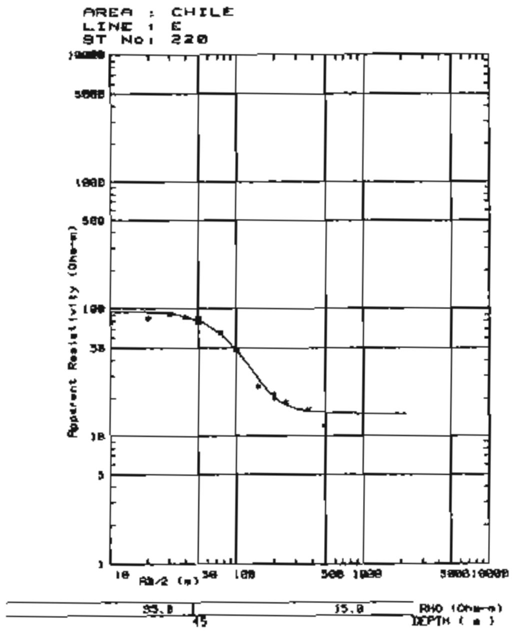
AREA : CHILE
LINE : E
ST No: 220
Apparent Resistivity (Ohm-m)
AB/2 (m)
RHO (Ohm-m)
95.0 15.0
DEPTH (m)
45

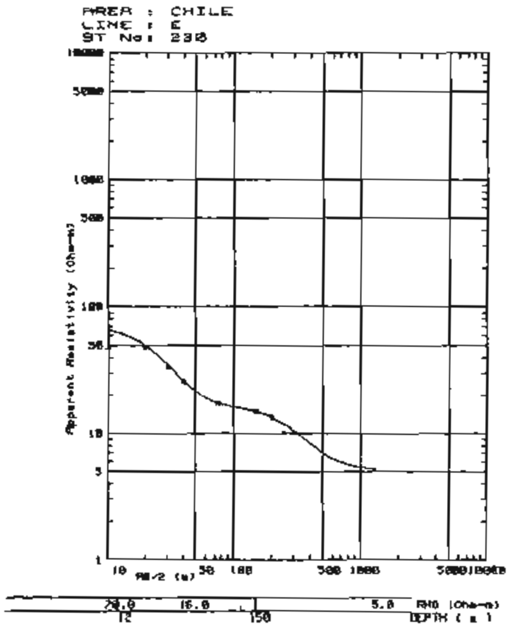
AREA : CHILE
LINE : E
ST No: 230
Apparent Resistivity (Ohm-m)
AB/2 (m)
RHO (Ohm-m)
70.0 16.0 5.0
DEPTH (m)
12 150

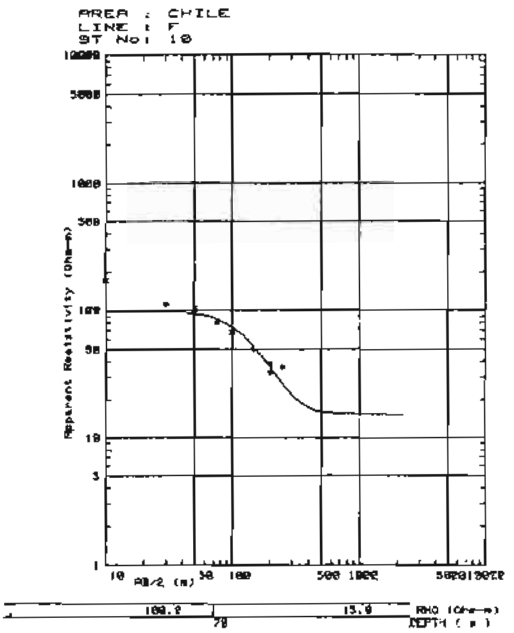
AREA : CHILE
LINE : F
ST No: 10
Apparent Resistivity (Ohm-m)
AB/2 (m)
100.0
13.0
RHO (Ohm-m)
70
DEPTH (m)

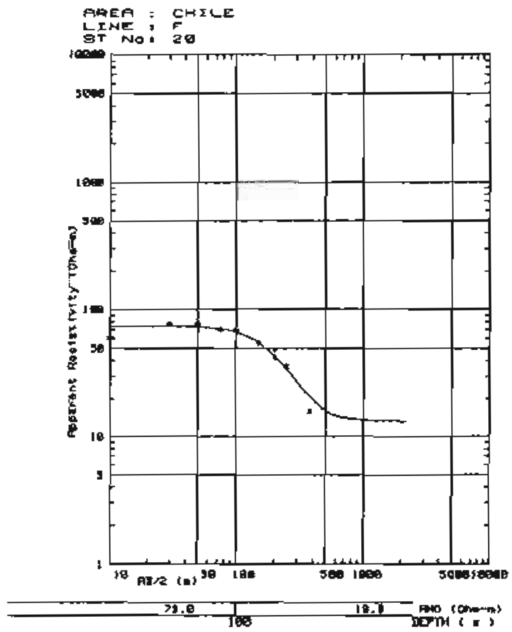
AREA : CHILE
LINE : F
ST No: 20
Apparent Resistivity (Ohm-m)
AB/2 (m)
RHO (Ohm-m)
100
DEPTH (m)

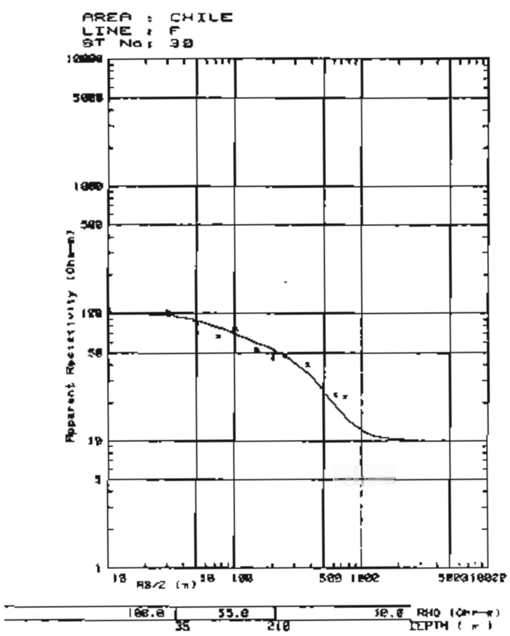
AREA : CHILE
LINE : F
ST No: 30
Apparent Resistivity (Ohm-m)
AB/2 (m)
100.0
55.0
RHO (Ohm-m)
35
210
DEPTH (m)

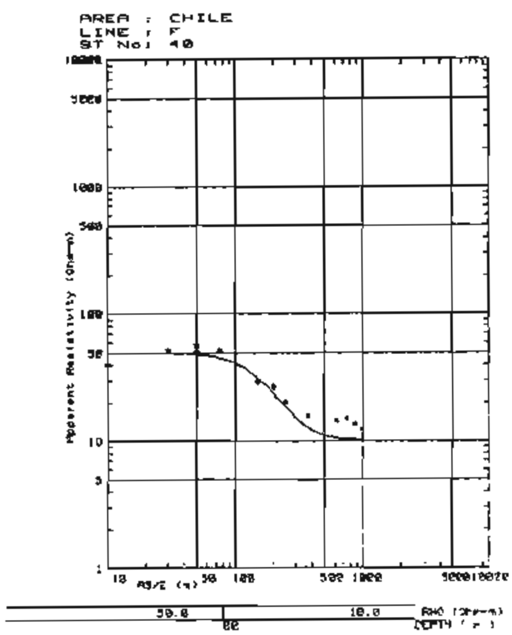
AREA : CHILE
LINE : F
ST No: 40
Apparent Resistivity (Ohm-m)
AB/2 (m)
50.0
10.0
RHO (Ohm-m)
DEPTH (m)

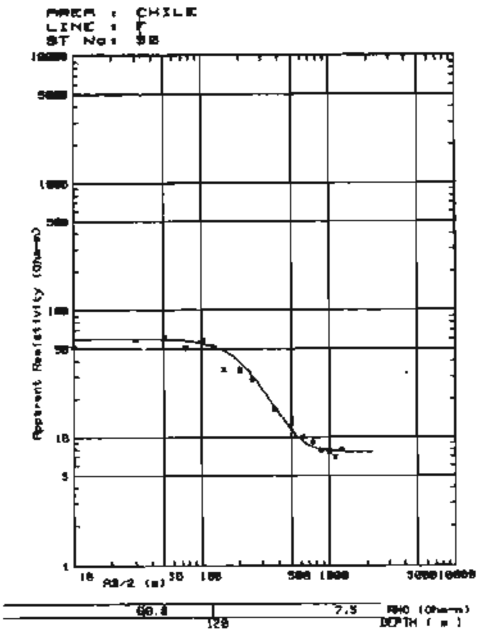
AREA : CHILE
LINE : F
ST No: 50
Apparent Resistivity (Ohm-m)
AB/2 (m)
60.0
7.5
RHO (Ohm-m)
120
DEPTH (m)

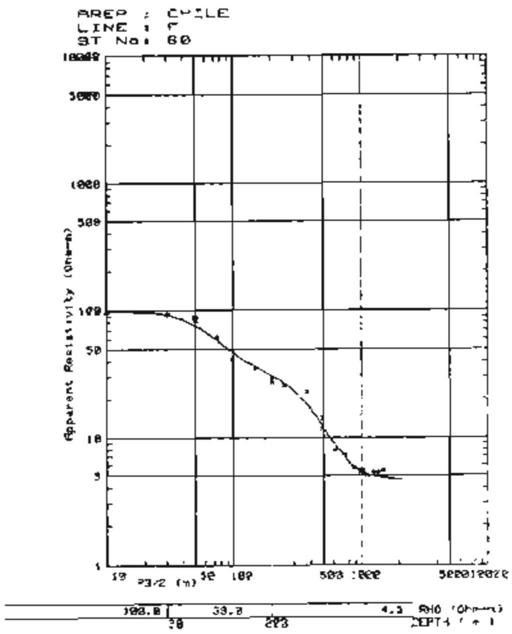
AREA : CHILE
LINE : F
ST No: 60
Apparent Resistivity (Ohm-m)
AB/2 (m)
100.0
33.0
4.3
RHO (Ohm-m)
30
273
DEPTH (m)

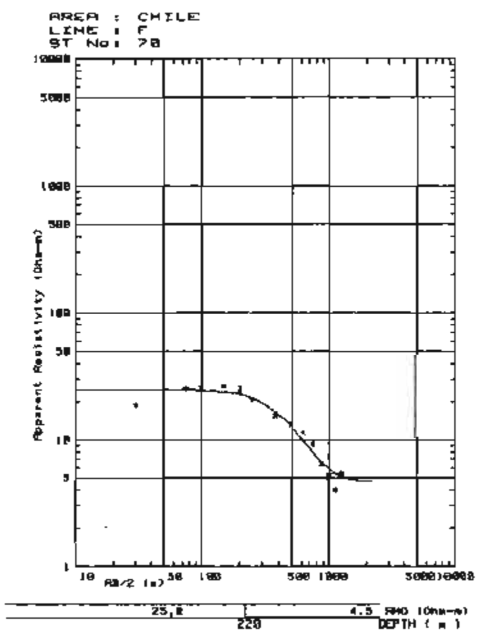
AREA : CHILE
LINE : F
ST No: 70
Apparent Resistivity (Ohm-m)
AB/2 (m)
25.0
4.5
RHO (Ohm-m)
220
DEPTH (m)

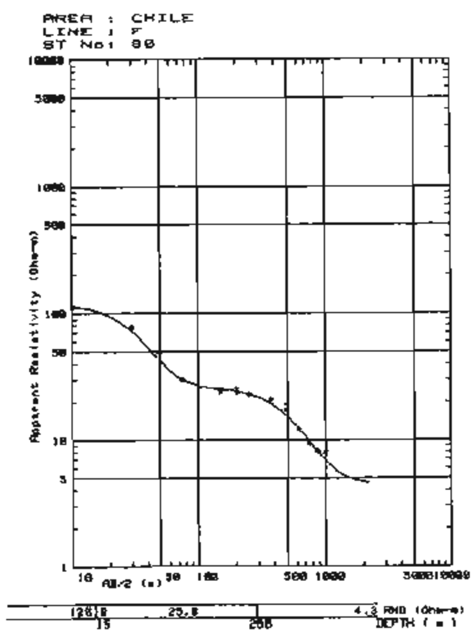
AREA : CHILE
LINE : F
ST No: 80
Apparent Resistivity (Ohm-m)
AB/2 (m)
120.0
25.0
4.3
RHO (Ohm-m)
15
200
DEPTH (m)

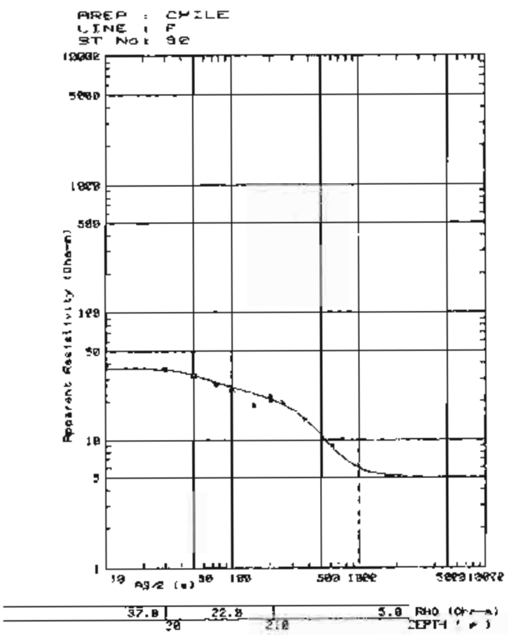
AREA : CHILE
LINE : F
ST No: 90
Apparent Resistivity (Ohm-m)
AB/2 (m)
37.0
22.0
5.0
RHO (Ohm-m)
20
210
DEPTH (m)

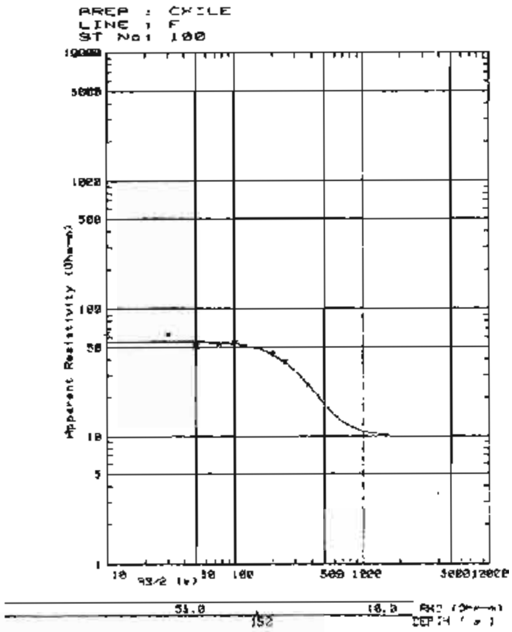
AREA : CHILE
LINE : F
ST No: 100
Apparent Resistivity (Ohm-m)
AB/2 (m)
51.0
10.0
RHO (Ohm-m)
152
DEPTH (m)

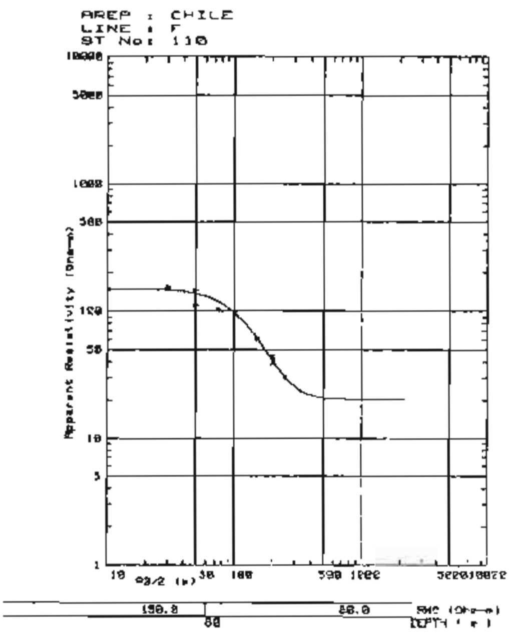
AREA : CHILE
LINE : F
ST No: 110
Apparent Resistivity (Ohm-m)
AB/2 (m)
150.0
30.0
RHO (Ohm-m)
60
DEPTH (m)

X-RAY DIFFRACTION

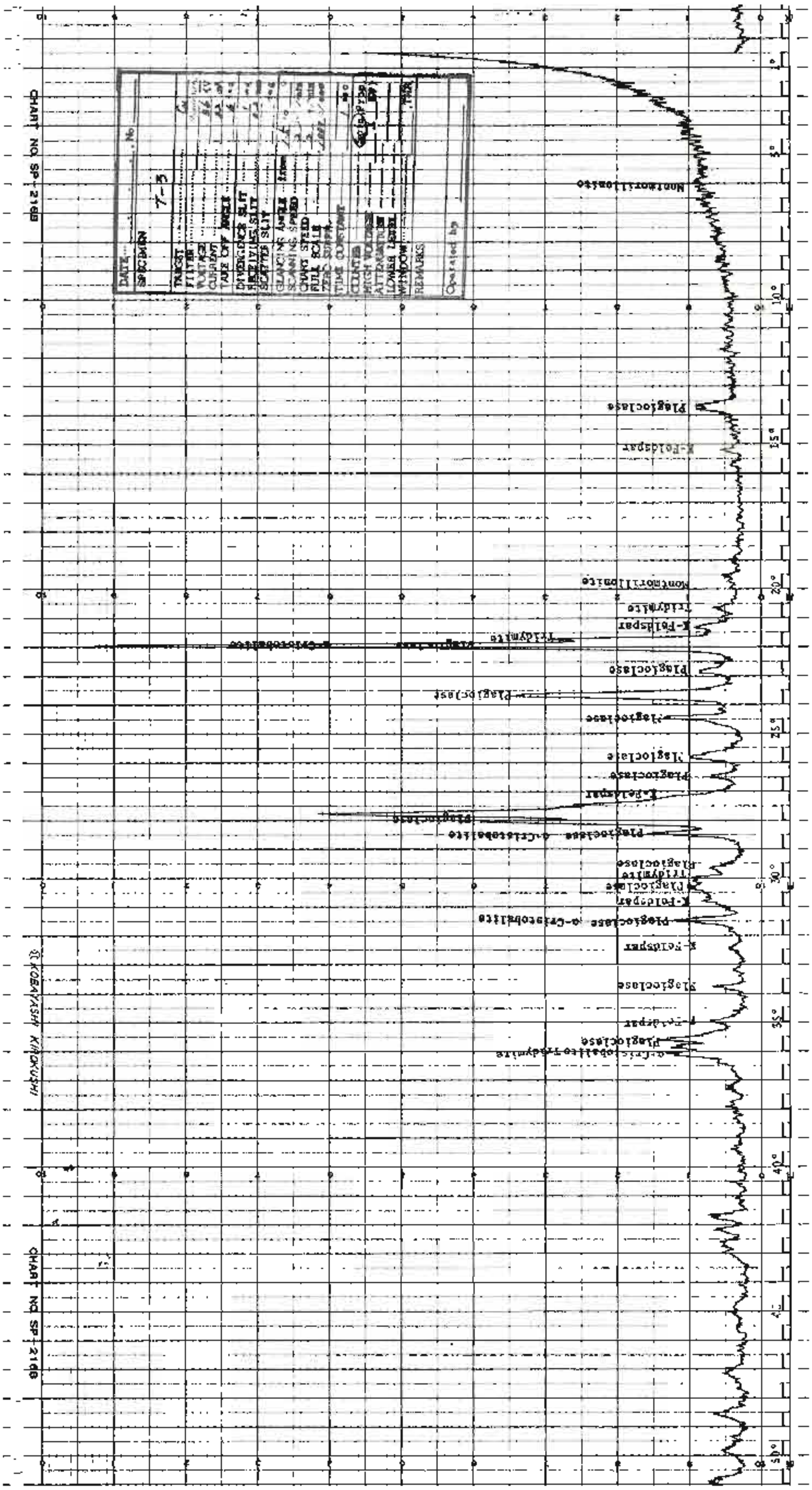
CHART NO SP-2168
SPECIMEN 7-3
Montmorillonite
Plagioclase
K-Feldspar
Tridymite
α-Cristobalite
KOBAYASHI KIROKUSHI

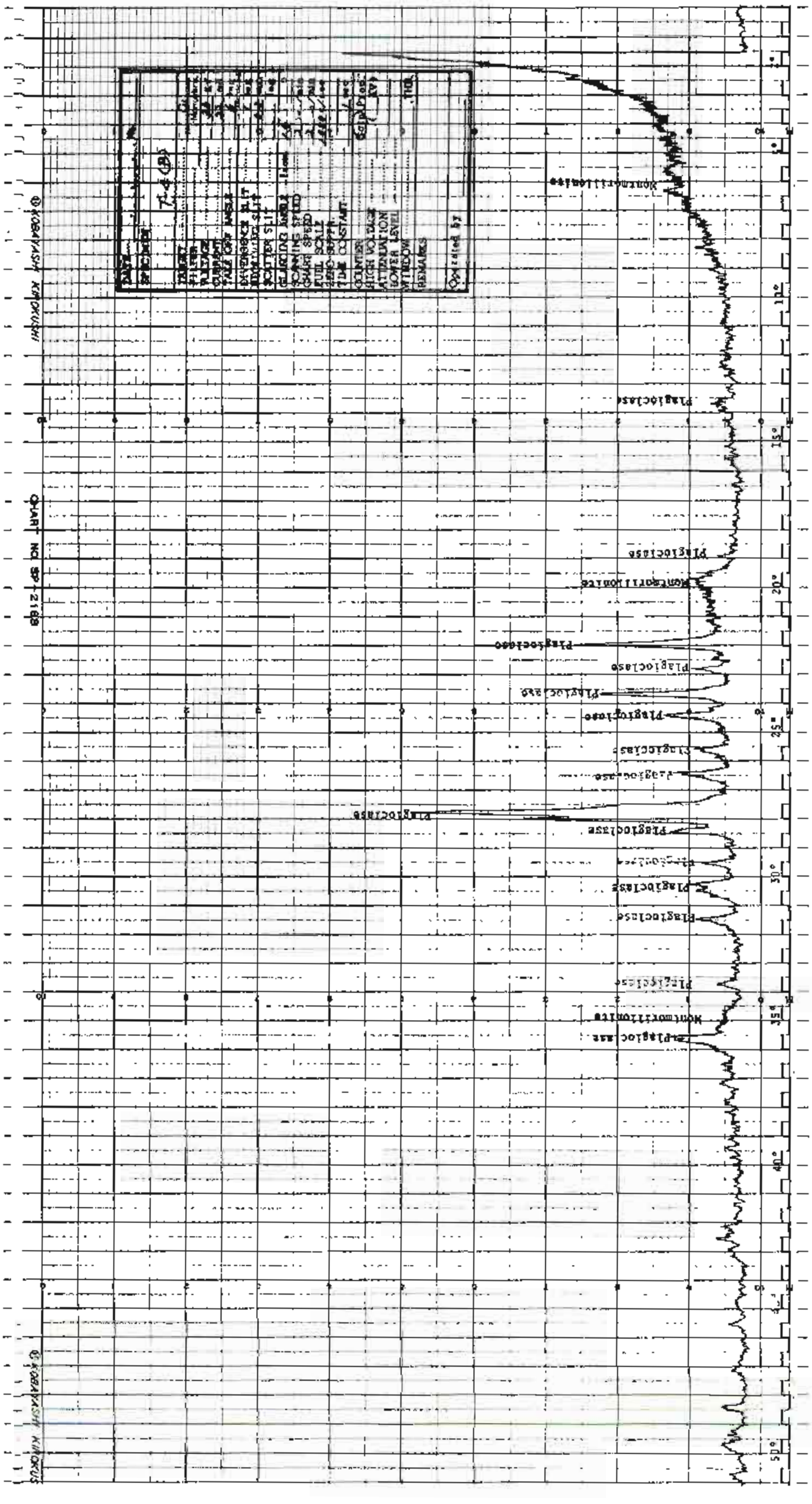
© KOBAYASHI KIROKUSHI
CHART NO. SP 2168
Montmorillonite
Plagioclase
Plagioclase
Montmorillonite
Plagioclase
Plagioclase
Plagioclase
Plagioclase
Plagioclase
Plagioclase
Plagioclase
Plagioclase
Plagioclase
Plagioclase
Plagioclase
Plagioclase
Montmorillonite
Plagioclase
10°
15°
20°
25°
30°
35°
40°
50°

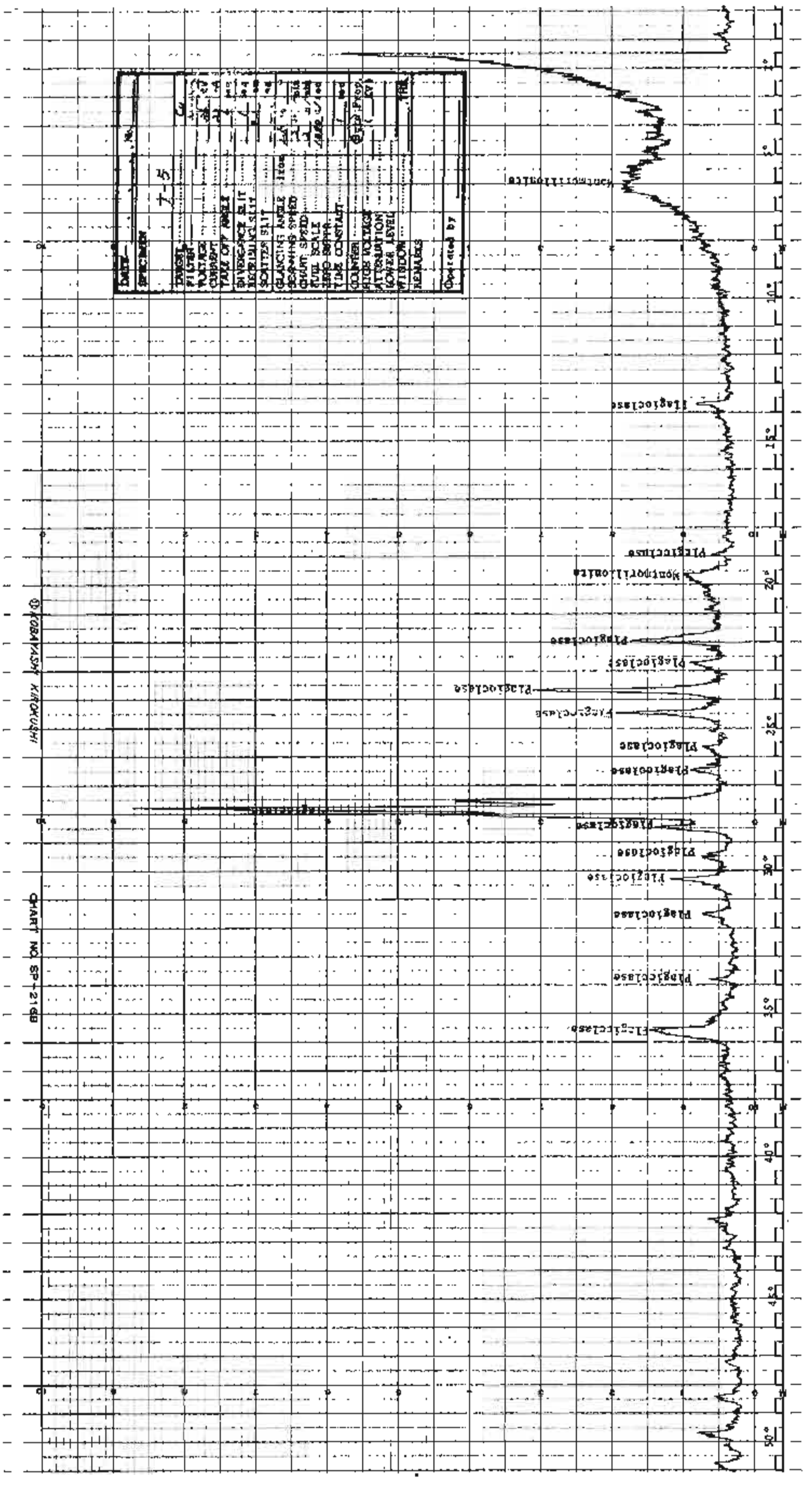

Montmorillonite
Plagioclase
KOBAYASHI KIROKUSHI

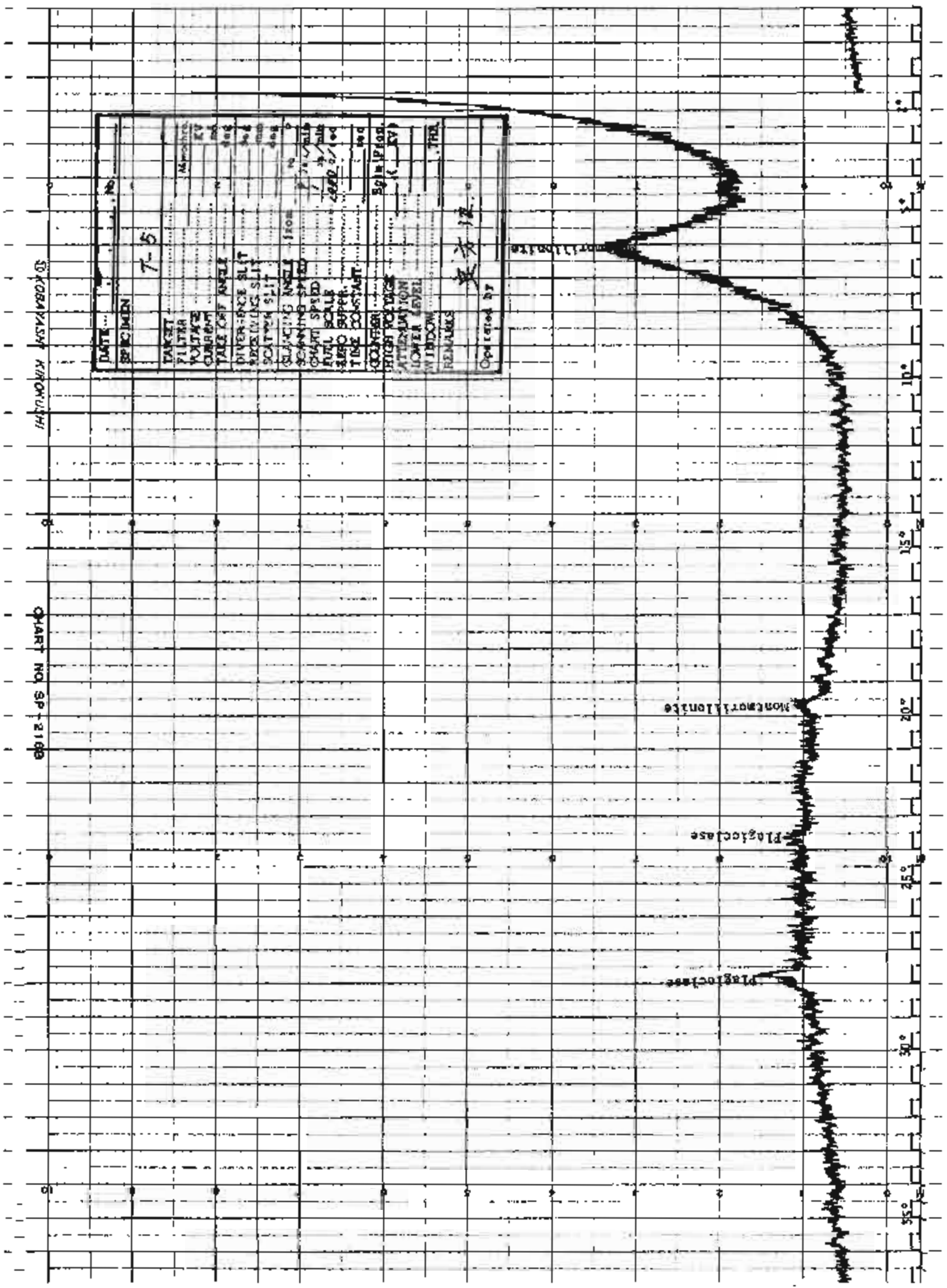
CHART NO. SP-2168
Montmorillonite
Montmorillonite
Plagioclase
Plagioclase
10°
15°
20°
25°
30°
35°

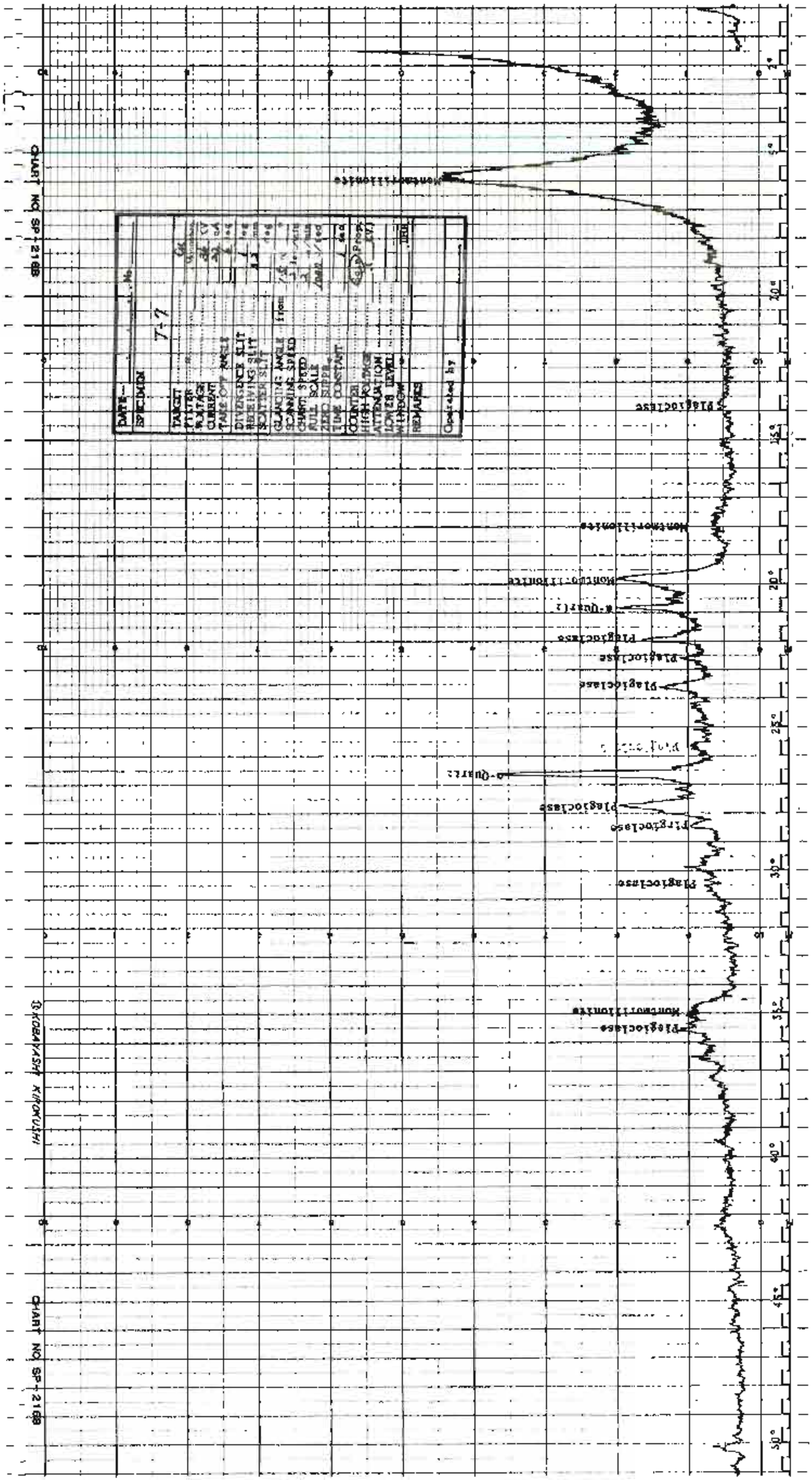

CHART NO. SP-216B
KOBAYASHI KIROKUSHI
T-7
Montmorillonite
Plagioclase
Montmorillonite
Montmo-illonite
α-Quartz
Plagioclase
Plagioclase
Plagioclase
α-Quartz
Plagioclase
Plagioclase
Plagioclase
Montmorillonite
Plagioclase

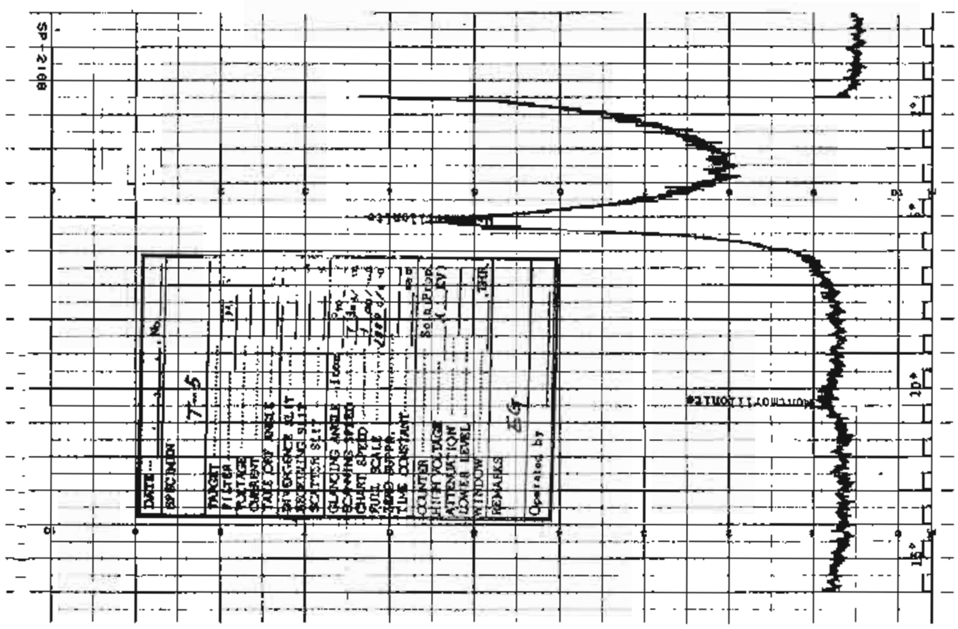

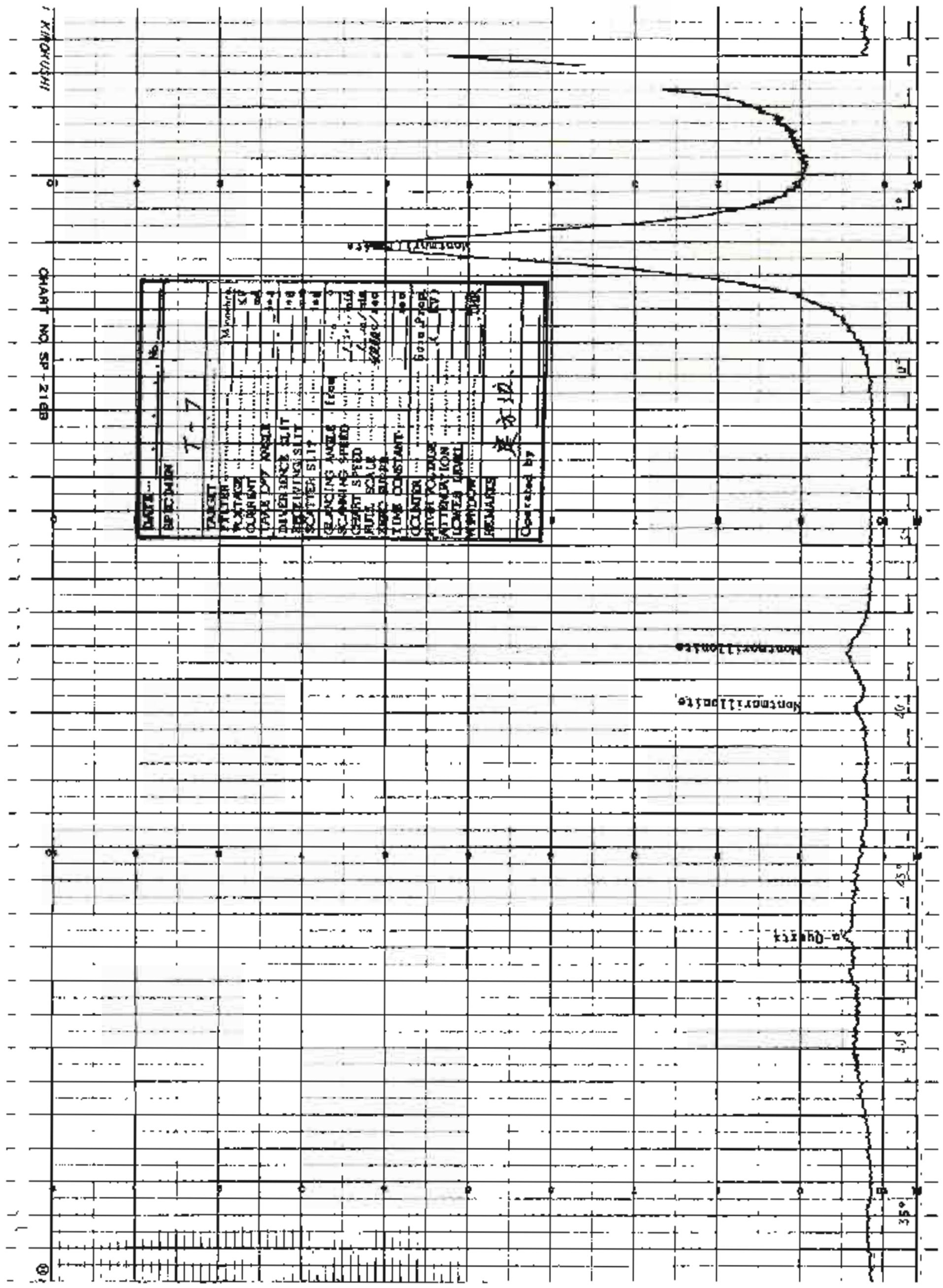
CHART NO. SP-21GB
Montmorillonite
Montmorillonite
α-Quartz

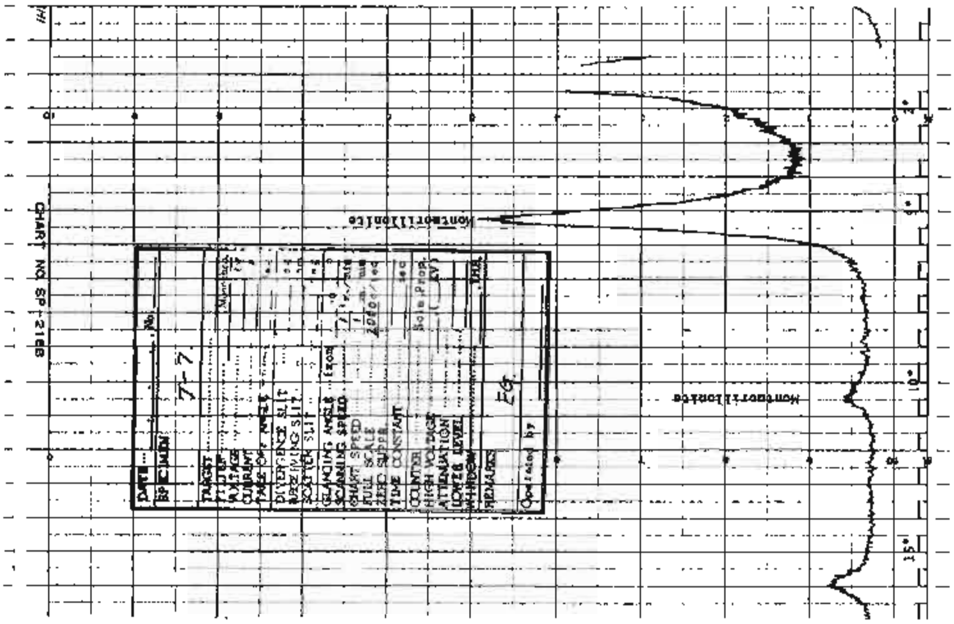
CHART NO. SP-216B
Montmorillonite
Montmorillonite
5°
10°
15°

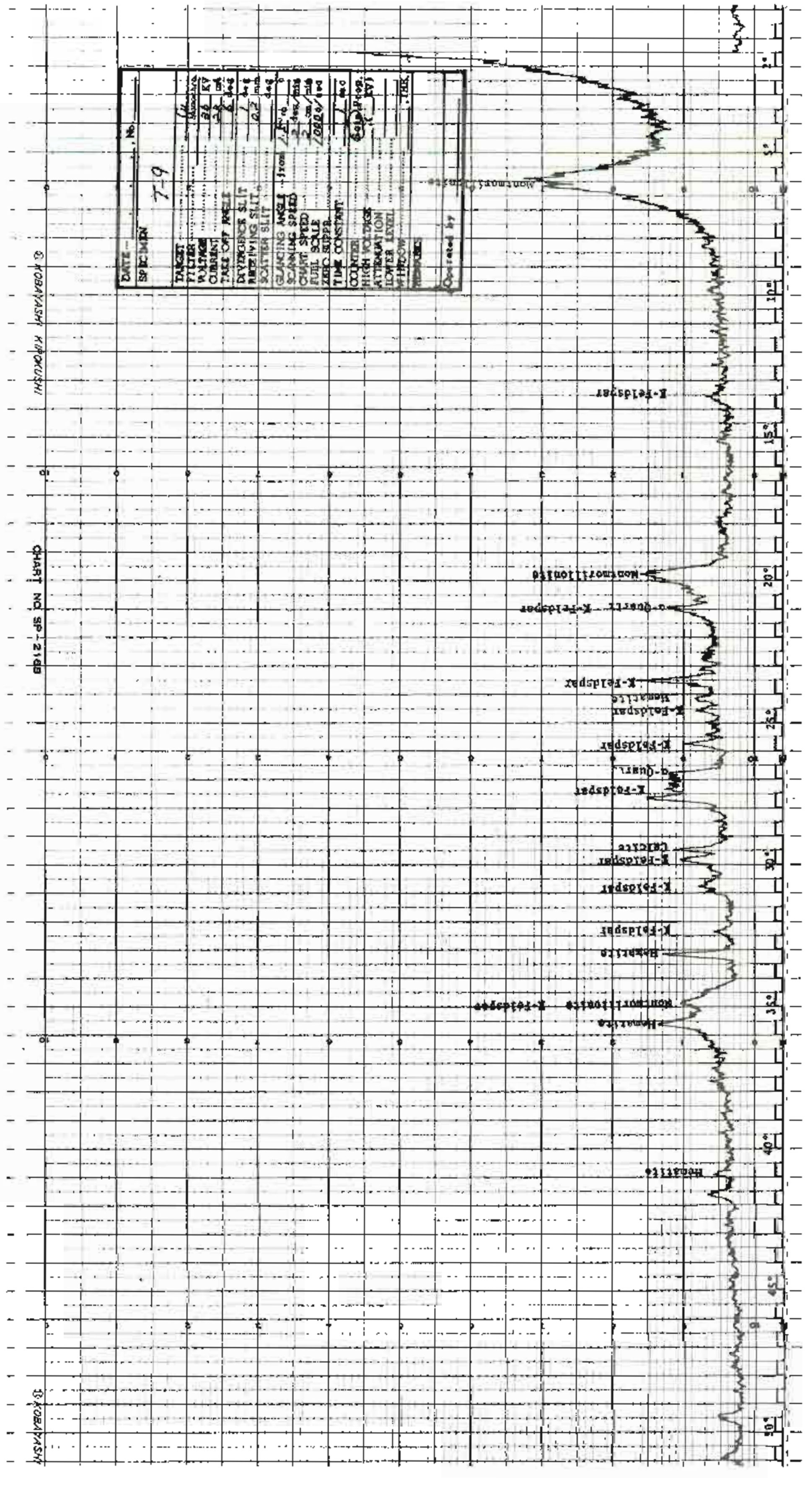

KOBAYASHI KIROKUSHI
CHART NO. SP-21GB
Montmorillonite
K-Feldspar
Montmorillonite
α-Quartz K-Feldspar
K-Feldspar
Hematite
K-Feldspar
K-Feldspar
α-Quartz
K-Feldspar
Calcite
K-Feldspar
K-Feldspar
K-Feldspar
Hematite
Montmorillonite K-Feldspar
Hematite
Hematite

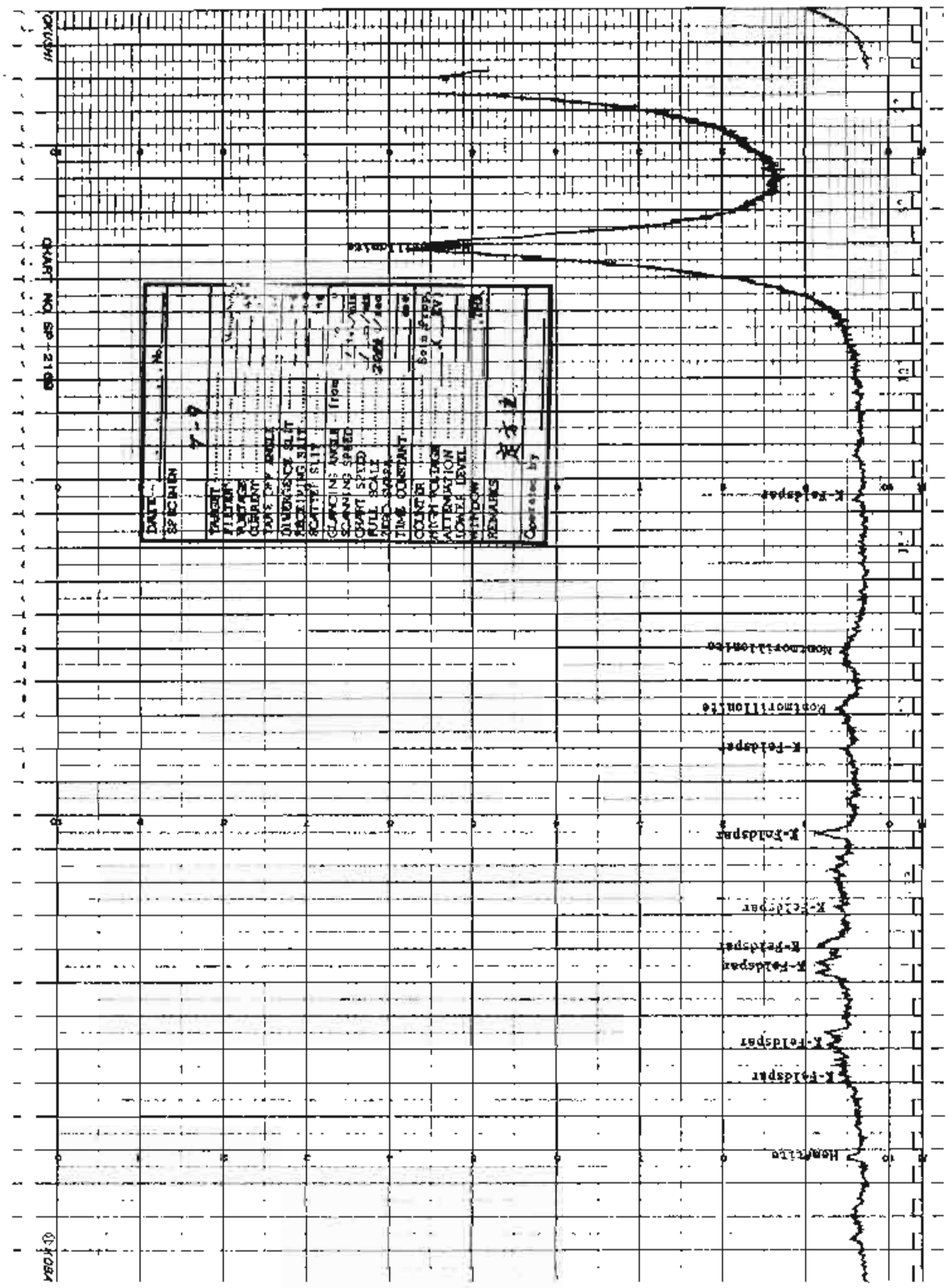
Montmorillonite
K-Feldspar
Montmorillonite
Montmorillonite
K-Feldspar
K-Feldspar
K-Feldspar
K-Feldspar
K-Feldspar
K-Feldspar
K-Feldspar
Hematite

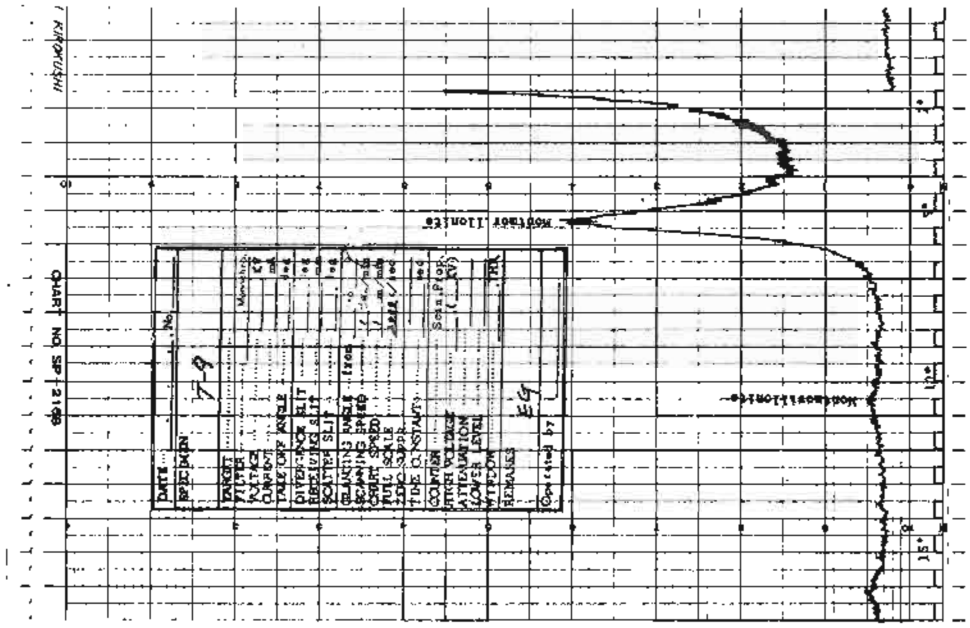
KIROKUSHI
Montmorillonite
Montmorillonite

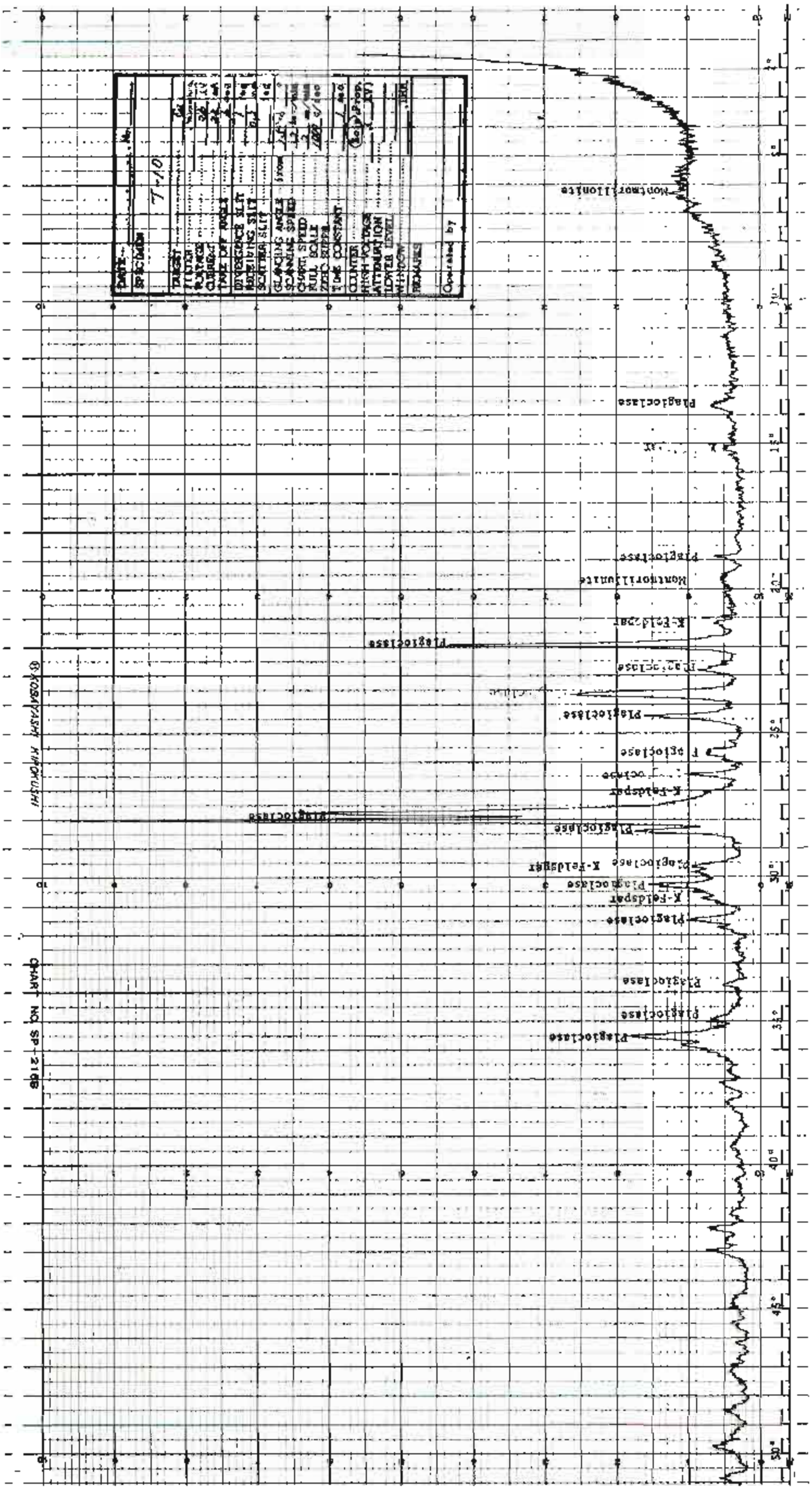
T-10
Montmorillonite
Plagioclase
K-Feldspar
KOBAYASHI KIROKUSHI
CHART NO. SP-216B
5°
10°
15°
20°
25°
30°
35°
40°
45°
50°

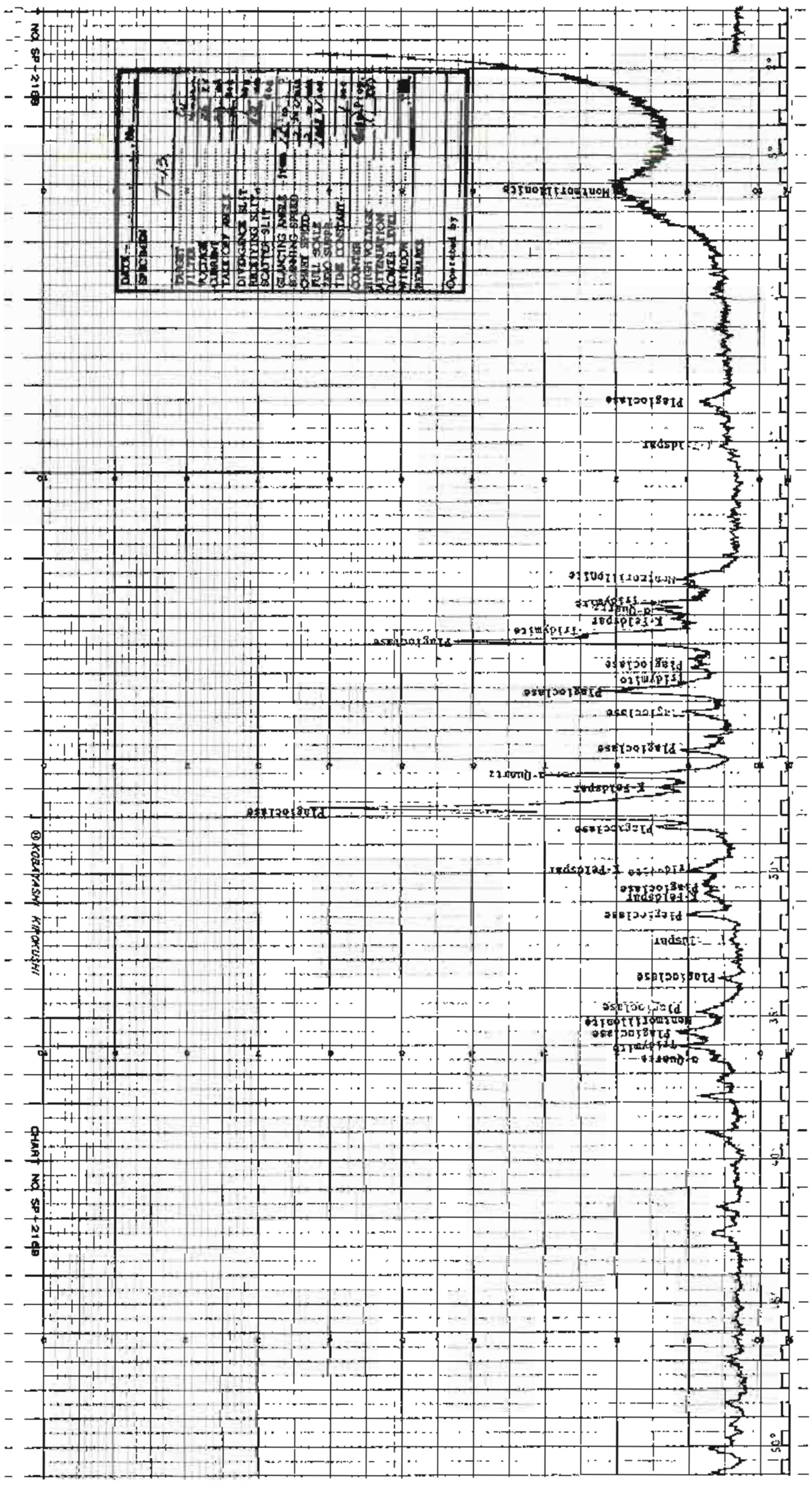

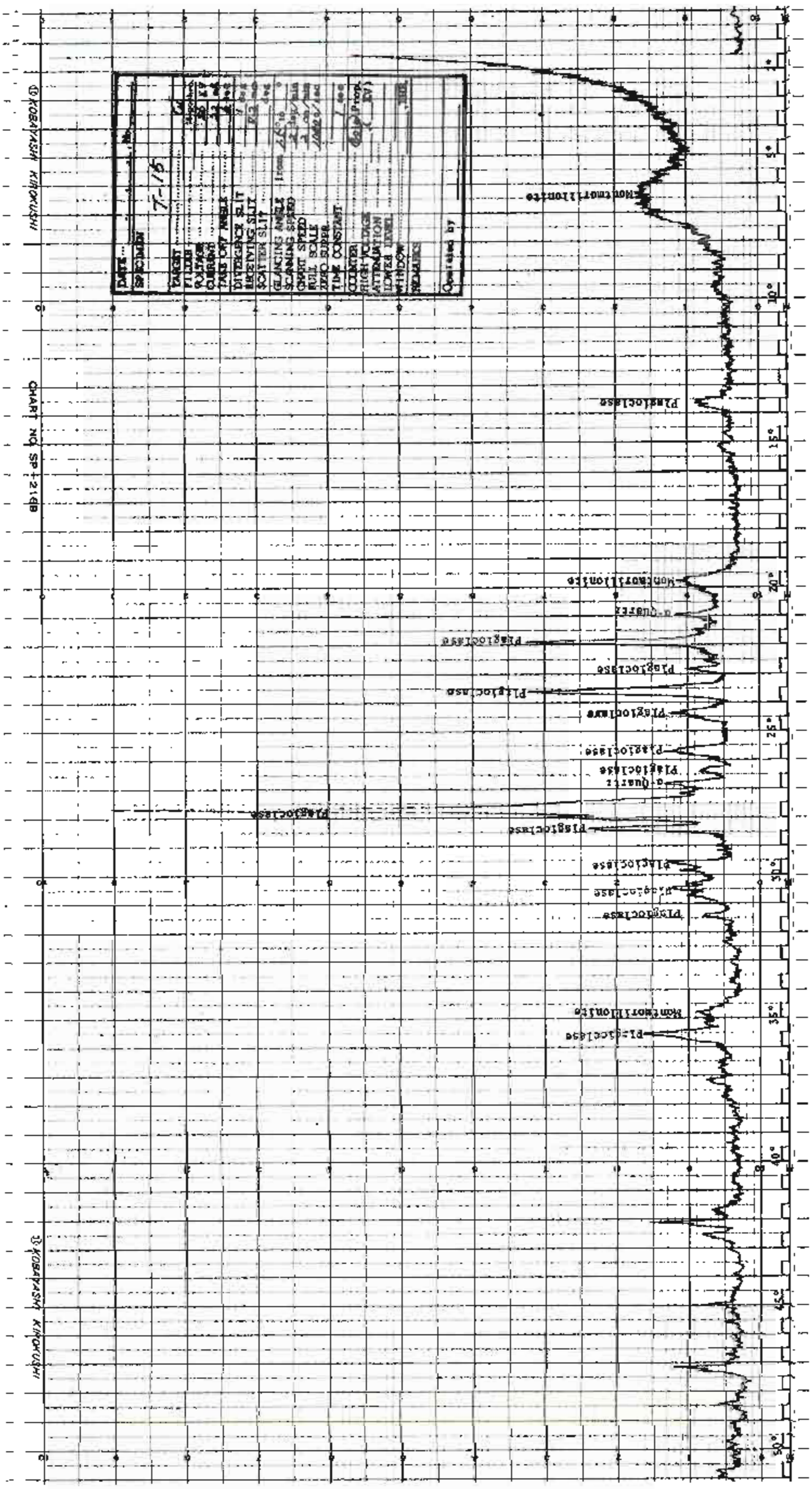

KOBAYASHI KIROKUSHI
CHART NO. SP-216B
7-15
Montmorillonite
Plagioclase
α-Quartz

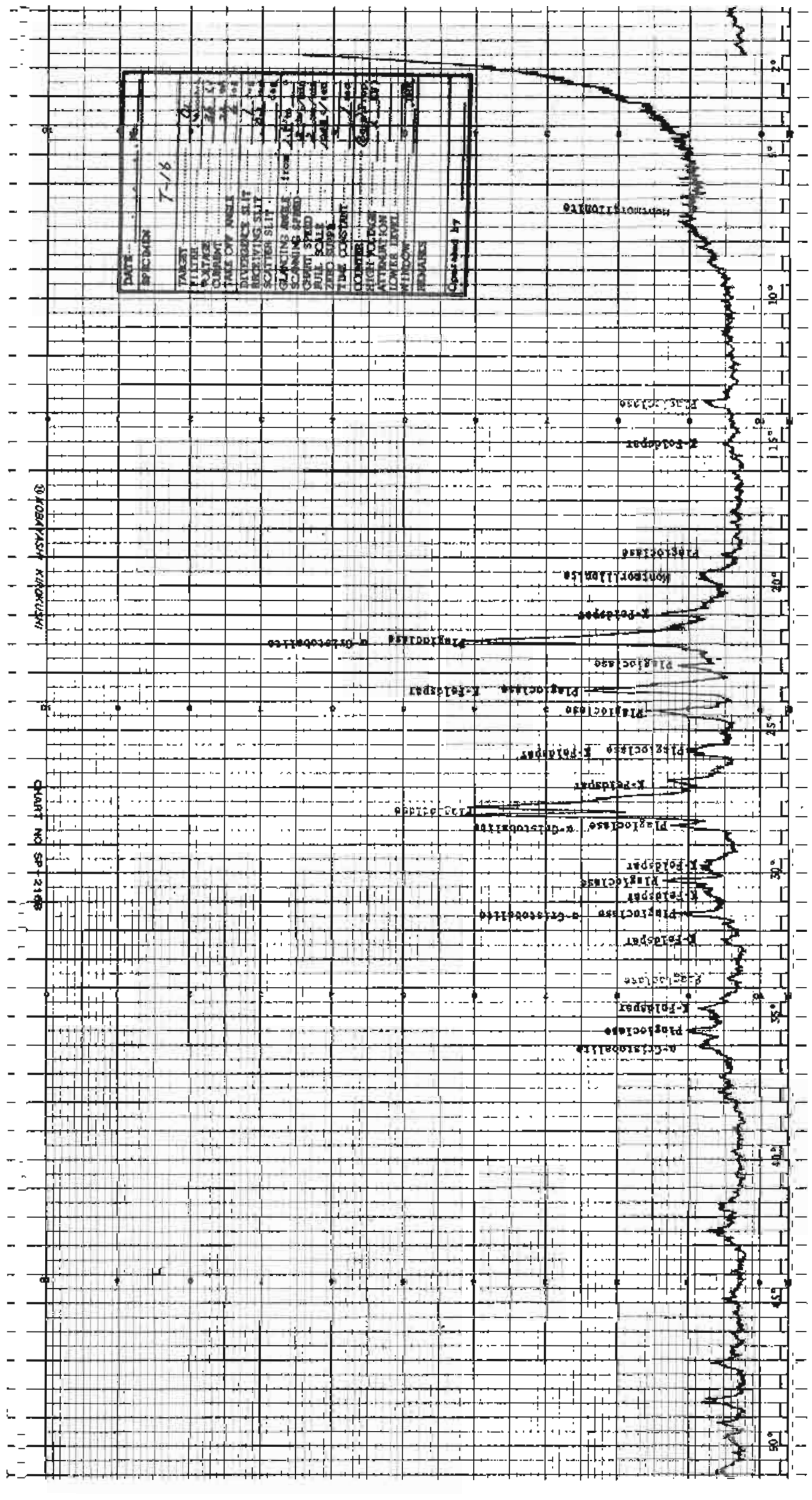
KOBAYASHI KIROKUSHI
CHART NO SP-216B
Montmorillonite
Plagioclase
K-feldspar
α-Cristobalite

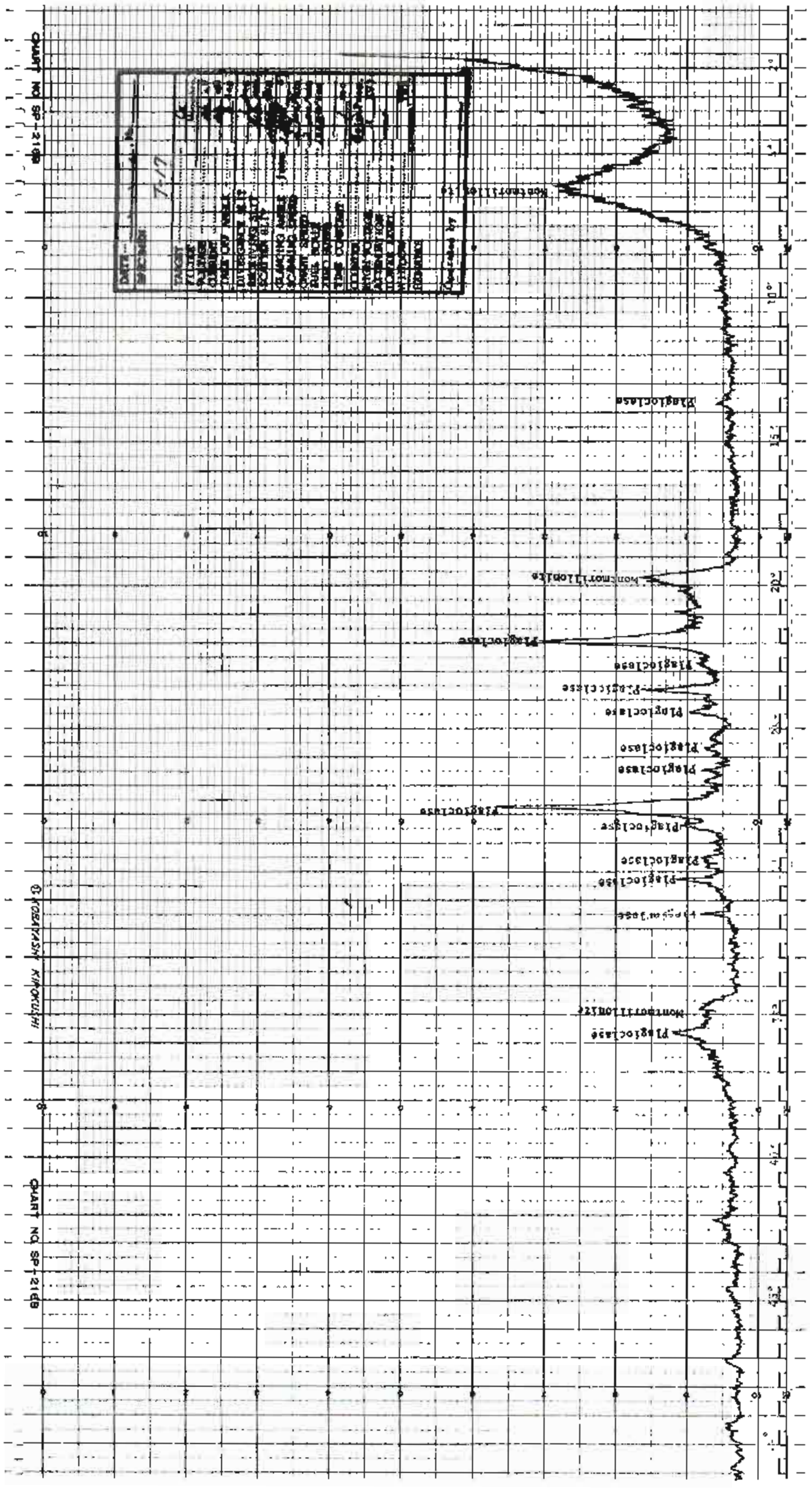
CHART NO. SP-216B
Montmorillonite
Plagioclase
Montmorillonite
Plagioclase
Plagioclase
Plagioclase
Plagioclase
Plagioclase
Plagioclase
Plagioclase
Plagioclase
Plagioclase
Plagioclase
Plagioclase
Montmorillonite
Plagioclase
CHART NO. SP-216B

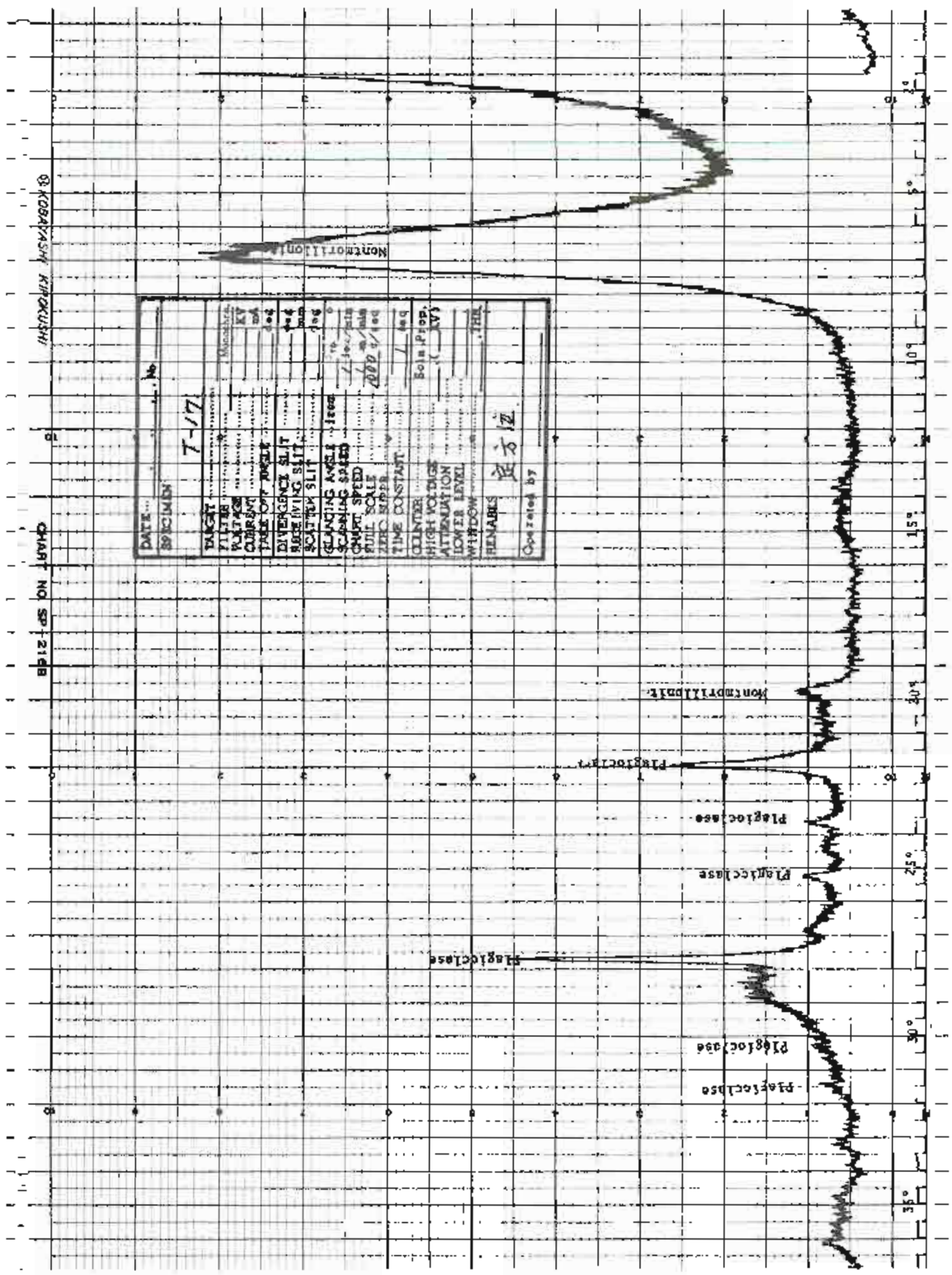
KOBAYASHI KIROKUSHI
CHART NO SP-216B
T-17
Montmorillonite
Montmorillonite
Plagioclase
Plagioclase
Plagioclase
Plagioclase
Plagioclase
Plagioclase

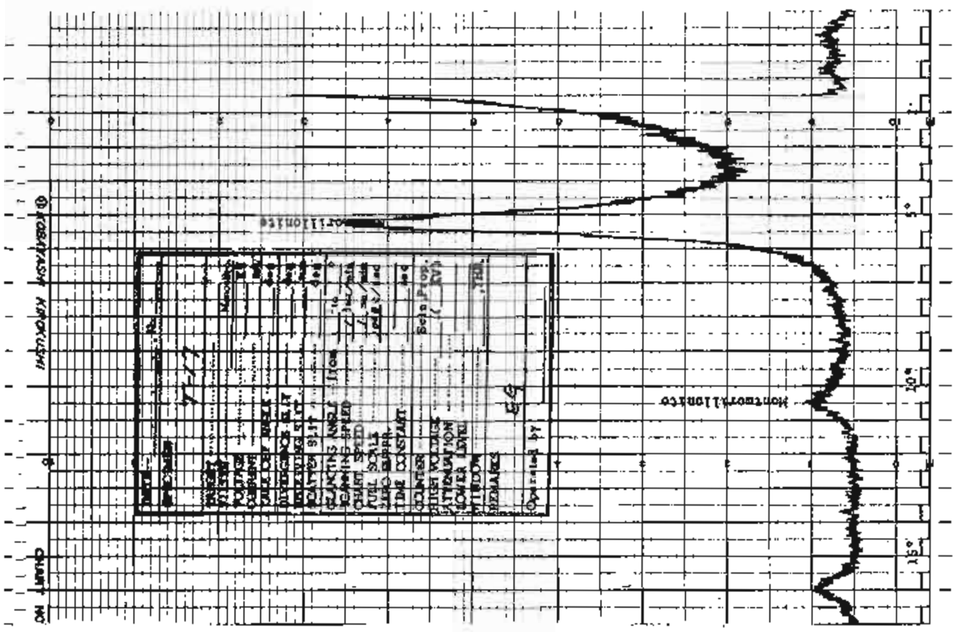

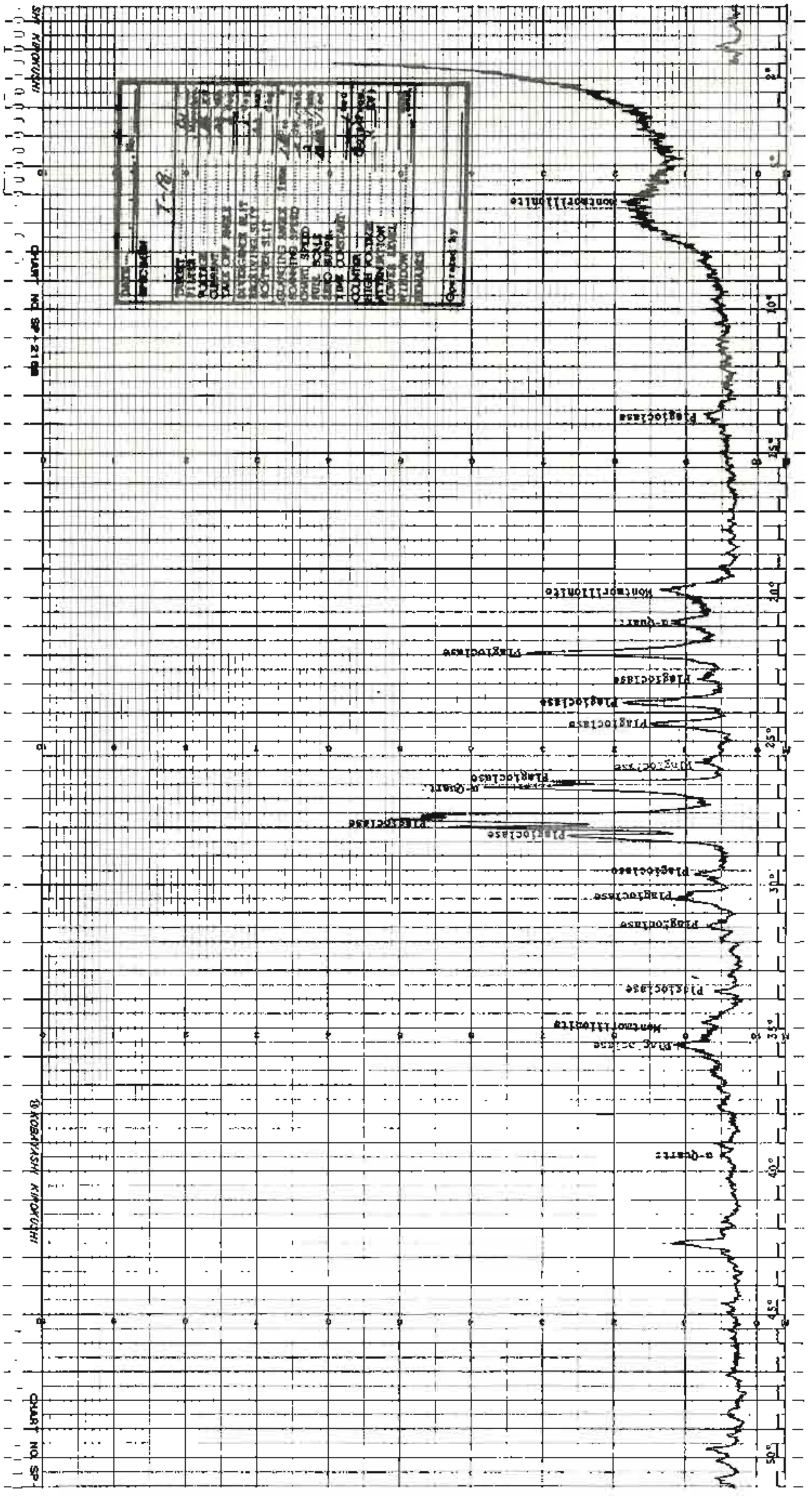

Montmorillonite
Plagioclase
α-Quartz
CHART NO. SP-21
KOBAYASHI KIROKUSHI

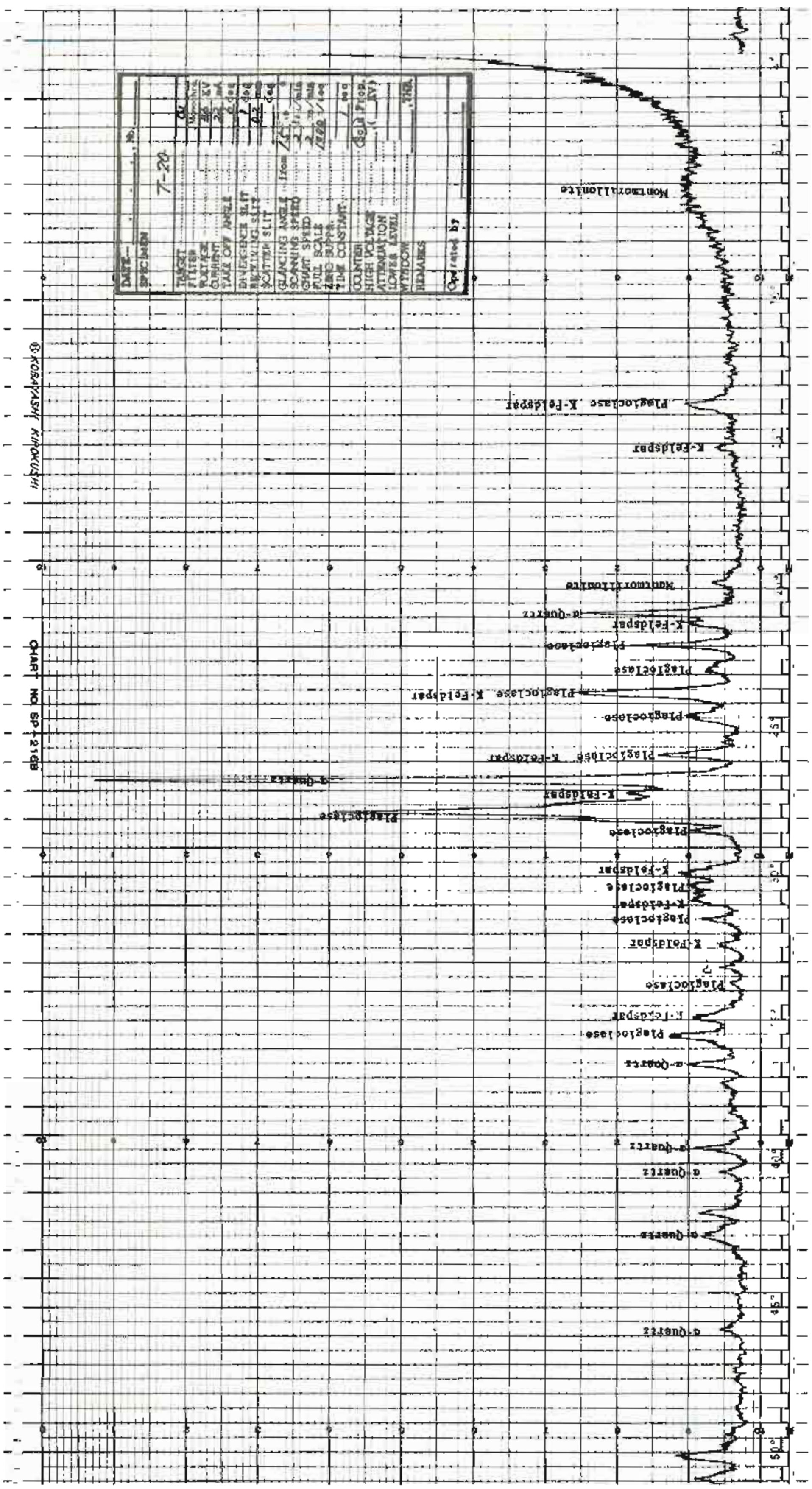
7-20
Montmorillonite
Plagioclase K-Feldspar
K-Feldspar
Montmorillonite
α-Quartz
K-Feldspar
Plagioclase
Plagioclase
Plagioclase K-Feldspar
Plagioclase
Plagioclase K-Feldspar
α-Quartz
K-Feldspar
Plagioclase
Plagioclase
K-Feldspar
Plagioclase
K-Feldspar
Plagioclase
K-Feldspar
Plagioclase
K-Feldspar
Plagioclase
α-Quartz
α-Quartz
α-Quartz
α-Quartz
α-Quartz
KOBAYASHI KIROKUSHI
CHART NO SP-216B

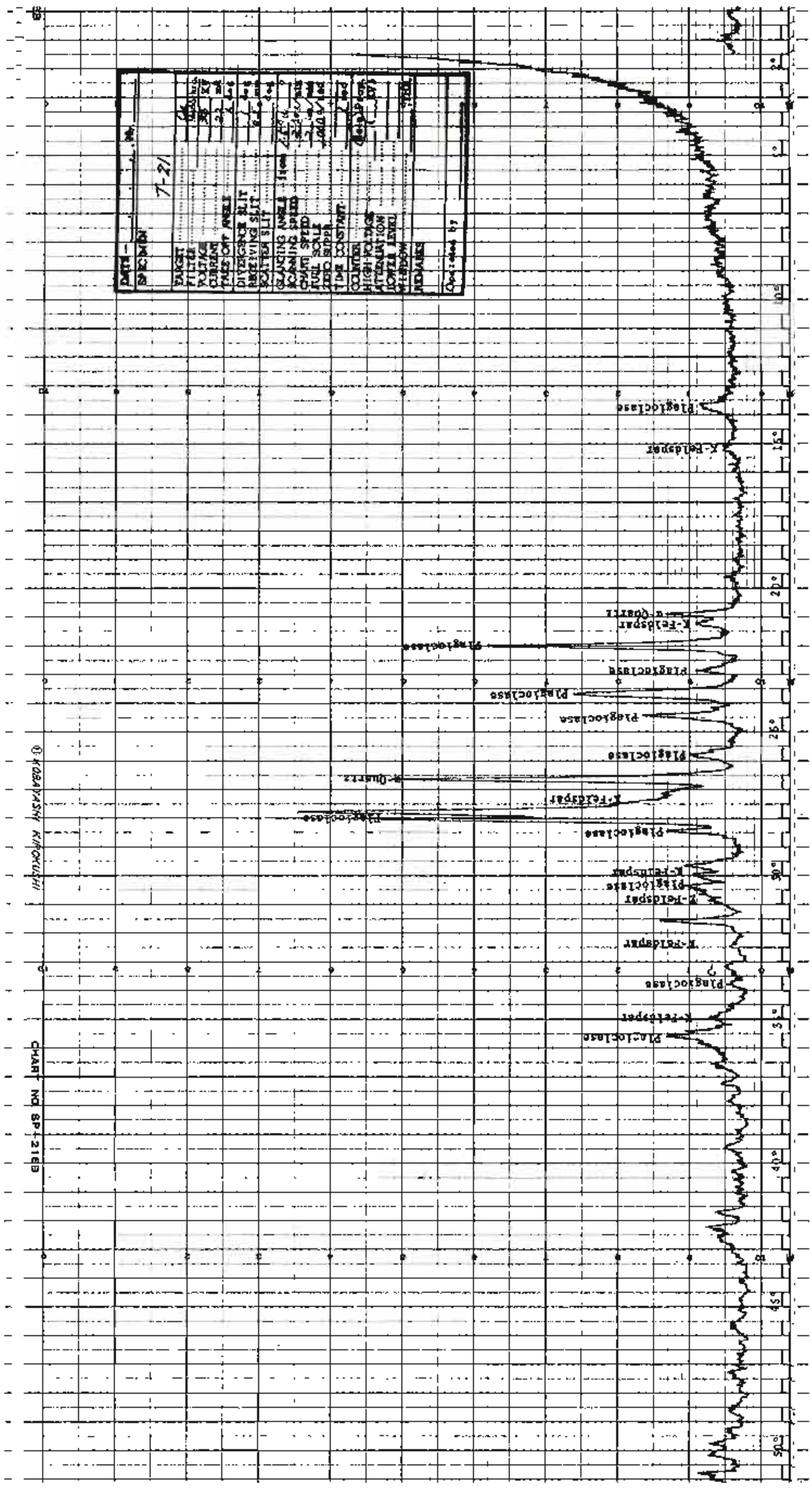

7-21
Plagioclase
K-Feldspar
α-Quartz
CHART NO. SP-216B

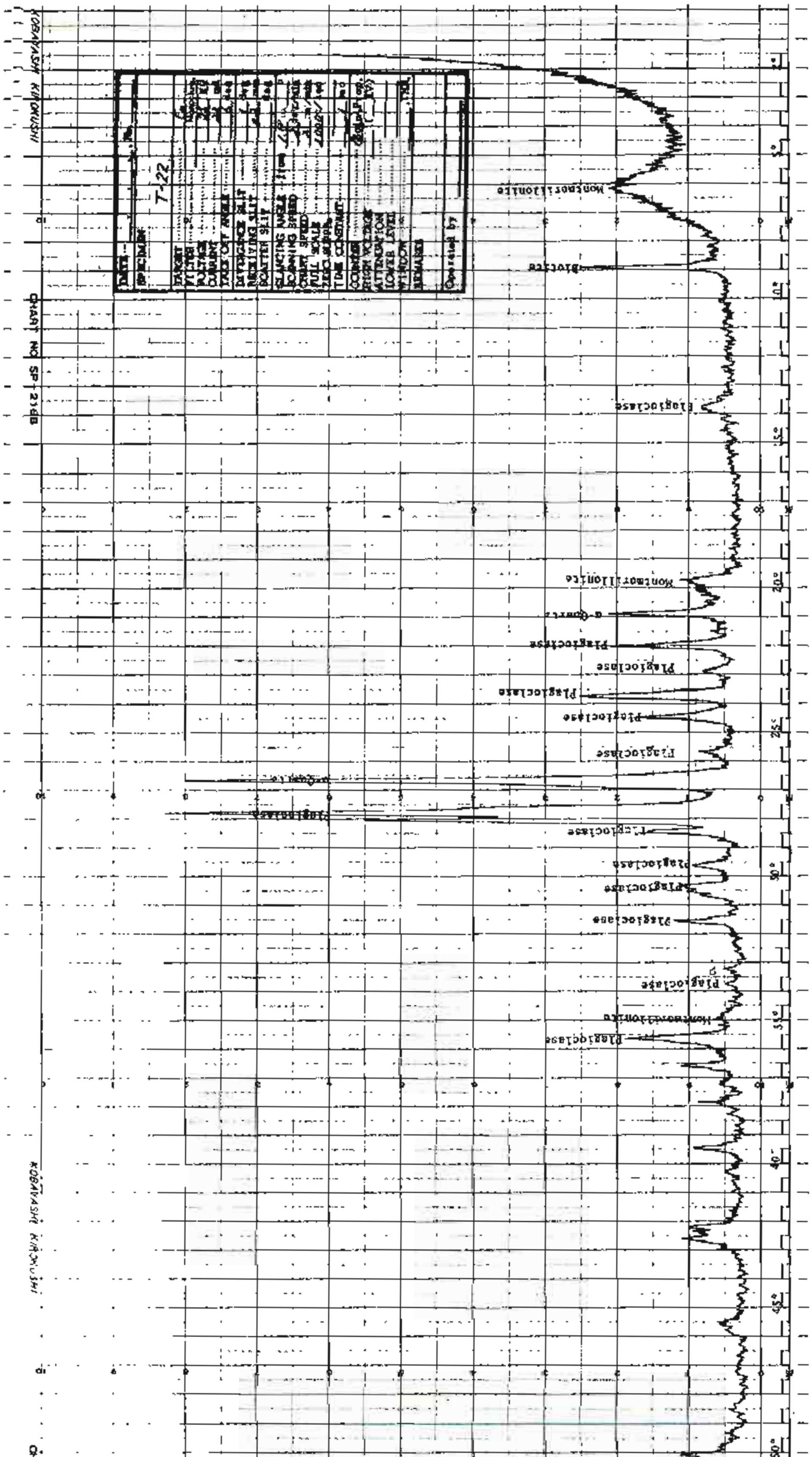
KOBAYASHI KIROKUSHI
CHART NO SP-21dB
T-22
Montmorillonite
Plagioclase
α-Quartz

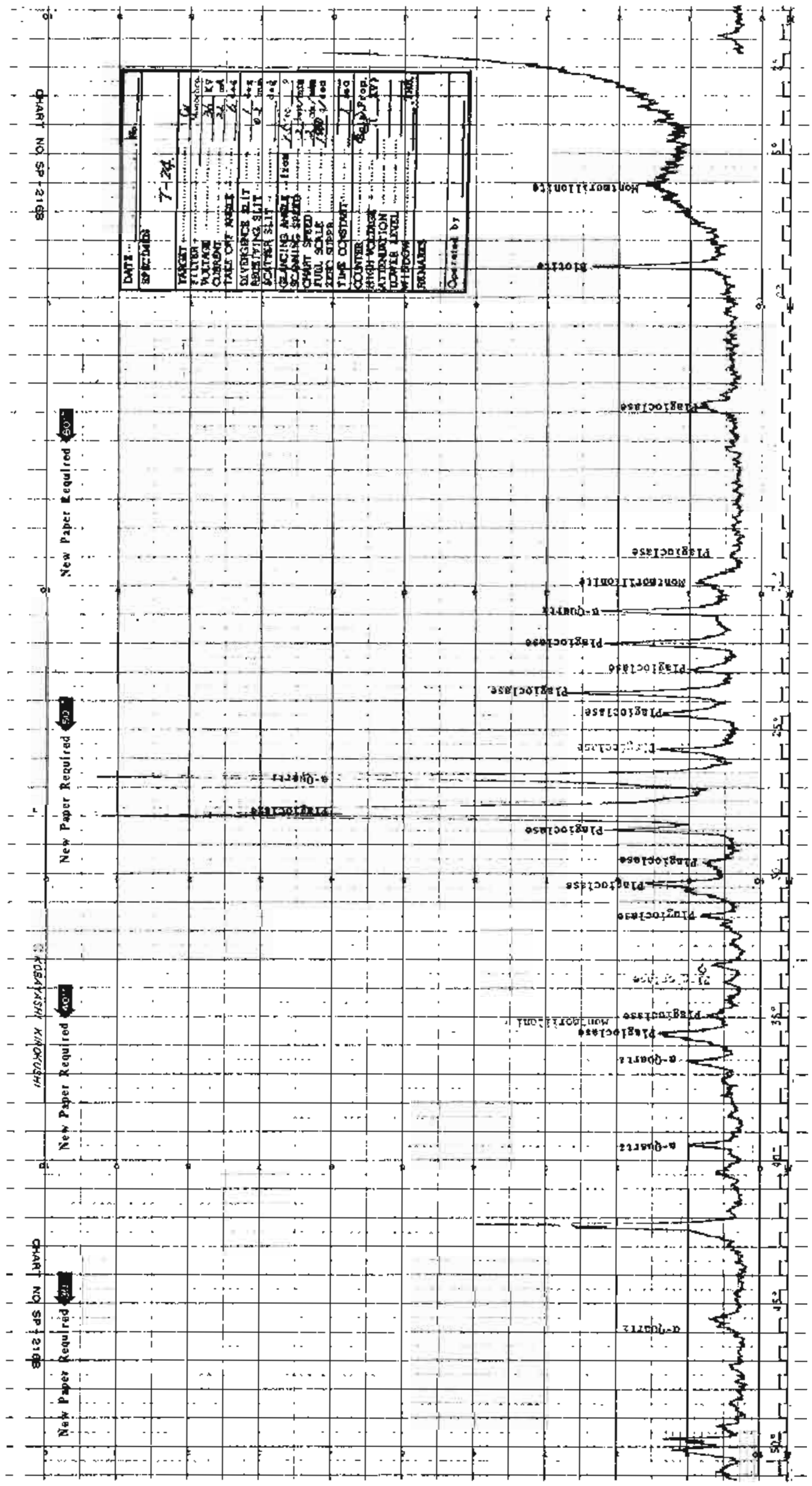

CHART NO SP-2168
New Paper Required
7-24
Montmorillonite
Biotite
Plagioclase
α-Quartz

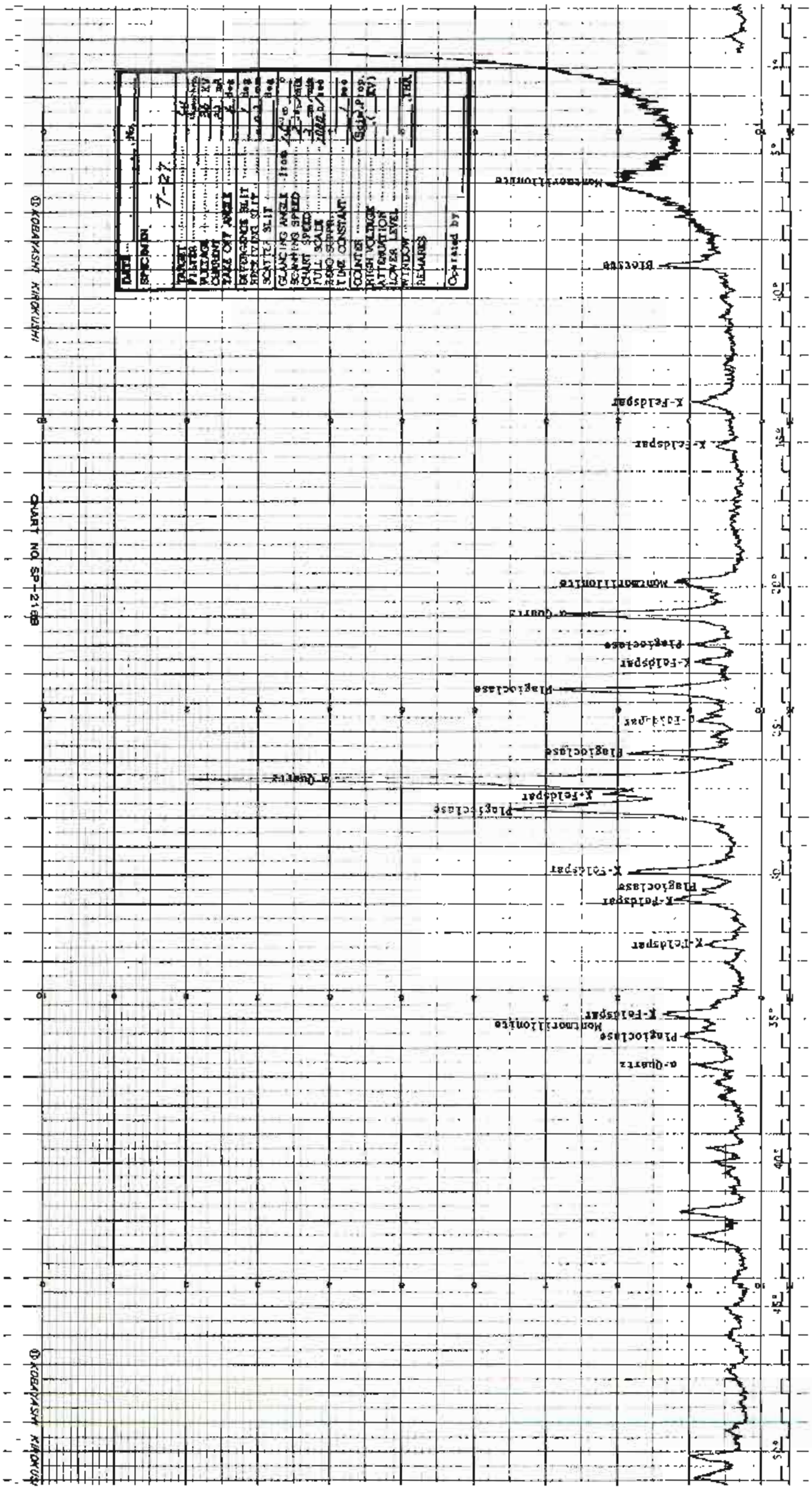

KOBAYASHI KIROKUSHI
CHART NO. SP-21GB
SPECIMEN 7-27
Montmorillonite
Biotite
K-Feldspar
K-Feldspar
Montmorillonite
α-Quartz
Plagioclase
K-Feldspar
Plagioclase
K-Feldspar
Plagioclase
α-Quartz
K-Feldspar
Plagioclase
K-Feldspar
Plagioclase
K-Feldspar
K-Feldspar
K-Feldspar
Montmorillonite
Plagioclase
α-Quartz
5°
10°
15°
20°
25°
30°
35°
40°
45°
50°

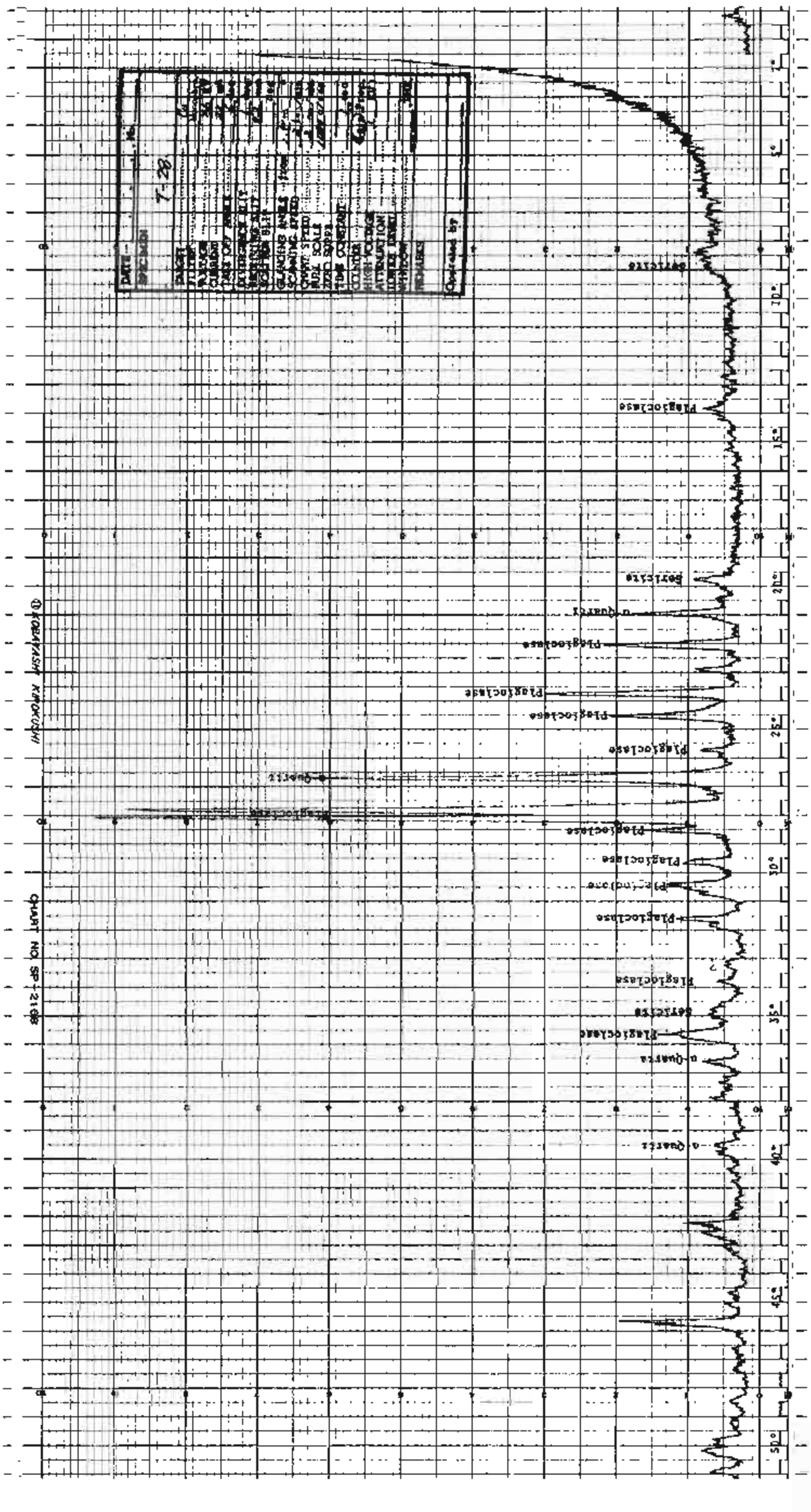

KOBAYASHI KIROKUSHI
CHART NO. SP-2108
T-28
Sericite
Plagioclase
α-Quartz
Quartz

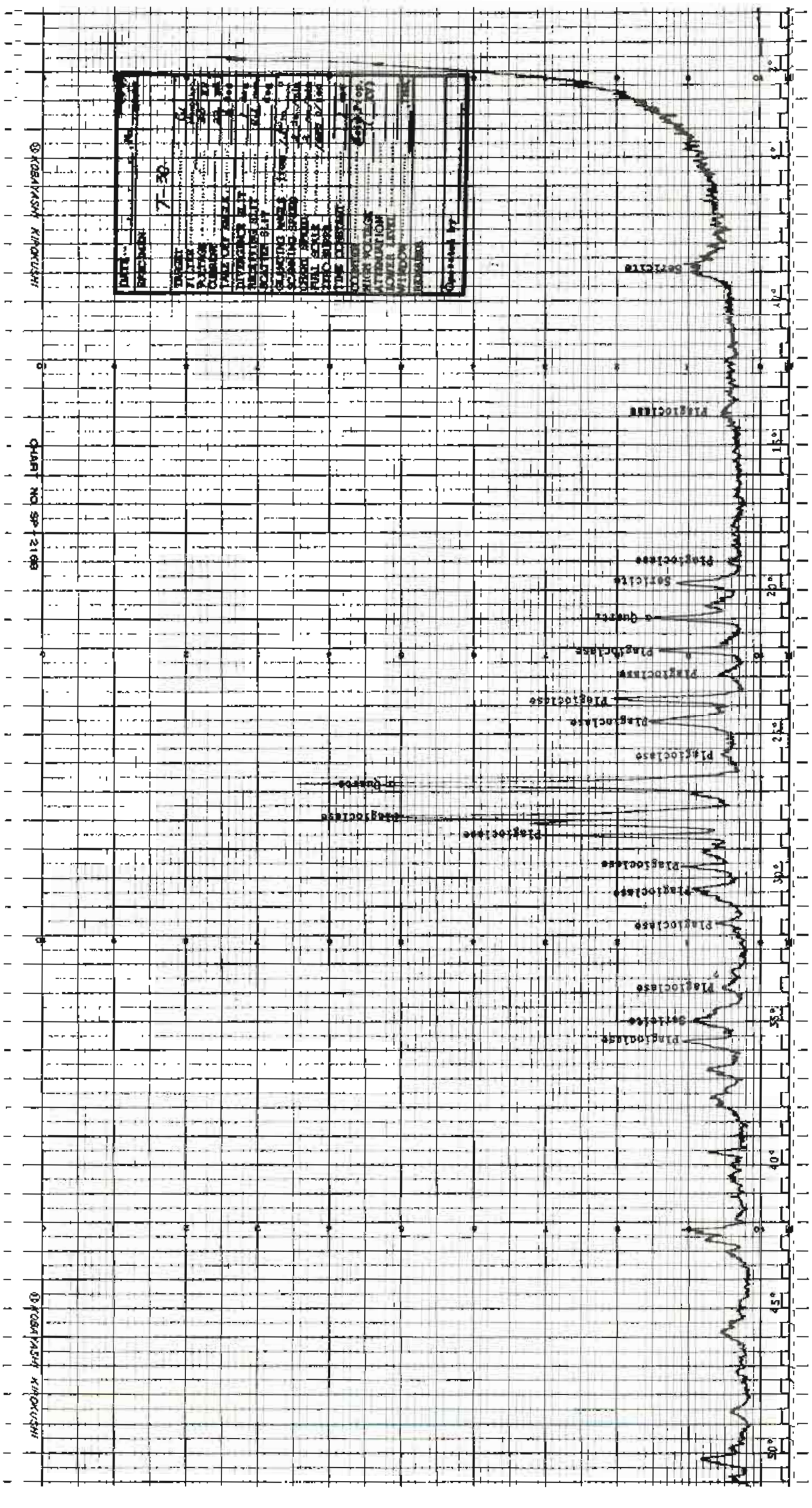
KOBAYASHI KIROKUSHI
CHART NO. SP-2168
7-30
Sericite
Plagioclase
Plagioclase
Sericite
α-Quartz
Plagioclase
Plagioclase
Plagioclase
Plagioclase
Plagioclase
α-Quartz
Plagioclase
Plagioclase
Plagioclase
Plagioclase
Plagioclase
Plagioclase
Sericite
Plagioclase
5°
10°
15°
20°
25°
30°
35°
40°
45°
50°

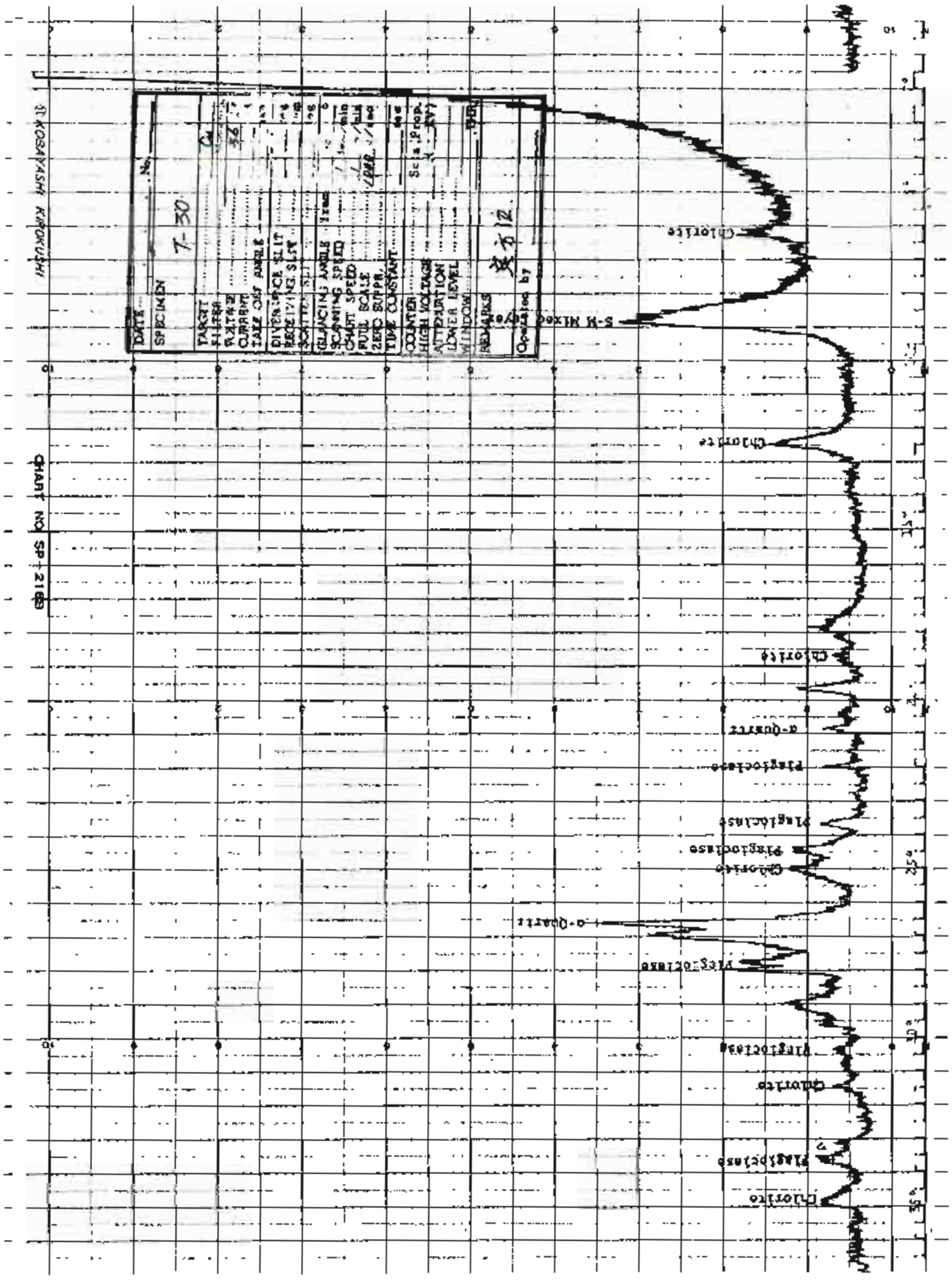

KOBAYASHI KIROKUSHI
CHART NO. SP-21
SPECIMEN
T-30
Chlorite
S-M Mixed
Chlorite
Chlorite
α-Quartz
Plagioclase
Plagioclase
Plagioclase
Chlorite
α-Quartz
Plagioclase
Plagioclase
Chlorite
Plagioclase
Chlorite

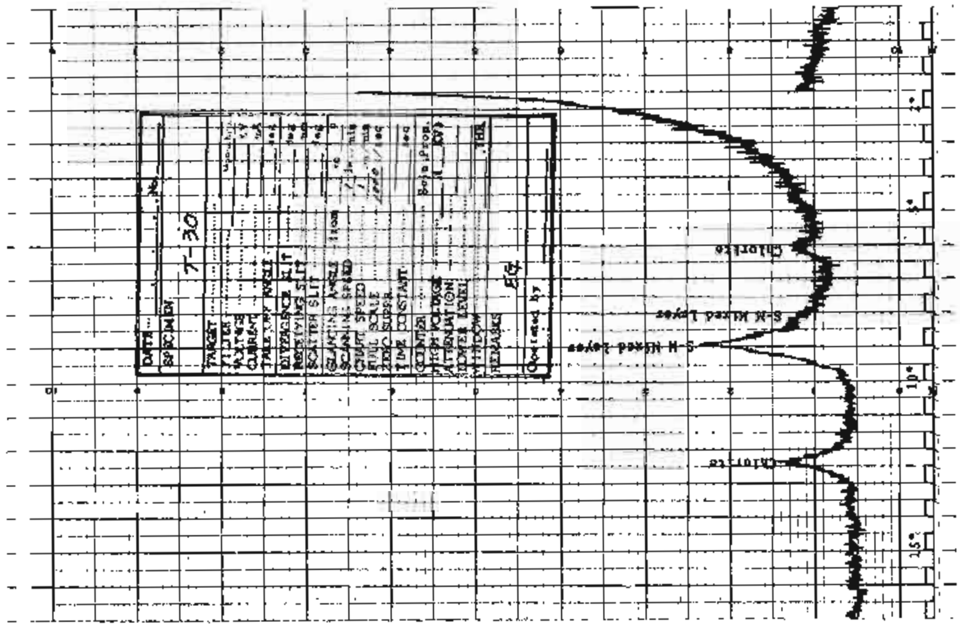
T-30
Chlorite
S-M Mixed Layer
Chlorite
S-M Mixed Layer

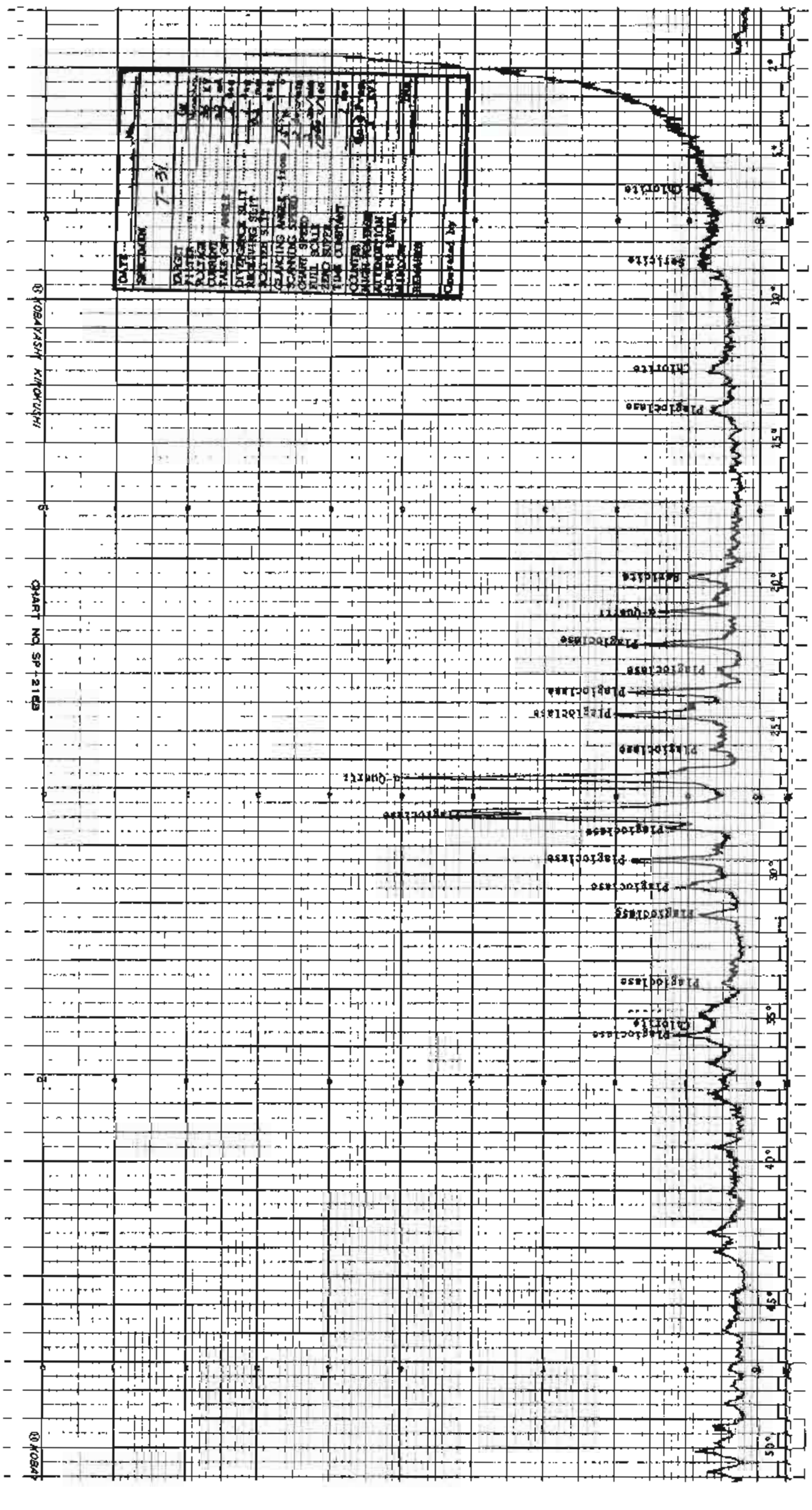
KOBAYASHI KIROKUSHI
CHART NO. SP-21
T-31
Chlorite
Sericite
Chlorite
Plagioclase
Sericite
α-Quartz
Plagioclase
Plagioclase
Plagioclase
Plagioclase
Plagioclase
α-Quartz
Plagioclase
Plagioclase
Plagioclase
Plagioclase
Plagioclase
Plagioclase
Chlorite
Plagioclase
5°
10°
15°
20°
25°
30°
35°
40°
45°
50°

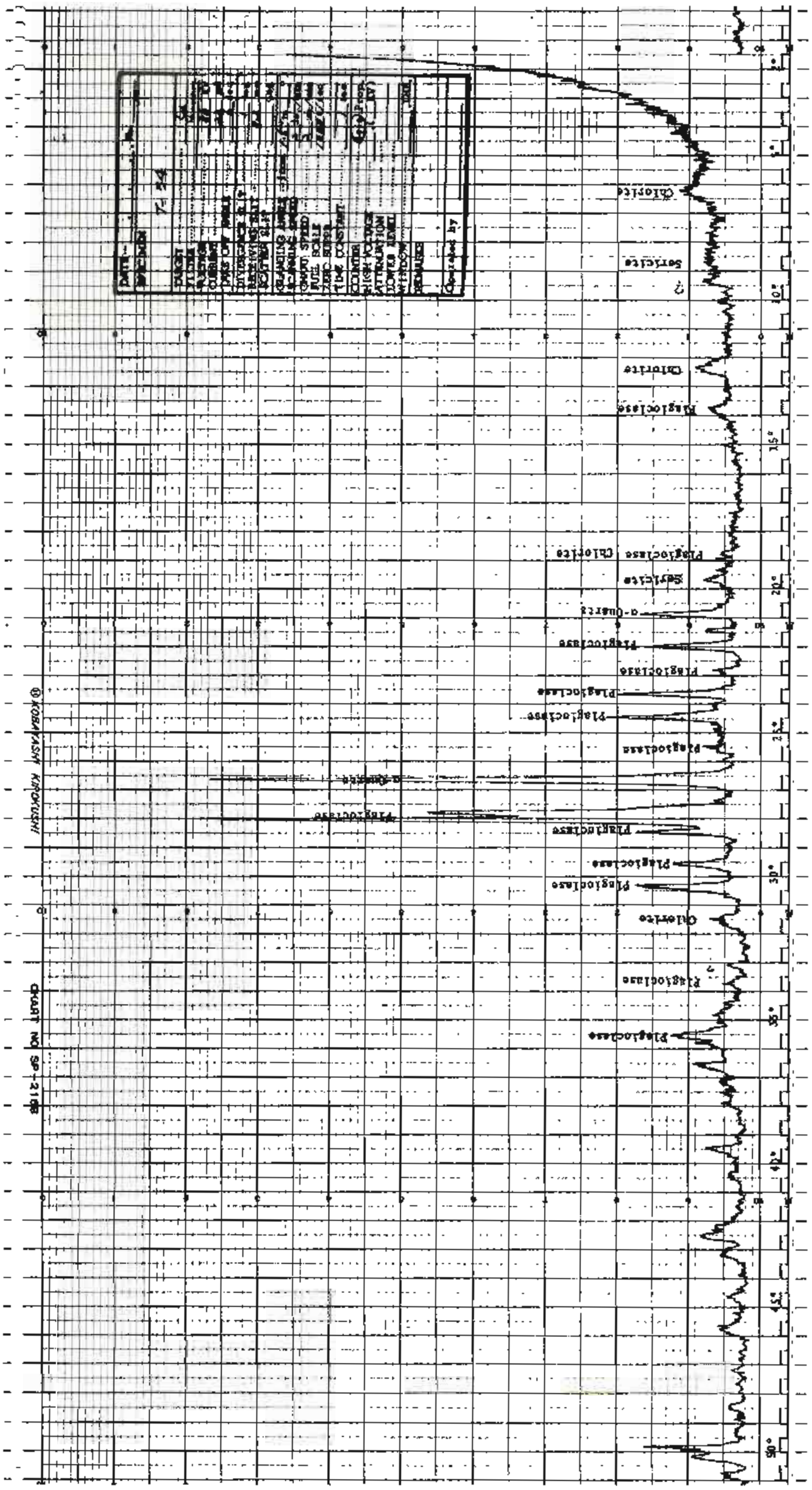
T-24
Chlorite
Sericite
Chlorite
Plagioclase
Plagioclase Chlorite
Sericite
α-Quartz
Plagioclase
Plagioclase
Plagioclase
Plagioclase
Plagioclase
α-Quartz
Plagioclase
Plagioclase
Plagioclase
Plagioclase
Chlorite
Plagioclase
Plagioclase
5°
10°
15°
20°
25°
30°
35°
40°
45°
50°
KOBAYASHI KIROKUSHI
CHART NO. SP-21DB

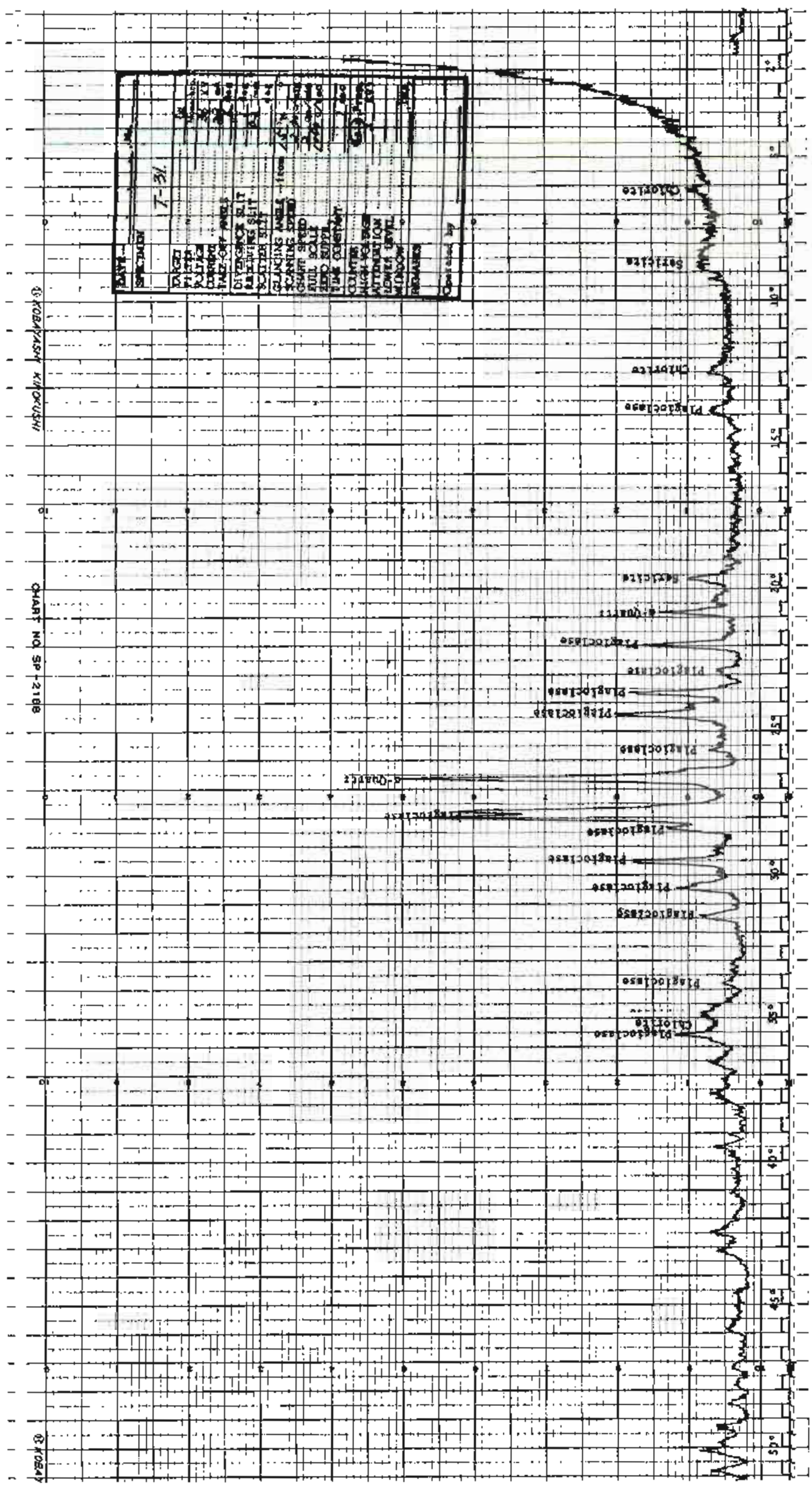
KOBAYASHI KIROKUSHI
CHART NO. SP-2188
T-31
Chlorite
Sericite
Chlorite
Plagioclase
Sericite
α-Quartz
Plagioclase
Plagioclase
Plagioclase
Plagioclase
Plagioclase
α-Quartz
Plagioclase
Plagioclase
Plagioclase
Plagioclase
Plagioclase
Plagioclase
Chlorite
Plagioclase

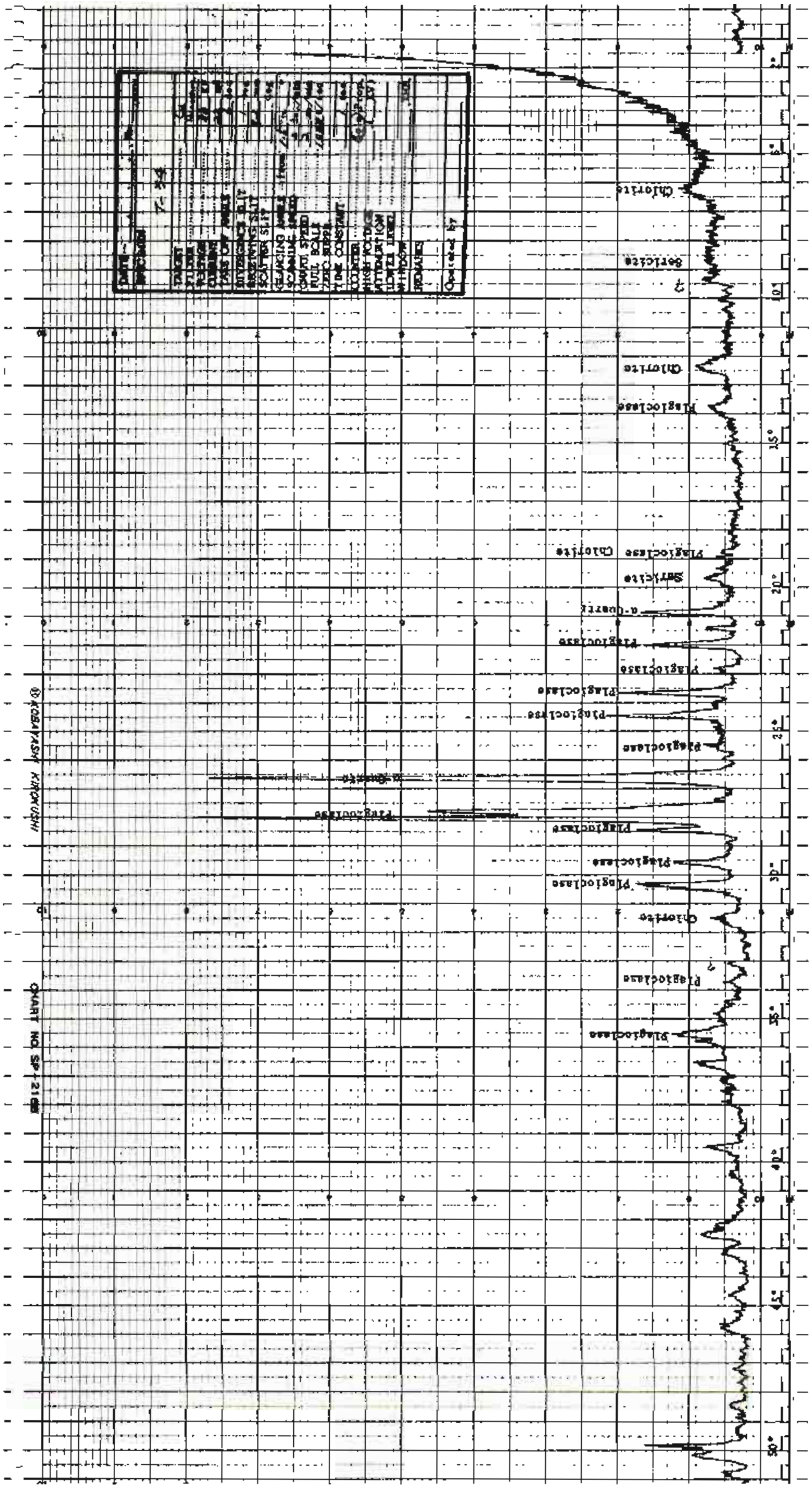
Chlorite
Sericite
Chlorite
Plagioclase
Plagioclase
Chlorite
Sericite
α-Quartz
Plagioclase
Plagioclase
Plagioclase
Plagioclase
Plagioclase
α-Quartz
Plagioclase
Plagioclase
Plagioclase
Plagioclase
Chlorite
Plagioclase
Plagioclase
KOBAYASHI KIROKUSHI
CHART NO. SP-216B

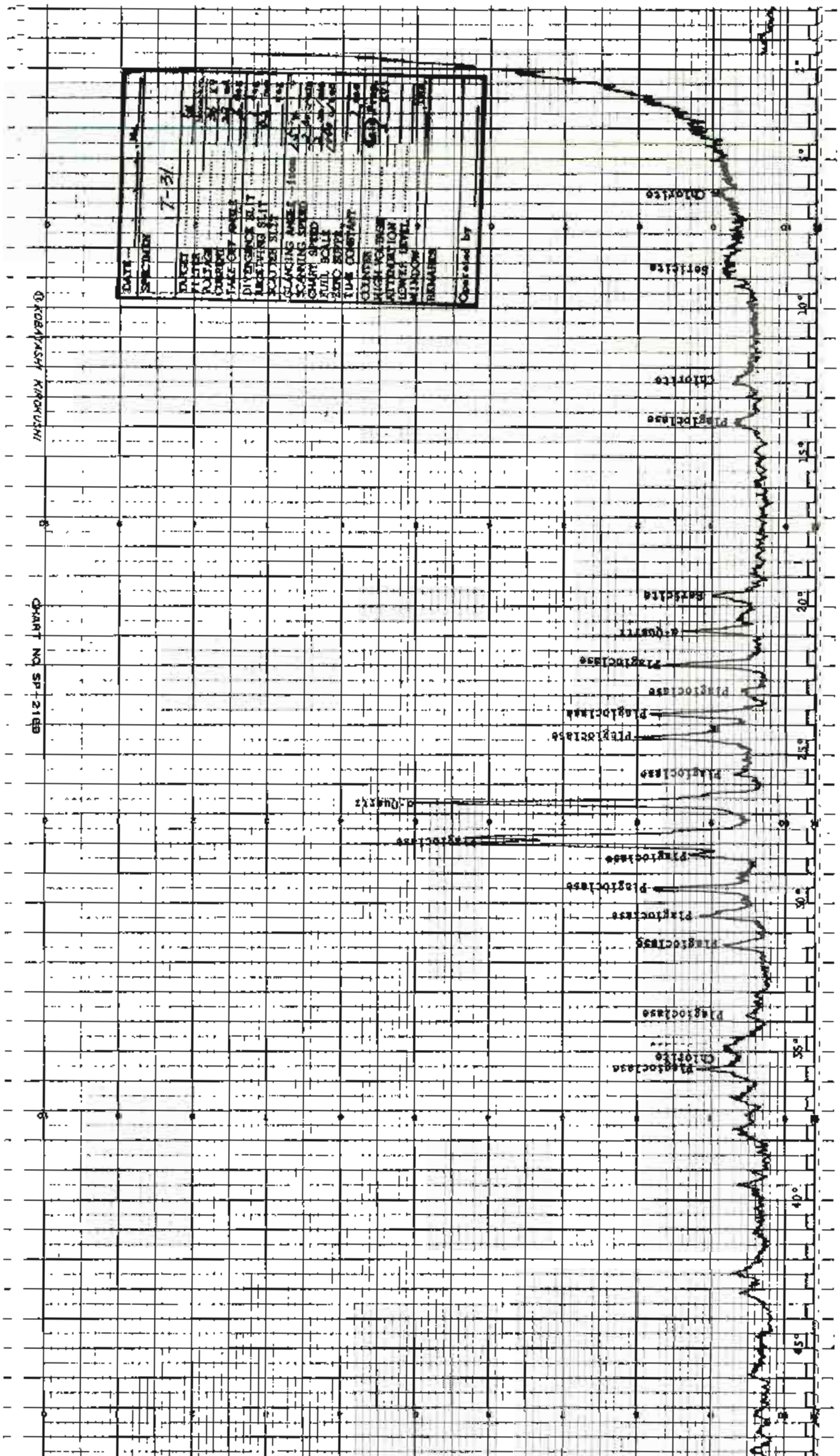

KOBAYASHI KIROKUSHI
CHART NO. SP-21BB
7-31
Chlorite
Sericite
Chlorite
Plagioclase
Sericite
α-Quartz
Plagioclase
Plagioclase
Plagioclase
Plagioclase
Plagioclase
α-Quartz
Plagioclase
Plagioclase
Plagioclase
Plagioclase
Plagioclase
Plagioclase
Chlorite
Plagioclase

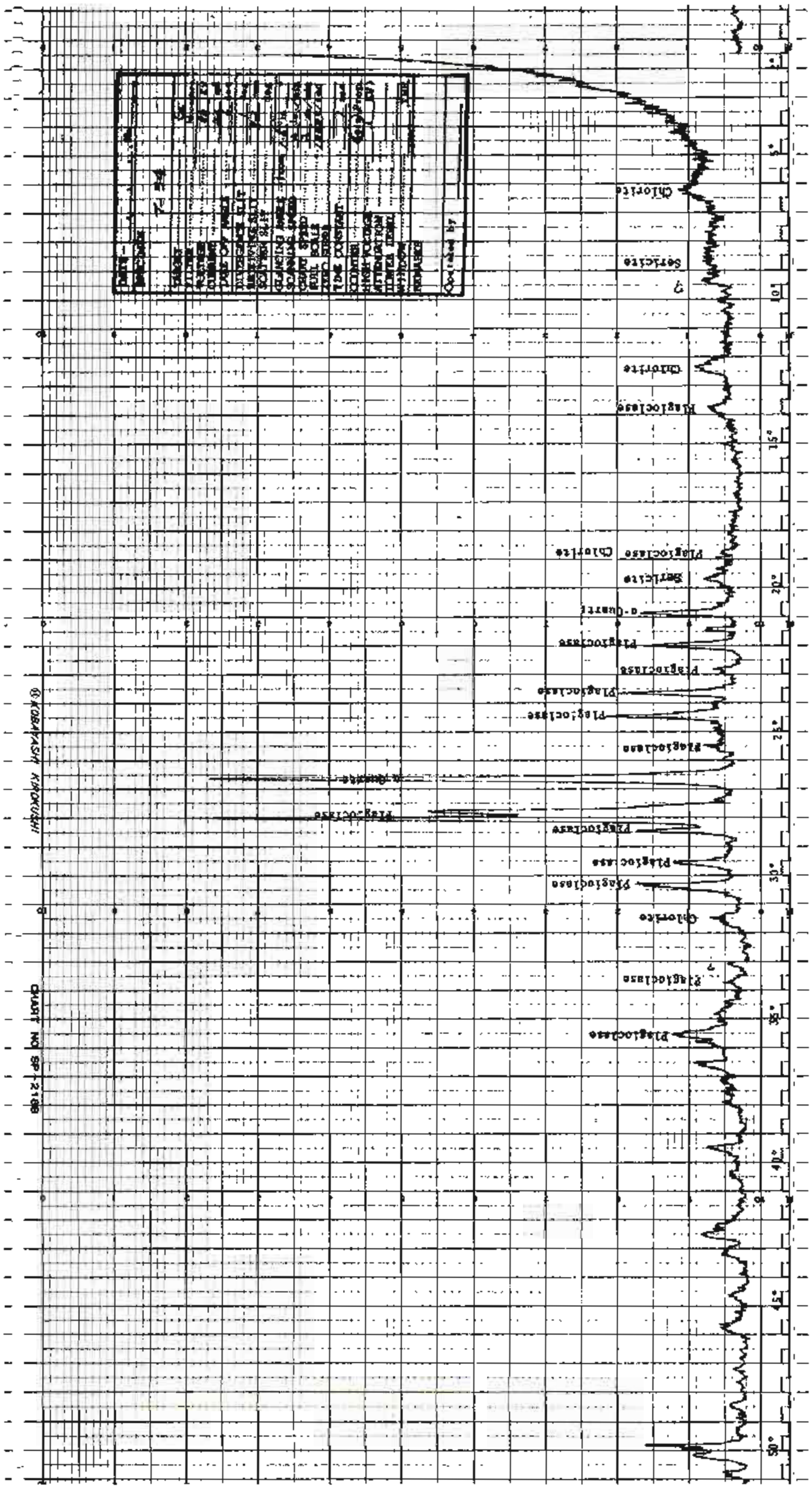
Chlorite
Sericite
Plagioclase
α-Quartz
© KOBAYASHI KIROKUSHI
CHART NO SP-2168
5°
10°
15°
20°
25°
30°
35°
40°
45°
50°

MICROSCOPIC PHOTOGRAPHS

Sample No. T-3 , 186m to 192m

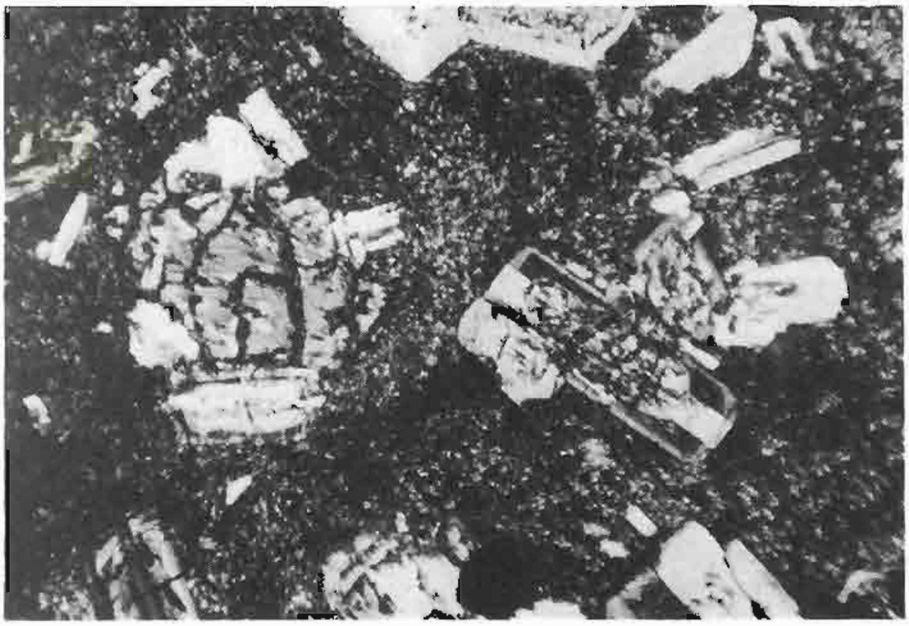

Two pyroxene andesite

x 40

Open nicols

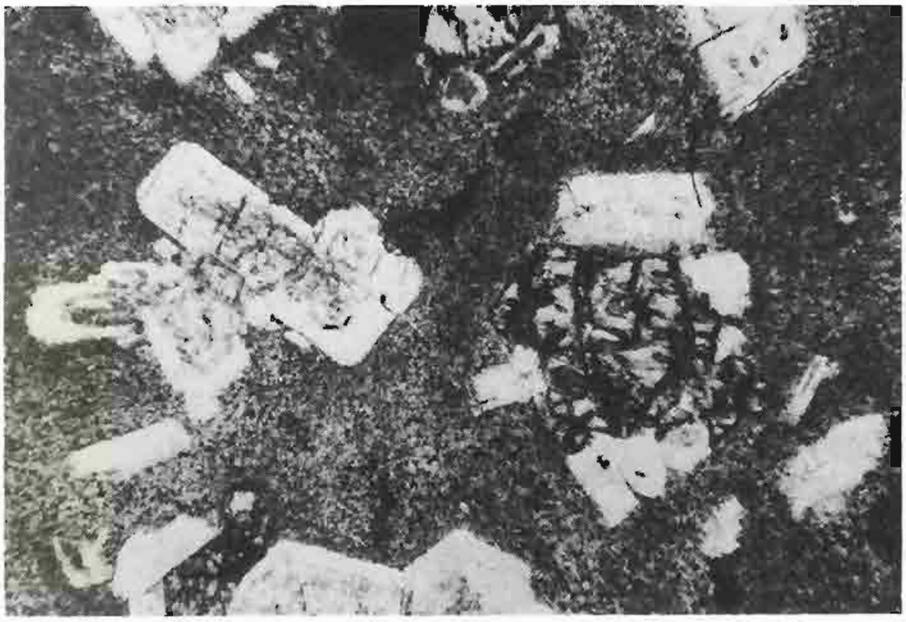

x 40

Cross nicols

Microscopic observation

: Weakly altered(montmorillonite) hyperthen, left phenocryst,and plagioclase, right pheno.

Sample No. T-4 , 215m to 221m

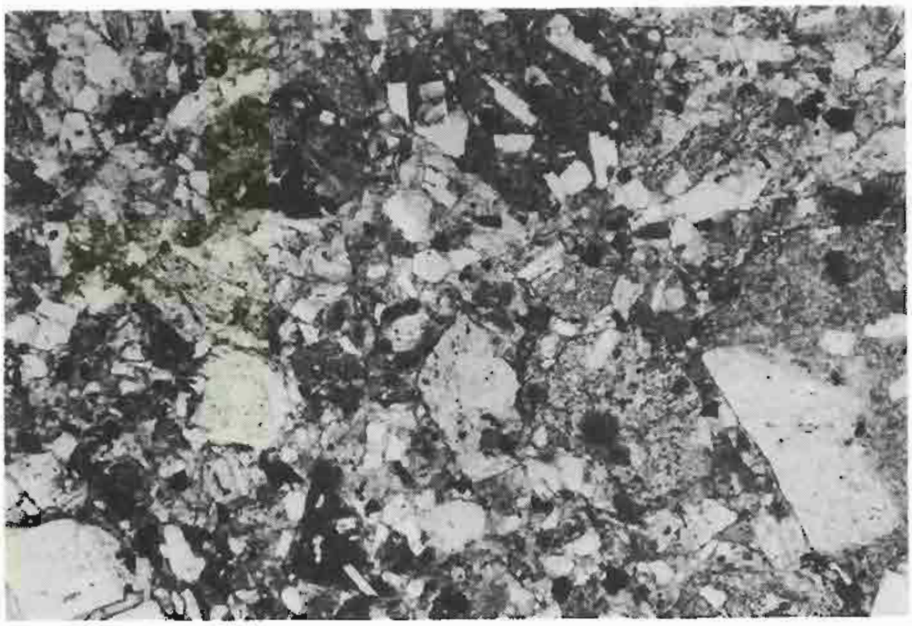

Andesitic coarse grained tuff

x 40

Open nicols

x 40

Cross nicols

Microscopic observation

: Pyroclastics consist of fragments of plagioclase and mafic crystal , glass and rock.
Matrix is consist of secondary montmorillonite.

Sample No. T-5 , 243m to 247m

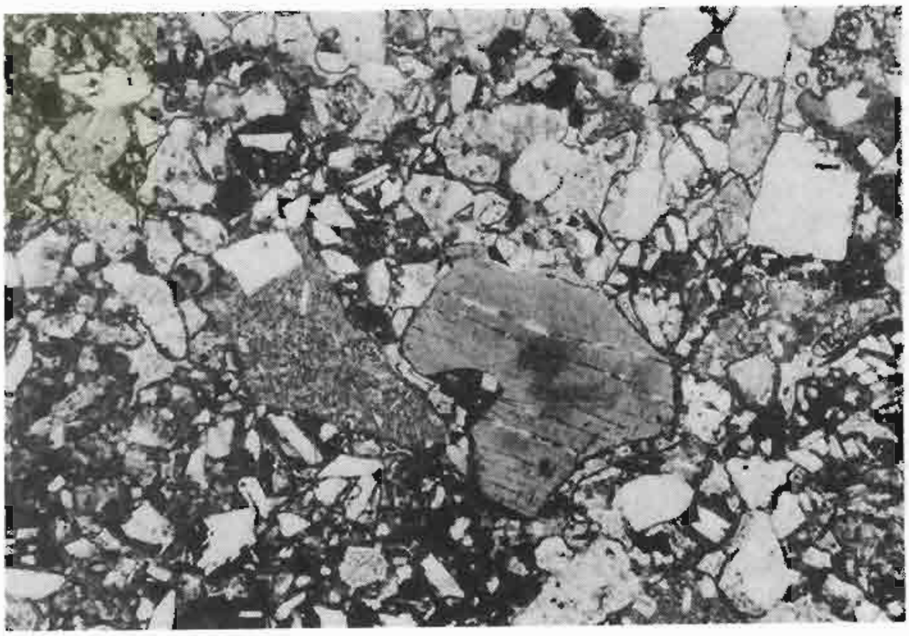

Andesitic coarse grained tuff

x 40

Open nicols

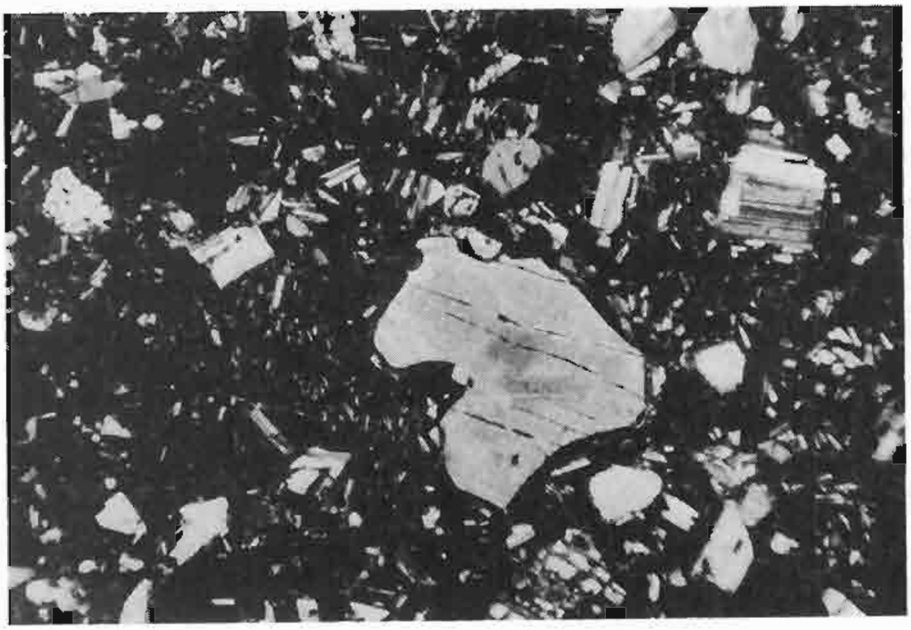

x 40

Cross nicols

Microscopic observation

: Pyroclastics containing large amounts of andesite breccia , glass fragments and crystal fragments of plagioclase , pyroxene and biotite.
Weak alteration of montmorillonite is recognized.

Sample No. T-7 , 315m to 320m

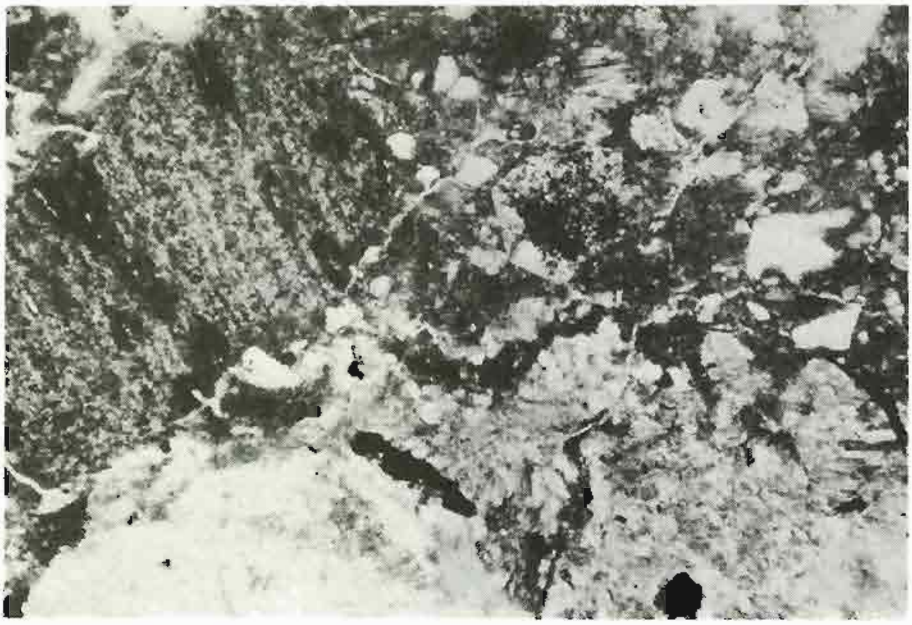

Andesitic coarse grained tuff

x 40

Open nicols

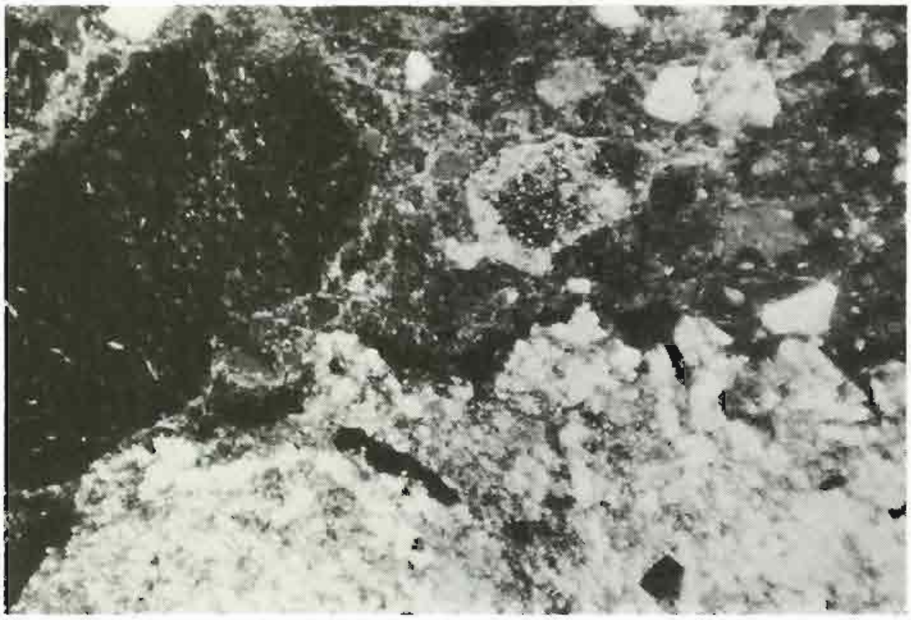

x 40

Cross nicols

Microscopic observation

: Plagioclase is main constituent crystal fragment and besides of it a small amount of quartz , K-feldspar are observed.
Pyroxene andesite and rhyolitic or dacitic rocks (left) are included.

Sample No. T-9 , 368m to 373m

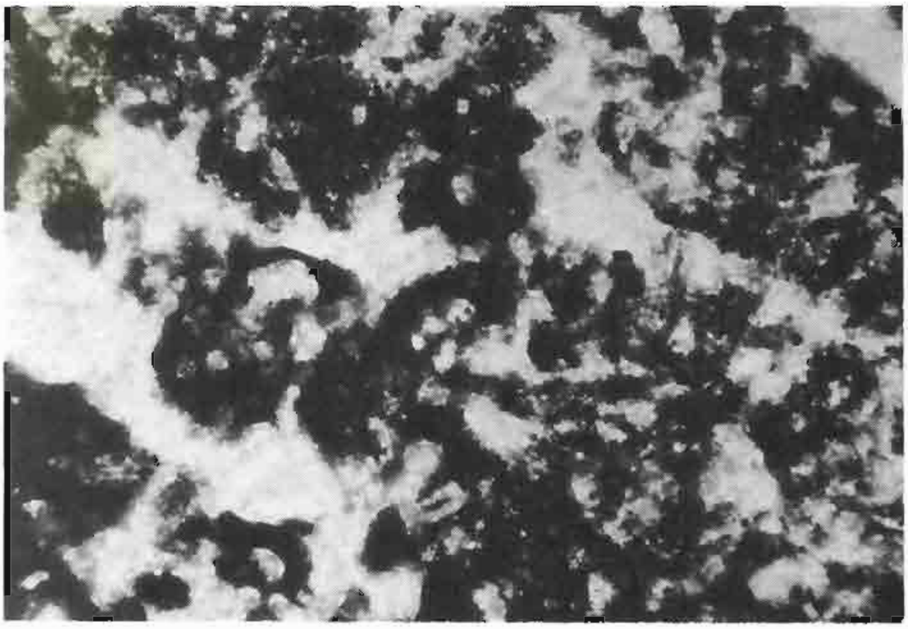

Fine grained tuff ?

x 130

Open nicols

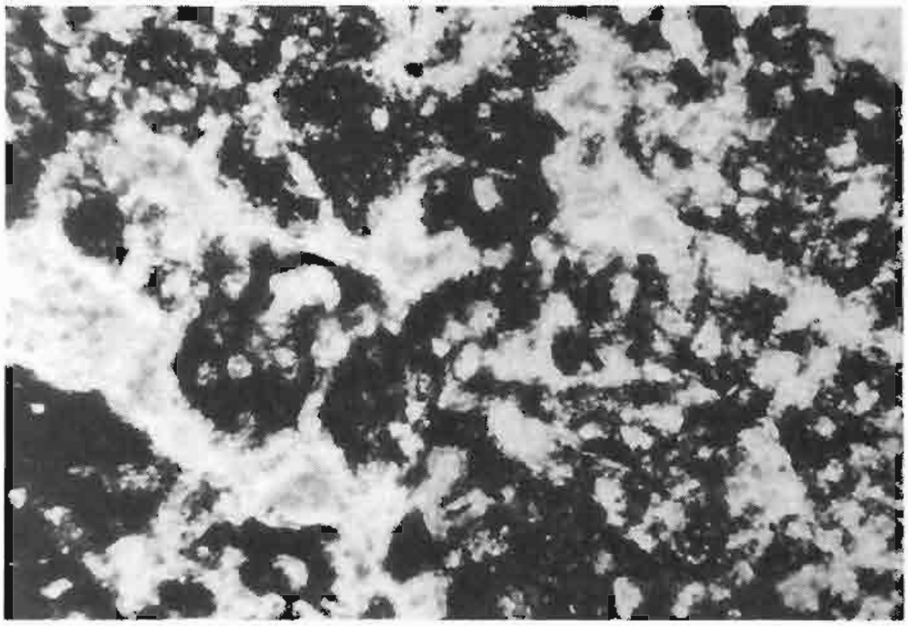

x 130

Cross nicols

Microscopic observation

: The rock is consist of fine grained opaque mineral (hematite ?) , clay mineral and calcite.

Sample No. T-10 , 402m to 404m

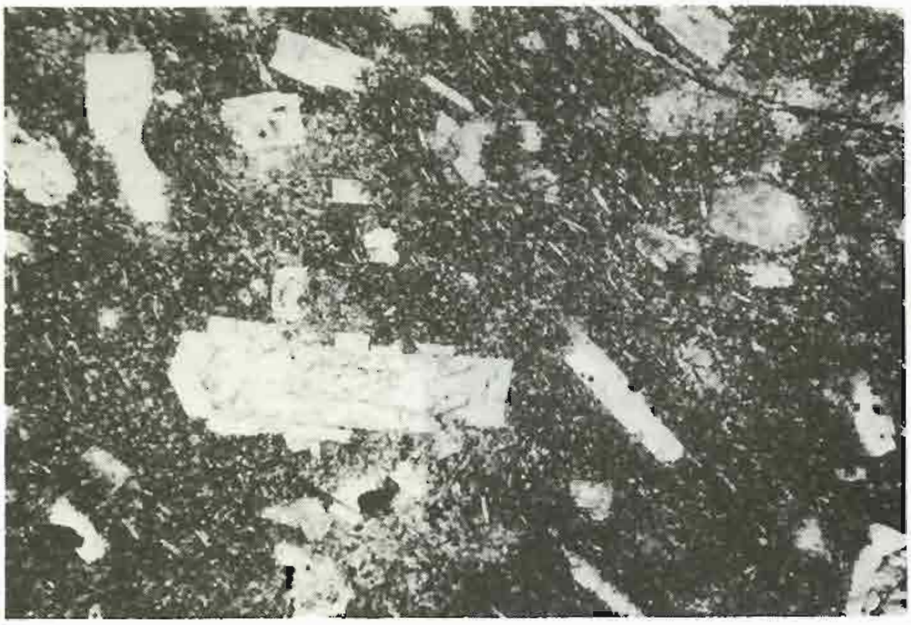

Pyroxene andesite

x 40

Open nicols

x 40

Cross nicols

Microscopic observation

: Pyroxene andesite characterized by the orientated arrangement of feldspar in the groundmass. Montmorillonite is observed along the crack and the clearvage of phenocrysts.

Sample No. T-13 , 489m to 492m

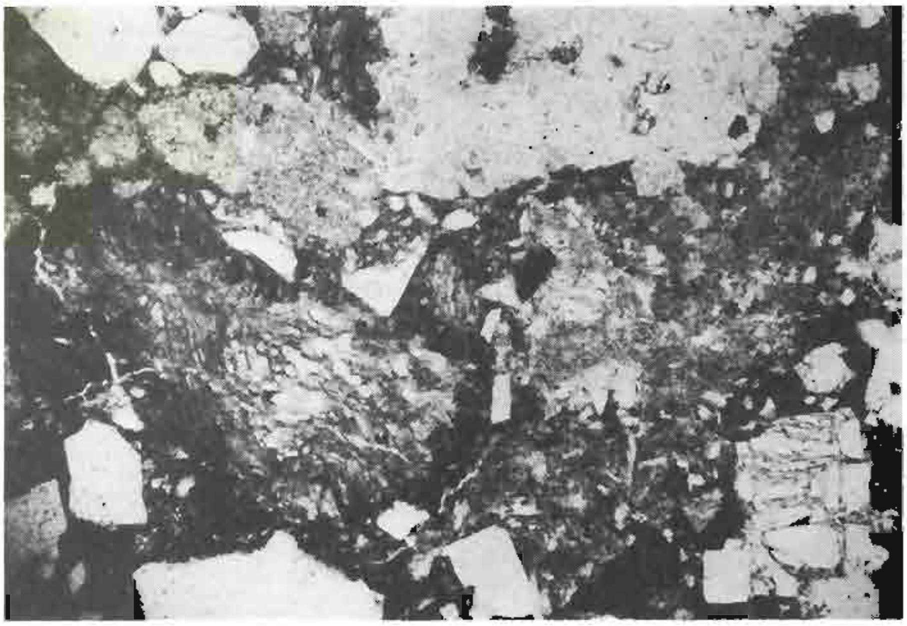

Dacitic lapilli tuff

x 40

Open nicols

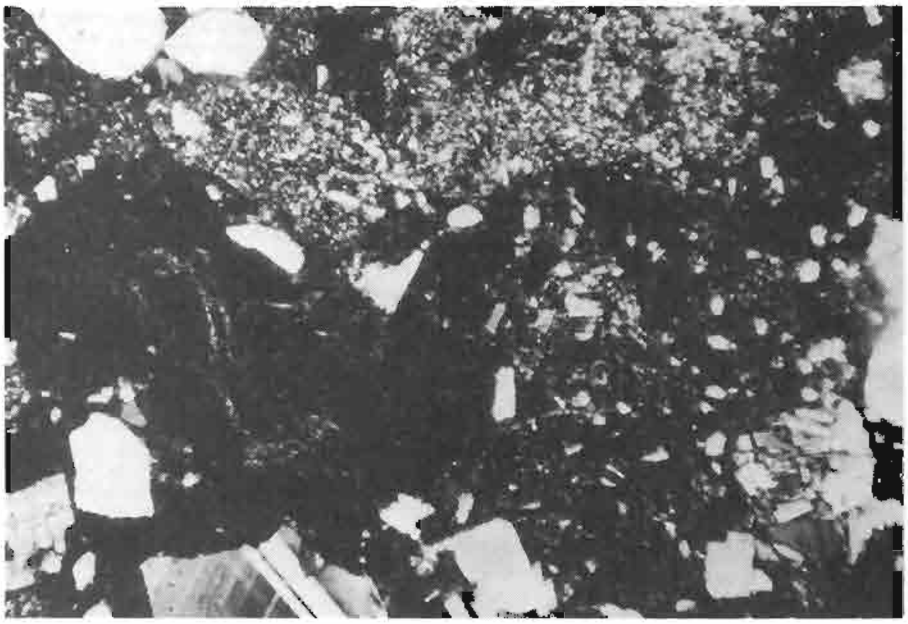

x 40

Cross nicols

Microscopic observation

: The lapilli tuff is characterized to contain a large amount of pumice. Breccia included is andesitic rock , and crystal flakes are plagioclase, opaque mineral and small amount of biotite. Pumice , glass and mafic mineral are completely altered to montmorillonite.

Sample No. T-15 , 550m to 552m

Andesite

x 40

Open nicols

x 40

Cross nicols

Microscopic observation

: Andesite breccia included in the formation. Mafic mineral and groundmass are completely altered to montmorillonite.

Sample No. T-16 , 580m to 583m

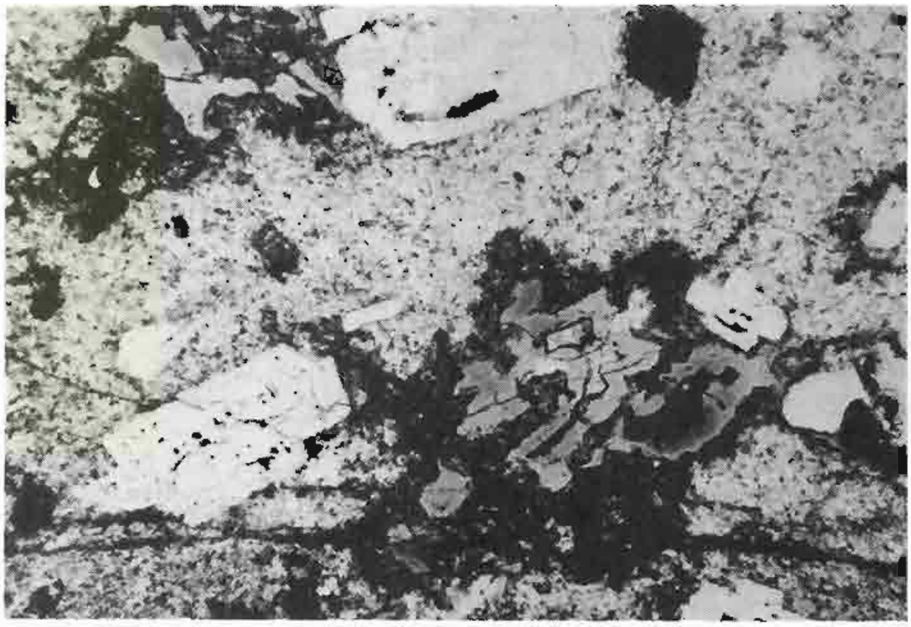

Lapilli tuff

x 40

Open nicols

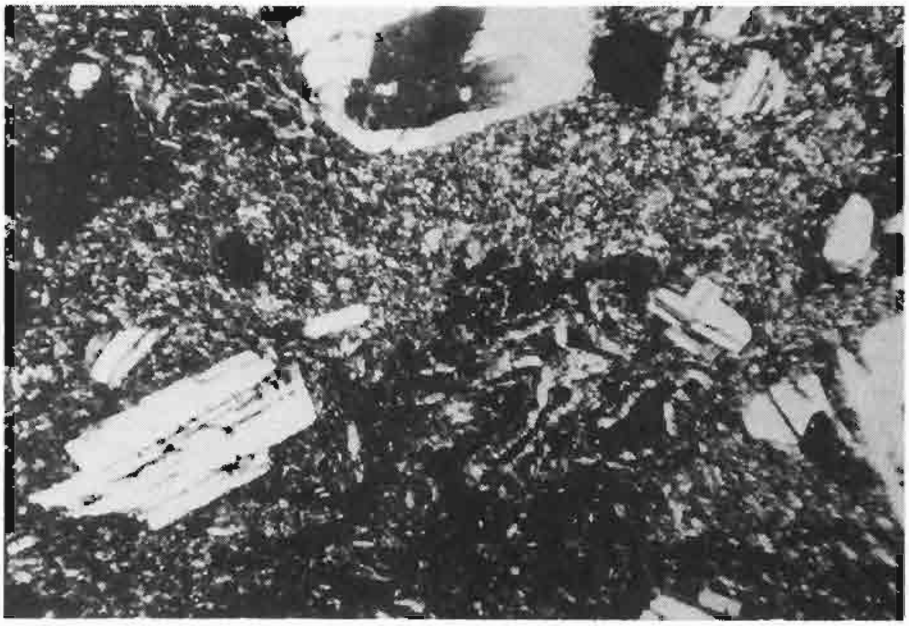

x 40

Cross nicols

Microscopic observation

: Mafic mineral and groundmass are strongly altered to montmorillonite.

Sample No. T-17 , 611m to 614m

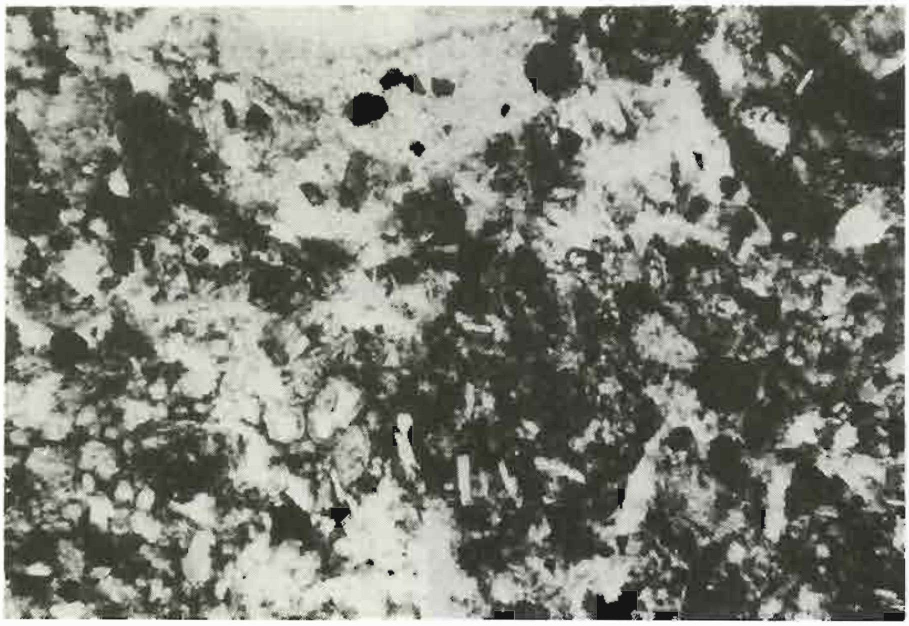

Lapilli tuff

x 40

Open nicols

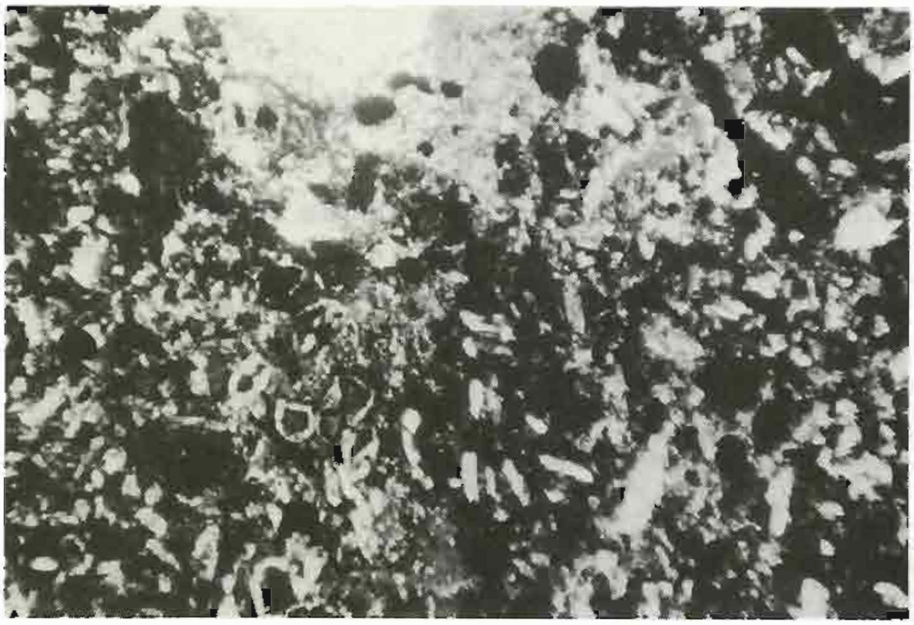

x 40

Cross nicols

Microscopic observation

: Strongly altered pyroclastic rock.
Large amounts of montmorillonite and limonite are observed in the groundmass.

Sample No. T-18 , 641m to 643m

Lapilli tuff

x 40

Open nicols

x 40

Cross nicols

Microscopic observation

: Pyroclastics rock consist of andesite , characterized by flow structure , and dacite. All of mafic mineral and groundmass are altered to montmorillonite and to silica mineral assemblage.

Sample No. T-20 , 702m to 704m

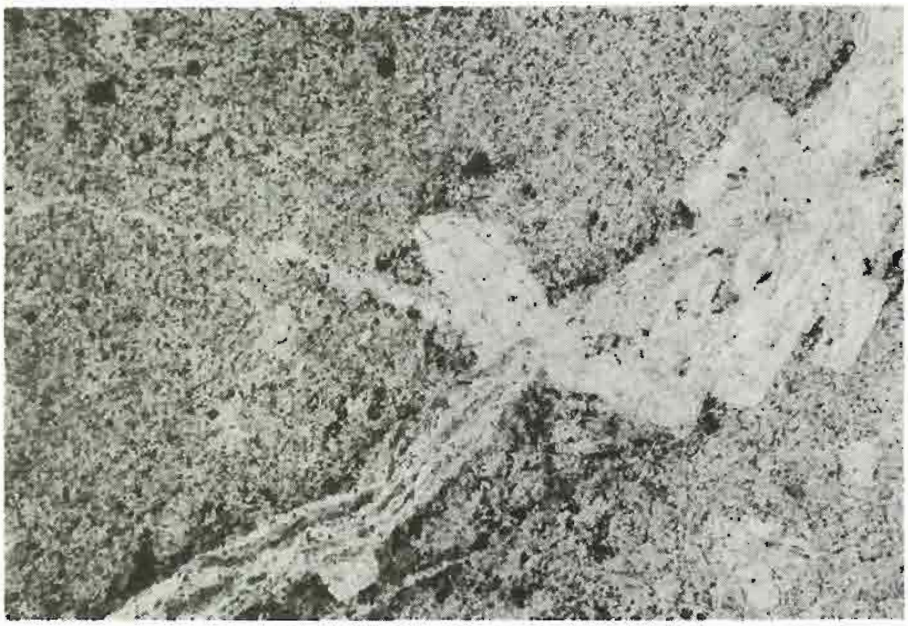

Andesite

x 40

Open nicols

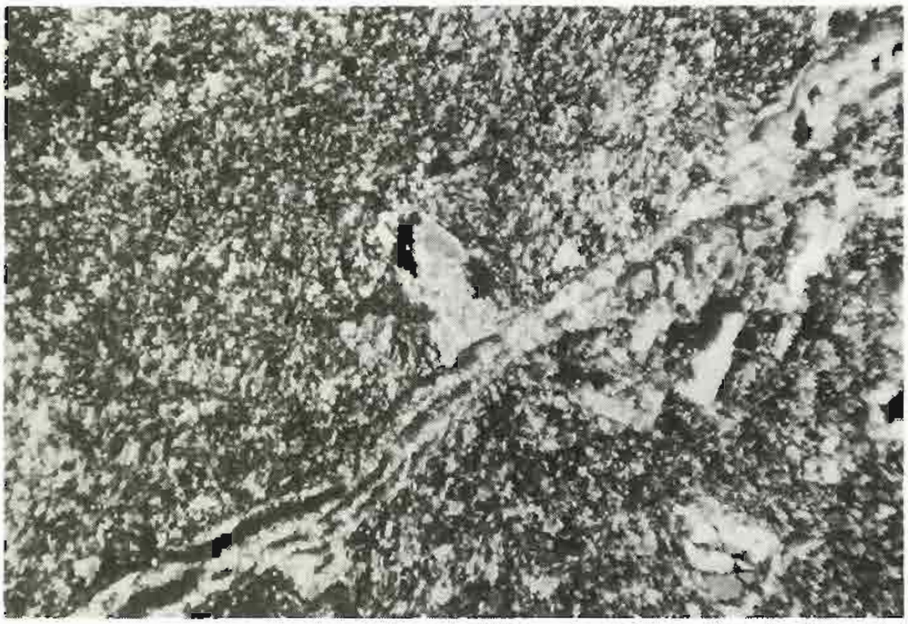

x 40

Cross nicols

Microscopic observation

: As a phenocryst plagioclase can be confirmed , and other mafic minerals are altered to montmorillonite. Groundmass consists of plagioclase , secondary fine grained quartz , montmorillonite. The vein consist of montmorillonite and fine grained secondary quartz.

Sample No. T-21 , 733m to 735m

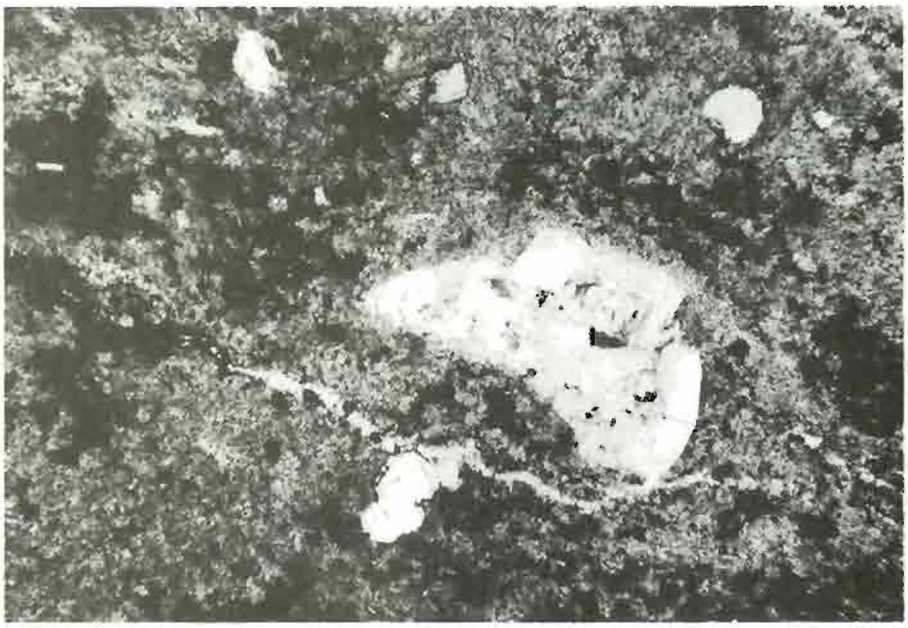

Andesite

x 40

Open nicols

x 40

Cross nicols

Microscopic observation

: The rock is characterized by fine grained andesite with few phenocryst of plagioclase showing flow structure. Groundmass consists of plagioclase , K-feldspar and opaque mineral. Mafic mineral and groundmass are altered to montmorillònite , calcite and other secondary minerals.

Secondary quartz veinlet is rarely observed.

Sample No. T-22 , 763m to 765m

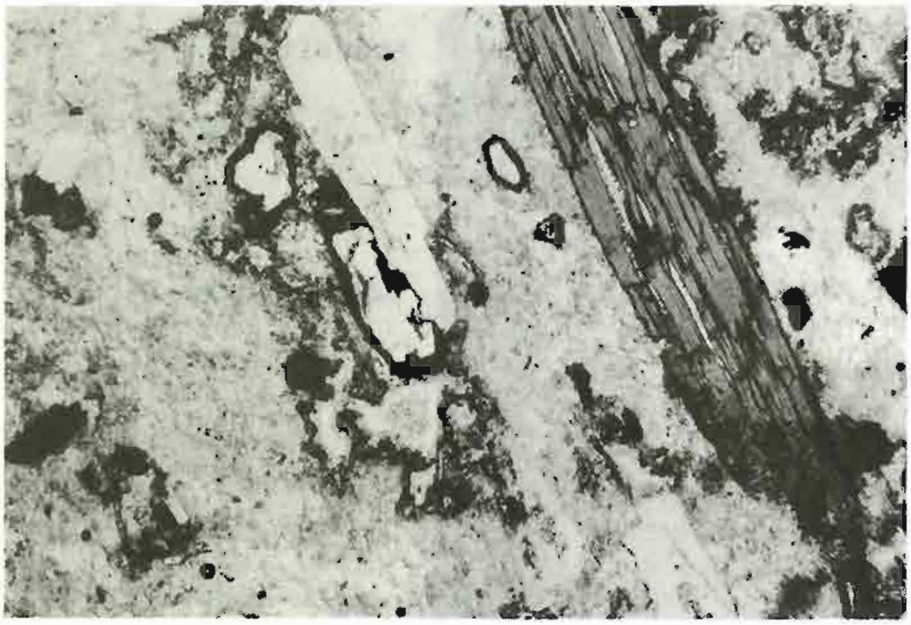

Strongly welded tuff or Dacite

x 40

Open nicols

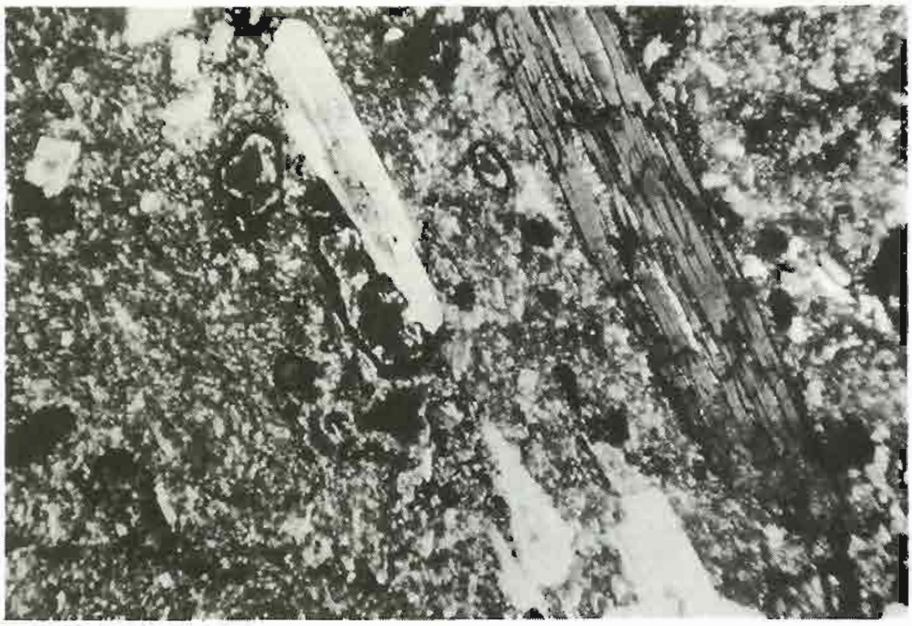

x 40

Cross nicols

Microscopic observation

: The rock is characterized by flow texture. Phenocrysts are composed of plagioclase ,biotite and hornblende , and its groundmass consists of plagioclase , quartz and K-feldspar. Groundmass and mafic mineral are strongly altered to montmorillonite and secondary quartz.

Sample No. T-24 , 812m to 814m

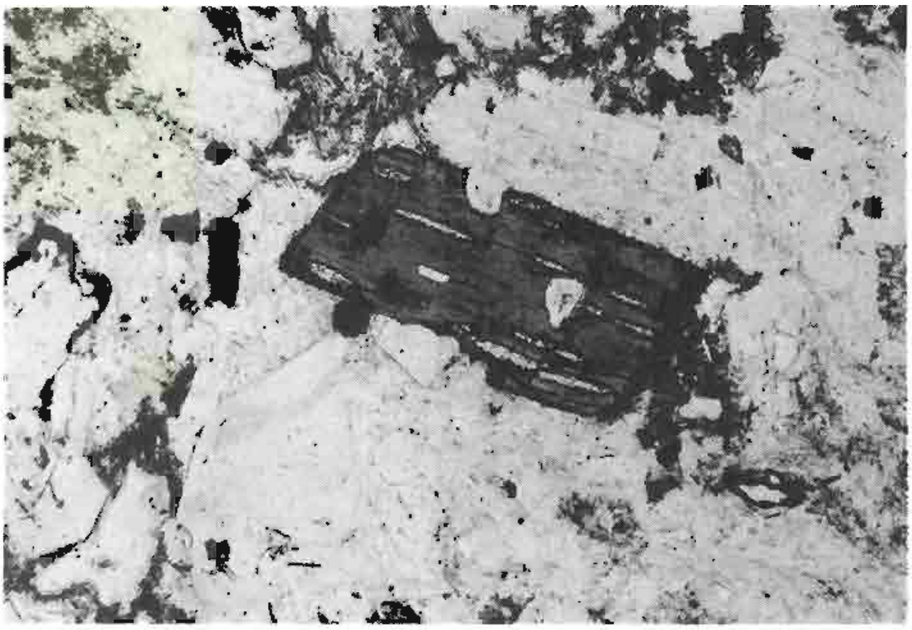

Strongly welded tuff or Dacite

x 40

Open nicols

x 40

Cross nicols

Microscopic observation

: The texture and rock forming minerals are same to Sample No. T-22.

Sample No. T-27 , 904m to 908m

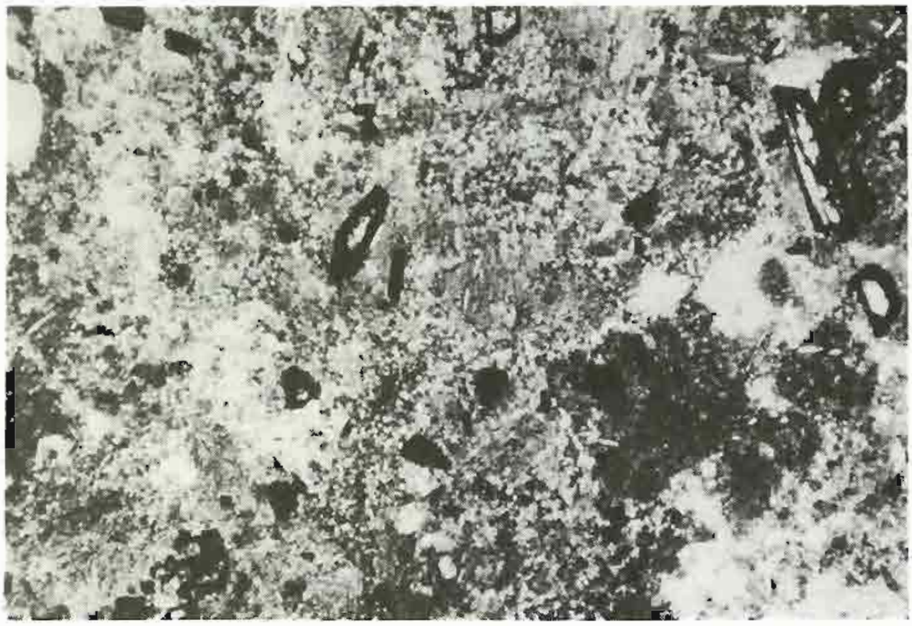

Dacitic tuff

x 40

Open nicols

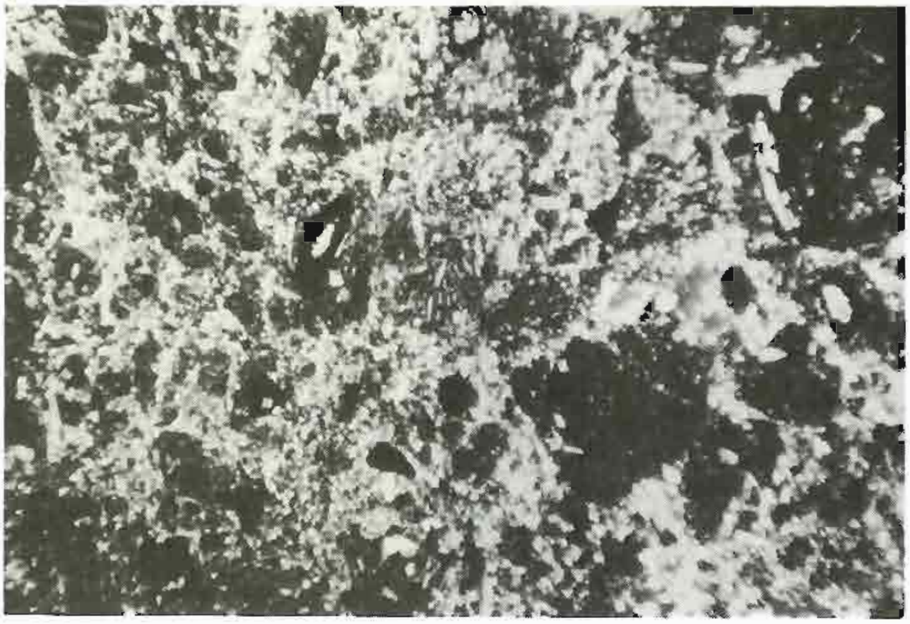

x 40

Cross nicols

Microscopic observation

: Phenocrysts are same to Sample No. T-22 , and its texture is clastic.
Groundmass is strongly altered to montmorillonite and also mafic mineral is altered montmorillonite spot with opasite rim.

Sample No. T-28 , 935m to 937m

Coarse grained andesite tuff

x 40

Open nicols

x 40

Cross nicols

Microscopic observation

: Andesitic tuff consist of andesite fragment , plagioclase and opaque mineral. Groundmass is strongly altered to chlorite calcite and fine grained secondary quartz.

Sample No. T-30 , 996m to 996.3m

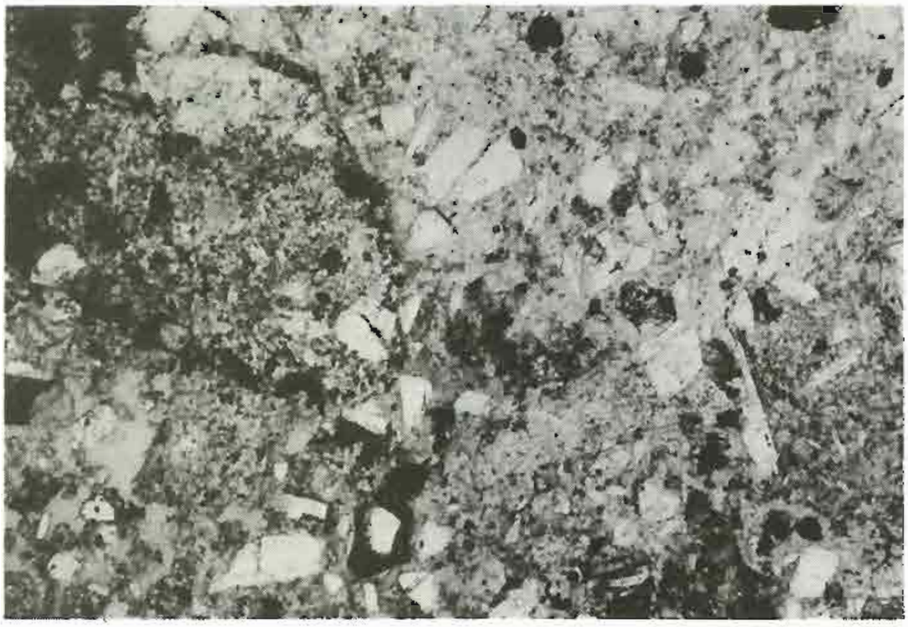

Coarse grained andesitic tuff

x 40

Open nicols

x 40

Cross nicols

Microscopic observation

: Breccia included , texture and alteration are same to Sample No. T-28.

Sample No. T-31 , 1039m to 1041m

Pyroxene andesite

x 40

Open nicols

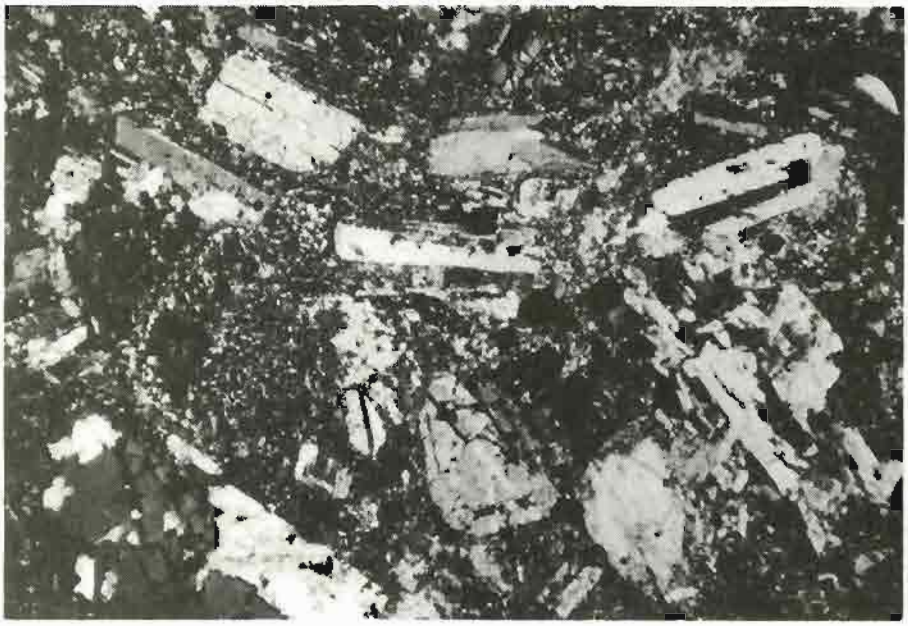

x 40

Cross nicols

Microscopic observation

: The rock consist of plagioclase , augite and opaque mineral as its phenocryst , and its groundmass is composed of plagioclase , secondary quartz , clay minerals and opaque. Groundmass and mafic minerals are altered to chlorite , and , especially , epidote is recognized in plagioclase phenocryst.

Sample No. T-34 , 1154m to 1157m

Andesite

x 40

Open nicols

x 40

Cross nicols

Microscopic observation

: The texture , phenocryst mineral , and alteration are same to Sample No. T-31.

TEMPERATURE AND PRESSURE LOGGING CONDITION

Temperature and Pressure Logging Condition

Logging No.	I	II		III		
	Temperature	Temperature 1	Temperature 2	Temperature 1	Temperature 2	Temperature 3
Logging Curve No.	①	②	③	④	⑤	⑥
Date	21/Oct/1980 Tue.	1/Nov/1980 Sat.	2/Nov/1980 Sun.	15/Nov/1980 Sat.	15/Nov/1980 Sat.	16/Nov/1980 Sun.
Weather	Fine	Fine	Cloudy	Fine	Fine	Fine
Temperature (ºC)	13.0	10.0	12.0	12.5	5.0	13.0
Atmosphere (mb)	600.0	600.0	599.0	598.0	602.0	599.0
Equipment	KTB 10004	KTB 10004	KTB 10004	KTB 10004	KTB 10004	KTB 10004
Drilling depth (m)	463.0	653.0	653.0	814.5	814.5	814.5
Logging depth (m)	300.0	652.0	652.0	800.0	800.0	800.0
Standing time (h)	144:05	4:30	23:40	7:30	16:30	31:00
Final circulation	15/Oct/1980 12:00	1/Nov/1980 10:00	1/Nov/1980 10:00	15/Nov/1980 2:00	15/Nov/1980 2:00	15/Nov/1980 2:00
Logging from	12:05	14:20	9:20	9:23	18:10	9:00
〃 till	13:03	15:33	11:04	11:02	19:49	10:34
〃 Final	13:15	16:35	11:40	11:34	20:18	10:58
Water level (-m)	73.0	0	7.0	0	0	0
Water level temp. (°C)	No data	No data	No data	No data	N 18.0	25.0
Bottom temp. (°C)	No data	67.4	111.2	114.5	132.8	142.6
Maximum temp. (°C) and its depth (-m)	60.3 300.0	67.4 652.0	111.2 652.0	114.5 800.0	132.8 800.0	142.6 800.0
Stationary point Thermometer Max. Temp. (°C)	60.0	63.0	112.0	118.0	132.0	142.0
Well diameter and its depth (inch, -m)	8 3/4 463.0	8 3/4 653.0	8 3/4 653.0	6 1/8 814.5	6 1/8 814.5	6 1/8 814.5
Casing pipe and its depth (inch, -m)	9 5/8 312.0	9 5/8 312.0	9 5/8 312.0	7 651.5	7 651.5	7 651.5
Slit pipe and its depth (inch, -m)	–	–	–	–	–	–
Circulation Water and its density	Bentonite mud 1.06	Bentonite mud 1.07	Bentonite mud 1.07	Bentonite mud 1.07	Bentonite mud 1.07	Bentonite mud 1.07
Remarks						

Temperature and Pressure Logging Condition

Logging No.	IV				
	Temperature 1	Temperature 2	Temperature 3	Temperature 4	Temperature 5
Logging Curve No.	⑦	⑧	⑨	⑩	⑪
Date	27/Nov/1980 Tue.	28/Nov/1980 Fri.	29/Nov/1980 Sat.	30/Nov/1980 Sun.	1/Dec/1980 Mon.
Weather	Fine	Fine	Fine	Fine	Fine
Temperature (°C)	4.0	16.0	15.0	16.0	13.0
Atmosphere (mb)	603.0	599.0	600.0	601.0	600.0
Equipment	KTB 10004	KTB 10004	KTB 10004	KTB 10004	KTB 10004
Drilling depth (m)	1,157.0	1,157.0	1,157.0	1,157.0	1,157.0
Logging depth (m)	1,150.0	1,150.0	1,150.0	1,150.0	1,150.0
Standing time (h)	10:20	23:00	48:00	72:00	
Final circulation	27/Nov/1980 9:00	27/Nov/1980 9:00	27/Nov/1980 9:00	27/Nov/1980 9:00	27/Nov/1980 9:00
Logging from	19:20	9:00	8:57	8:56	9:00
〃 till	21:20	11:21	11:16	11:33	11:35
〃 Final	22:05	12:04	11:55	12:08	12:13
Water level (-m)	0	0	0.5	1.5	2.0
Water level temp. (°C)	14.0	19.0	19.0	20.0	22.0
Bottom temp. (°C)	146.1	158.9	165.5	168.8	170.5
Maximum temp. (°C) and its depth (-m)	146.1 1,150.0	158.9 1,150.0	165.5 1,150.0	169.3 1,150.0	170.5 1,150.0
Stationary point Thermometer Max. Temp. (°C)	144.0	154.0	164.0	167.5	169.0
Well diameter and its depth (inch, -m)	6 1/8 1,157	6 1/8 1,157	6 1/8 1,157	6 1/8 1,157	6 1/8 1,157
Casing pipe and its depth (inch, -m)	7, 651.5	7, 651.5	7, 651.5	7, 651.5	7, 651 5
Slit pipe and its depth (inch, -m)	5, 648.0~1,157.0	5, 648.0~1,157.0	5, 648.0~1,157.0	5, 648.0~1,157.0	5, 648.0~1,157.0
Circulation Water and its density	Cool water –	Cool water –	Cool water –	Cool water –	Cool water –
Remarks					

Temperature and Pressure Logging Condition

Logging No.	V			
	Pressure 1	Pressure 2	Pressure 3	Temperature 1
Logging Curve No.	P 1 . 2 . 3	P 4 . 5 . 6	P 7	⑫
Date	1/Dec/1980 Sun.	1/Dec/1980 Sun.	4/Dec/1980 Tue.	4/Dec/1980 Tue.
Weather	Fine	Fine	Fine	Fine
Temperature (°C)	16.0	16.0	15.0	15.0
Atmosphere (mb)	602	602	599	599
Equipment	KPG 10201	KPG 10201	KPG 7727	KTB 10004
Drilling depth (m)	1,157	1,157	1,157	1,157
Logging depth (m)	200	200	500	1,150
Standing time (h)	–	–	–	after injection
Final circulation	–	–	–	–
Logging from	15:50	15:50	10:10	15:00
〃 till	16:08	16:08	10:45	16:38
〃 Final	21:15	21:15	14:00	17:35
Water level (-m)	–	–	–	–
Water level temp. (°C)	–	–	–	–
Bottom temp. (°C)	–	–	–	166.8
Maximum temp. (°C)	–	–	–	166.8
and its depth (-m)	–	–	–	1,150
Stationary point Thermometer Max. Temp. (°C)	–	–	–	165
Well diameter and its depth (inch, -m)	6 1/8 1,157	6 1/8 1,157	6 1/8 1,157	6 1/8 1,157
Casing pipe and its depth (inch, -m)	7, 651.5	7, 651.5	7, 651.5	7, 651.5
Slit pipe and its depth (inch, -m)	5, 648~1,157	5, 648~1,157	5, 648~1,157	5, 648~1,157
Circulation water and	Cool water	Cool water	Cool water	Cool water
its density	–	-	–	–
Remarks				

CALCULATION OF ANALIZED RESERVOIR TEMPERATURE

Calculation of Analized Reservoir Temperature (II 1, 2 Curve No.②,③)

Depth (m)	Cooling time (t)			Standing time (θ)	(t + θ)	θ / (t + θ)	Measured Temp. (°C)
100	A) Drilling Date	2/Sep/1980	3:00	1) 4.5	1) 1451.5	1) 0.0031	1) 48.0
	B) Final circulation	1/Nov/1980	10:00	2) 24.0	2) 1471.0	2) 0.0163	2) 44.7
	C) Hours from A till B	1447 h					
200	A) Drilling Date	10/Sep/1980	11:00	1) 4.9	1) 1251.9	1) 0.0039	1) 50.7
	B) Final circulation	1/Nov/1980	10:00	2) 24.3	2) 1271.3	2) 0.0191	2) 51.1
	C) Hours from A till B	1247 h					
300	A) Drilling Data	14/Sep/1980	15:00	1) 5.0	1) 1152.0	1) 0.0043	1) 51.8
	B) Final circulation	1/Nov/1980	10:00	2) 24.5	2) 1171.5	2) 0.0209	2) 56.3
	C) Hours from A till B	1147 h					
400	A) Drilling Date	13/Oct/1980	4:00	1) 5.2	1) 467.2	1) 0.0111	1) 54.4
	B) Final circulation	1/Nov/1980	10:00	2) 24.8	2) 486.8	2) 0.0509	2) 59.7
	C) Hours from A till B	462 h					
500	A) Drilling Date	27/Oct/1980	12:00	1) 5.3	1) 123.3	1) 0.0430	1) 57.8
	B) Final circulation	1/Nov/1980	10:00	2) 25.0	2) 143.0	2) 0.1748	2) 77.2
	C) Hours from A till B	118 h					
600	A) Drilling Date	30/Oct/1980	9:00	1) 5.4	1) 54.4	1) 0.0993	1) 59.8
	B) Final circulation	1/Nov/1980	10:00	2) 25.8	2) 74.8	2) 0.3449	2) 93.9
	C) Hours from A till B	49 h					

Calculation of Analized Reservoir Temperature (III. 1 ~ 3, Curve No.④~⑥)

Depth(m)	Cooling time (t)	Standing time (θ)	(t + θ)	θ/(t + θ)	Measured Temp. (°C)
100	A) Drilling Date 2/Sep/1980 3:00 B) Final circulation 15/Nov/1980 2:00 C) Hours from A till B 2447.0 h	1) 7.6 2) 16.3 3) 31.4	1) 2454.6 2) 2463.3 3) 2478.4	1) 0.0031 2) 0.0066 3) 0.0127	1) 44.4 2) 45.5 3) 43.9
200	A) Drilling Date 10/Sep/1980 11:00 B) Final circulation 15/Nov/1980 2:00 C) Hours from A till B 1575.0 h	1) 7.7 2) 16.5 3) 31.6	1) 1582.7 2) 1591.5 3) 1606.6	1) 0.0048 2) 0.0104 3) 0.0197	1) 51.9 2) 54.6 3) 53.5
300	A) Drilling Date 14/Sep/1980 15:00 B) Final circulation 15/Nov/1980 2:00 C) Hours from A till B 1475.0 h	1) 7.9 2) 16.7 3) 31.8	1) 1482.9 2) 1491.7 3) 1506.8	1) 0.0053 2) 0.0112 3) 0.0314	1) 57.3 2) 60.3 3) 59.1
400	A) Drilling Date 13/Oct/1980 4:00 B) Final circulation 15/Nov/1980 2:00 C) Hours from A till B 790.0 h	1) 8.2 2) 16.8 3) 31.9	1) 798.2 2) 806.8 3) 821.9	1) 0.0103 2) 0.0208 3) 0.0388	1) 64.3 2) 69.3 3) 71.0
500	A) Drilling Date 27/Oct/1980 12:00 B) Final circulation 15/Nov/1980 2:00 C) Hours from A till B 446.0 h	1) 8.4 2) 16.9 3) 32.1	1) 454.4 2) 462.9 3) 478.1	1) 0.0185 2) 0.0365 3) 0.0671	1) 72.1 2) 78.1 3) 82.7
600	A) Drilling Date 30/Oct/1980 9:00 B) Final circulation 15/Nov/1980 2:00 C) Hours from A till B 377.0 h	1) 8.6 2) 17.3 3) 32.3	1) 385.6 2) 394.3 3) 409.3	1) 0.0223 2) 0.0439 3) 0.0789	1) 77.7 2) 88.8 3) 93.4
700	A) Drilling Date 10/Nov/1980 5:00 B) Final circulation 15/Nov/1980 2:00 C) Hours from A till B 117.0 h	1) 8.8 2) 17.5 3) 32.5	1) 125.8 2) 134.5 3) 149.5	1) 0.0700 2) 0.1301 3) 0.2174	1) 90.5 2) 103.1 3) 109.4
800	A) Drilling Date 14/Nov/1980 15:00 B) Final circulation 15/Nov/1980 2:00 C) Hours from A till B 11.0 h	1) 9.0 2) 17.8 3) 32.7	1) 20.0 2) 28.8 3) 43.7	1) 0.4500 2) 0.6180 3) 0.7483	1) 114.5 2) 132.5 3) 142.6

Calculation of Analized Reservoir Temperature (IV 1 ~ 5, Curve No⑦~⑪)

Depth (m)	Cooling time (t)			Standing Time (θ)	(t + θ)	θ / (t + θ)	Measured Temp. (°C)
100	A) Drilling Date	2/Sep/1980	3.00	1) 10.6	1) 2,080.65	1) 0.0051	1) 49.2
	B) Final circulation	27/Nov/1980	9:00	2) 23.2	2) 2,093.2	2) 0.0111	2) 44.3
	C) Hours from A till B	2070 h		3) 48.1	3) 2,118.1	3) 0.0227	3) 43.8
				4) 72.1	4) 2,142.1	4) 0.0337	4) 44.0
				5) 96.3	5) 2,166.2	5) 0.0445	5) 46.6
200	A) Drilling Date	10/Sep/1980	11:00	1) 10.8	1) 1,880.8	1) 0.0057	1) 57.3
	B) Final circulation	27/Nov/1980	9:00	2) 23.4	2) 1,893.4	2) 0.0124	2) 57.6
	C) Hours from A till B	1870 h		3) 48.3	3) 1,918.3	3) 0.0252	3) 56.3
				4) 72.3	4) 1,942.3	4) 0.0372	4) 57.0
				5) 96.4	5) 1,966.4	5) 0.0490	5) 56.9
300	A) Drilling Date	14/Sep/1980	15:00	1) 11.0	1) 1,781.0	1) 0.0062	1) 65.4
	B) Final circulation	27/Nov/1980	9:00	2) 23.6	2) 1,793.6	2) 0.0132	2) 67.9
	C) Hours from A till B	1770 h		3) 48.5	3) 1,818.5	3) 0.0267	3) 64.8
				4) 72.5	4) 1,842.5	4) 0.0393	4) 66.4
				5) 96.6	5) 1,866.6	5) 0.0518	5) 66.9
400	A) Drilling Date	13/Oct/1980	4:00	1) 11.1	1) 1,096.1	1) 0.0101	1) 77.1
	B) Final circulation	27/Nov/1980	9:00	2) 23.8	2) 1,108.8	2) 0.0215	2) 78.3
	C) Hours from A till B	1085 h		3) 48.7	3) 1,133.7	3) 0.0430	3) 77.7
				4) 72.7	4) 1,157.7	4) 0.0628	4) 79.8
				5) 96.9	5) 1,181.9	5) 0.0820	5) 81.8
500	A) Drilling Date	27/Oct/1980	12:00	1) 11.3	1) 752.3	1) 0.0150	1) 86.9
	B) Final circulation	27/Nov/1980	9:00	2) 24.0	2) 765.0	2) 0.0314	2) 89.1
	C) Hours from A till B	741 h		3) 48.9	3) 789.9	3) 0.0619	3) 90.8
				4) 72.9	4) 813.9	4) 0.0896	4) 93.3
				5) 97.1	5) 838.1	5) 0.1159	5) 94.8
600	A) Drilling Date	30/Oct/1980	9:00	1) 11.4	1) 683.4	1) 0.0167	1) 94.9
	B) Final circulation	27/Nov/1980	9:00	2) 24.2	2) 696.2	2) 0.0348	2) 99.6
	C) Hours from A till B	672 h		3) 49.1	3) 721.1	3) 0.0681	3) 102.3
				4) 73.1	4) 745.1	4) 0.0981	4) 106.3
				5) 97.3	5) 769.3	5) 0.1265	5) 108.3
700	A) Drilling Date	10/Nov/1980	5:00	1) 11.6	1) 423.6	1) 0.0274	1) 105.1
	B) Final circulation	27/Nov/1980	9:00	2) 24.4	2) 436.4	2) 0.0559	2) 111.7
	C) Hours from A till B	412 h		3) 49.3	3) 461.3	3) 0.1069	3) 117.2
				4) 73.3	4) 485.3	4) 0.1510	4) 120.6
				5) 97.5	5) 509.5	5) 0.1914	5) 124.4
800	A) Drilling Date	14/Nov/1980	15:00	1) 11.7	1) 317.7	1) 0.0368	1) 112.6
	B) Final circulation	27/Nov/1980	9:00	2) 24.6	2) 330.6	2) 0.0744	2) 121.4
	C) Hours from A till B	306 h		3) 49.5	3) 355.5	3) 0.1392	3) 127.7
				4) 73.5	4) 379.5	4) 0.1937	4) 131.7
				5) 97.8	5) 463.8	5) 0.2422	5) 136.6
900	A) Drilling Date	19/Nov/1980	4:00	1) 11.9	1) 208.9	1) 0.0570	1) 120.1
	B) Final circulation	27/Nov/1980	9:00	2) 24.8	2) 221.8	2) 0.1118	2) 130.7
	C) Hours from A till B	197 h		3) 49.7	3) 246.7	3) 0.2015	3) 138.5
				4) 73.8	4) 270.8	4) 0.2725	4) 143.2
				5) 98.0	5) 295.0	5) 0.3322	5) 146.3
1,000	A) Drilling Date	22/Nov/1980	2:00	1) 12.0	1) 139.0	1) 0.0863	1) 127.9
	B) Final circulation	27/Nov/1980	9:00	2) 25.0	2) 152.0	2) 0.1645	2) 139.5
	C) Hours from A till B	127 h		3) 49.9	3) 176.9	3) 0.2821	3) 147.1
				4) 74.1	4) 201.1	4) 0.3685	4) 152.1
				5) 98.2	5) 225.2	5) 0.4361	5) 155.8
1,100	A) Drilling Date	24/Nov/1980	20:00	1) 12.2	1) 73.2	1) 0.1667	1) 138.6
	B) Final circulation	27/Nov/1980	9:00	2) 25.2	2) 86.2	2) 0.2923	2) 151.5
	C) Hours from A till B	61 h		3) 50.1	3) 111.1	3) 0.4509	3) 159.2
				4) 74.4	4) 135.4	4) 0.5495	4) 163.2
				5) 98.4	5) 159.4	5) 0.6173	5) 167.2
1,150	A) Drilling Date	26/Nov/1980	14:00	1) 12.3	1) 31.3	1) 0.3930	1) 146.1
	B) Final circulation	27/Nov/1980	9:00	2) 25.4	2) 44.4	2) 0.5721	2) 158.9
	C) Hours from A till B	19h		3) 50.3	3) 69.3	3) 0.7258	3) 165.5
				4) 74.5	4) 93.5	4) 0.7968	4) 169.3
				5) 94.6	5) 113.6	5) 0.8327	5) 171.5

PHOTOGRAPHS

Geological survey

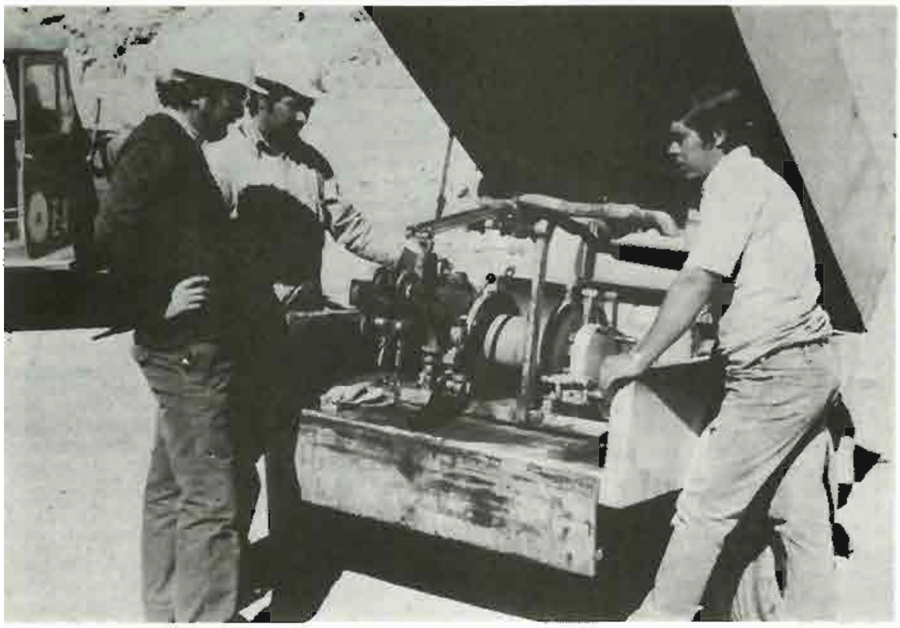

Logging survey

X-RAY DIFFRACTION

MAPAS

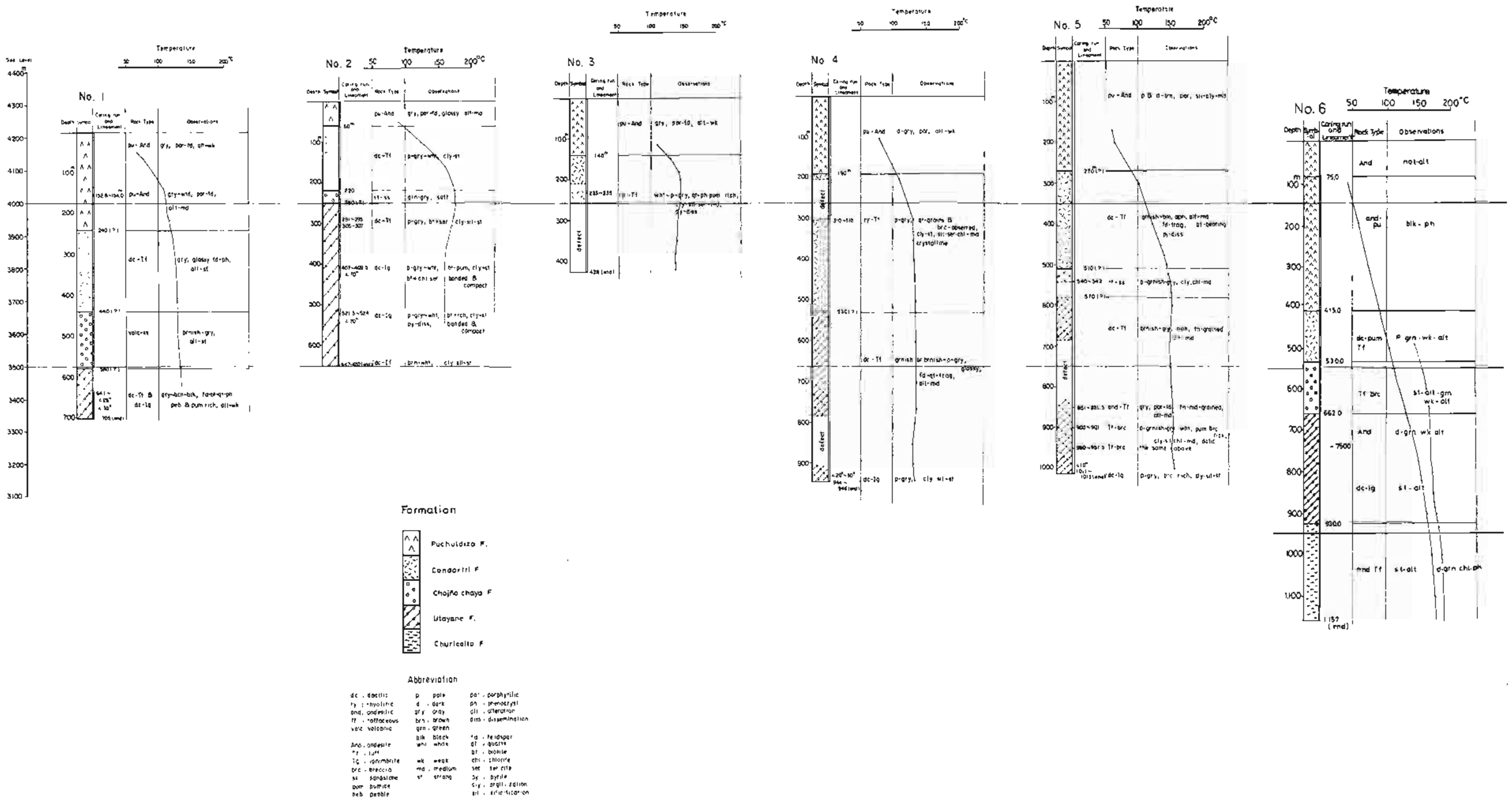

Fig I -2-1 GEOLOGIC DRILL LOG WITH TEMPERATURE CURVE

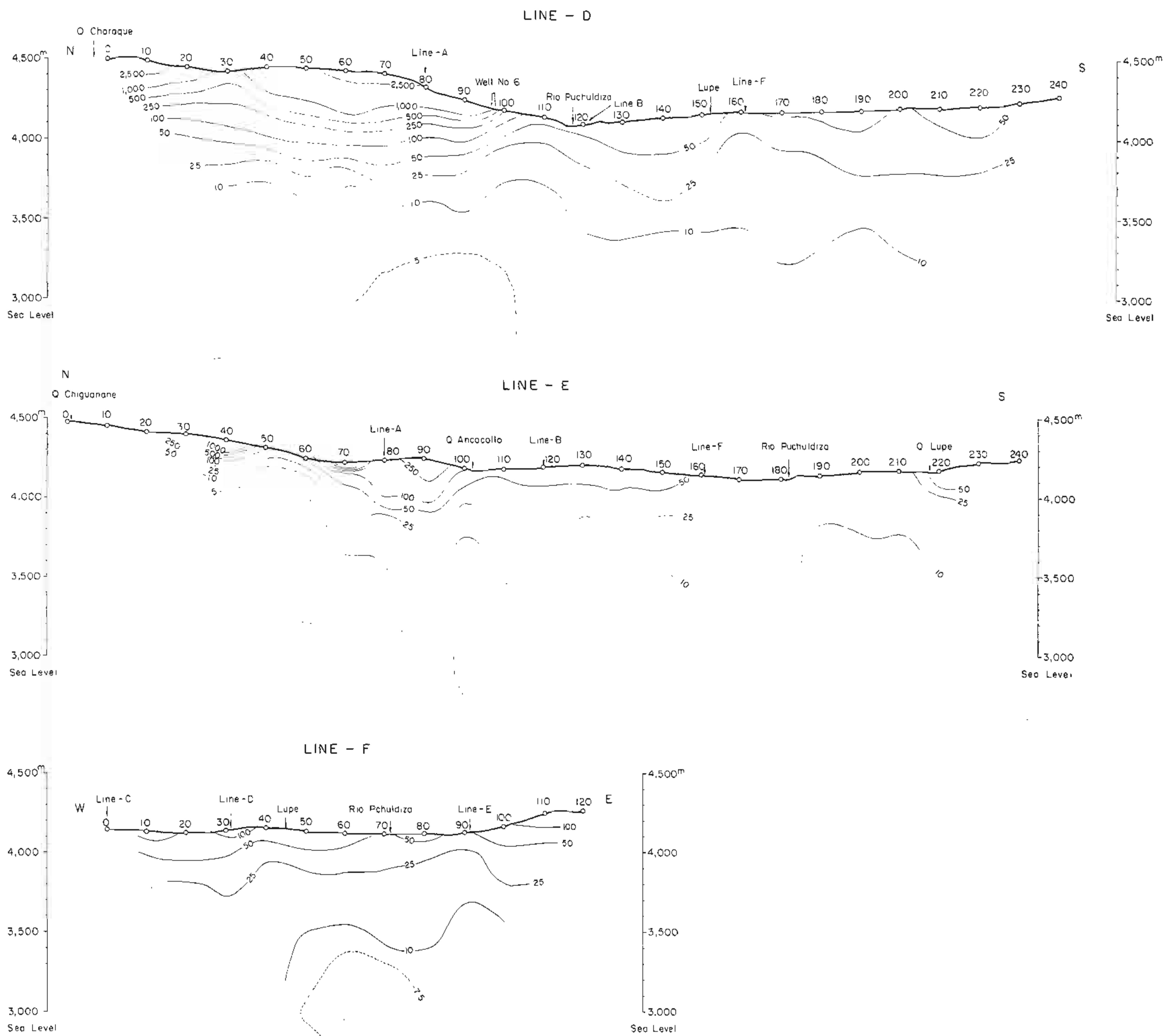

Geothermal Power Development Project
in Puchuldiza
the Republic of Chile

APPARENT RESISTIVITY SECTION
(LINE - D,E,F)
(Unit Ω-m)

1 : 25,000

0 500 1,000 1,500m

Oct. ~ Dec. 1979

Fig. I-3-1

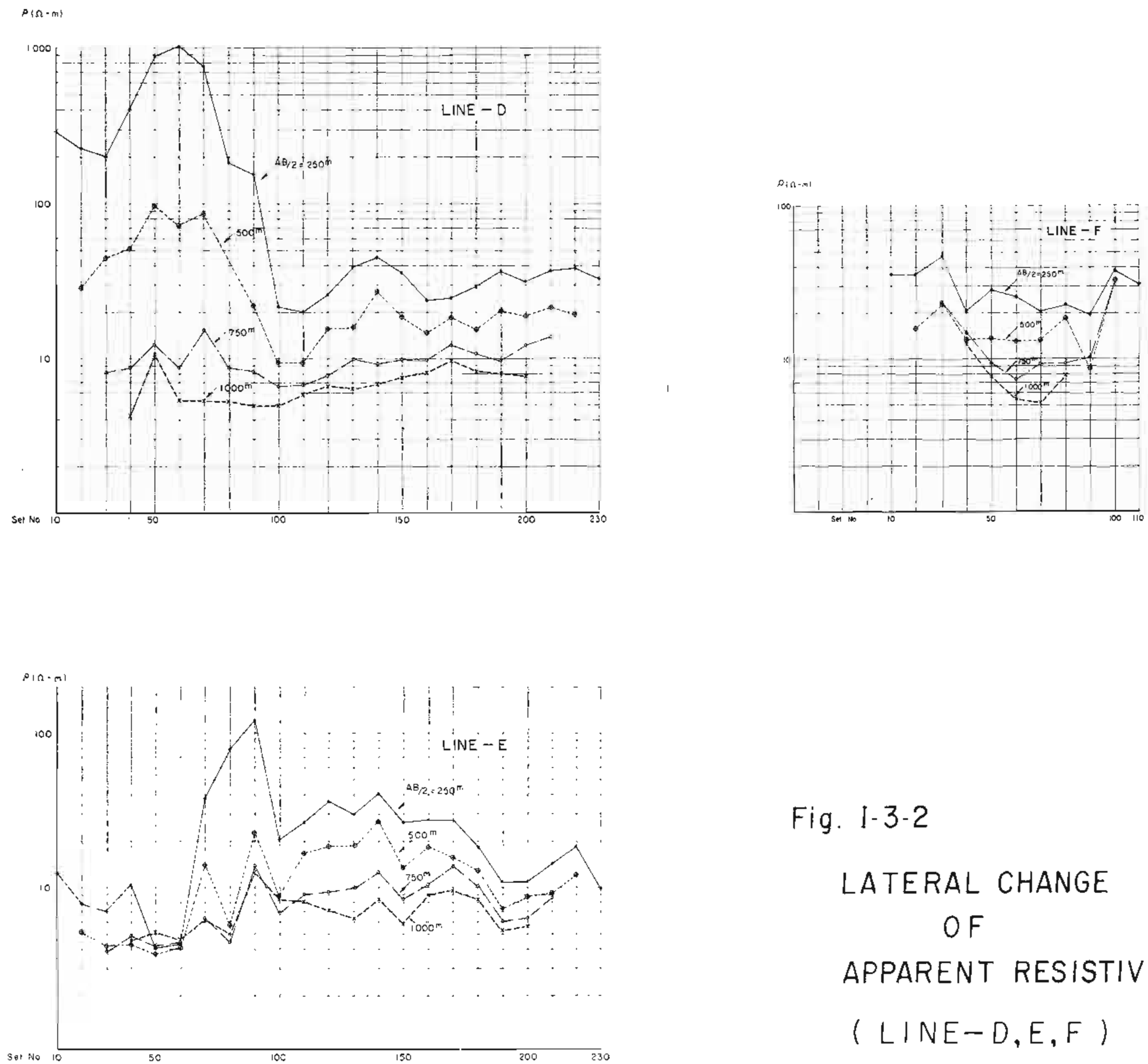

Fig. I-3-2

LATERAL CHANGE
OF
APPARENT RESISTIVITY
(LINE–D,E,F)

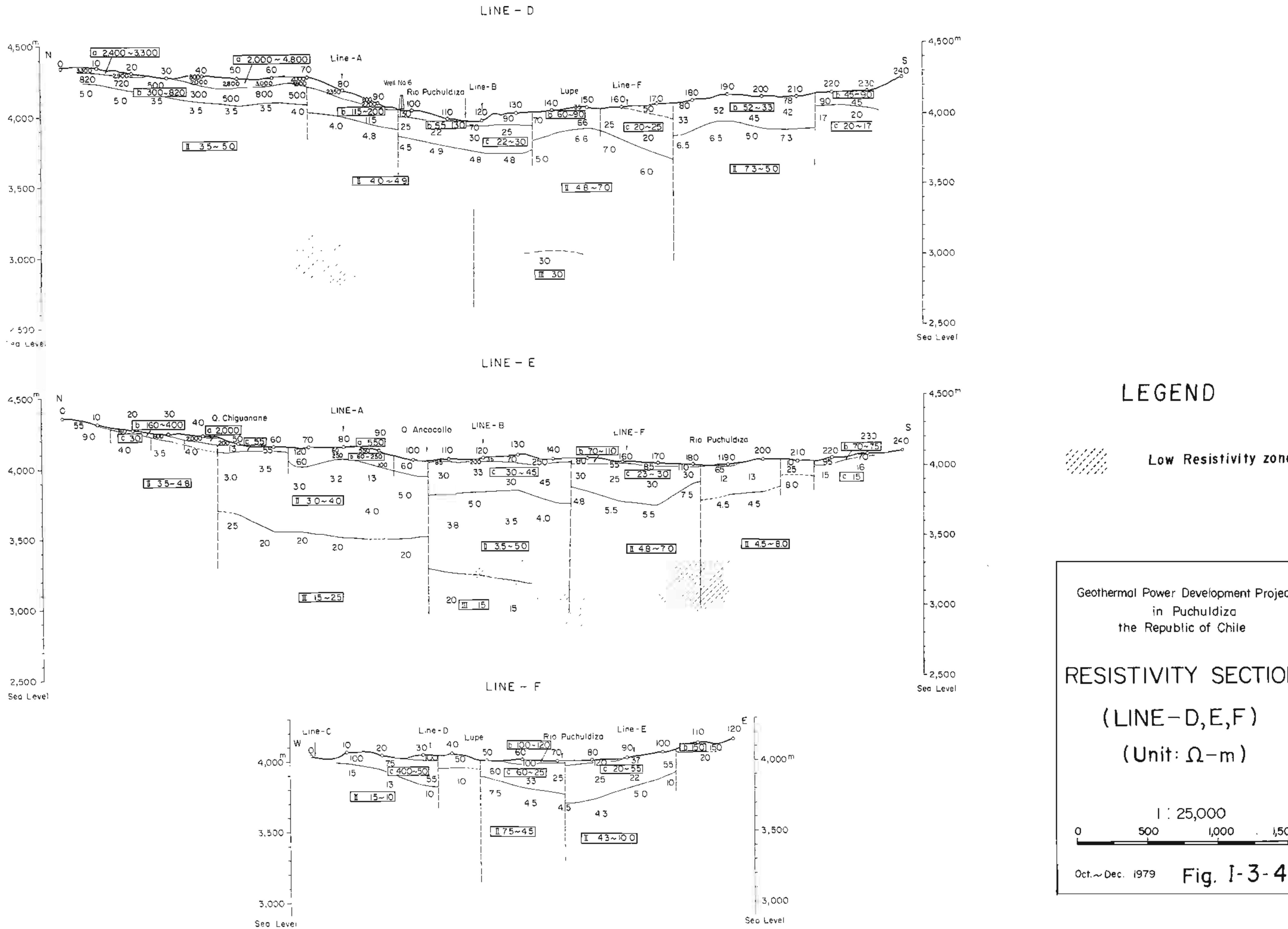

Geothermal Power Development Project
in Puchuldiza
the Republic of Chile

RESISTIVITY SECTION
(LINE-D,E,F)
(Unit: Ω-m)

1 : 25,000

Oct.~Dec. 1979

Fig. I-3-4

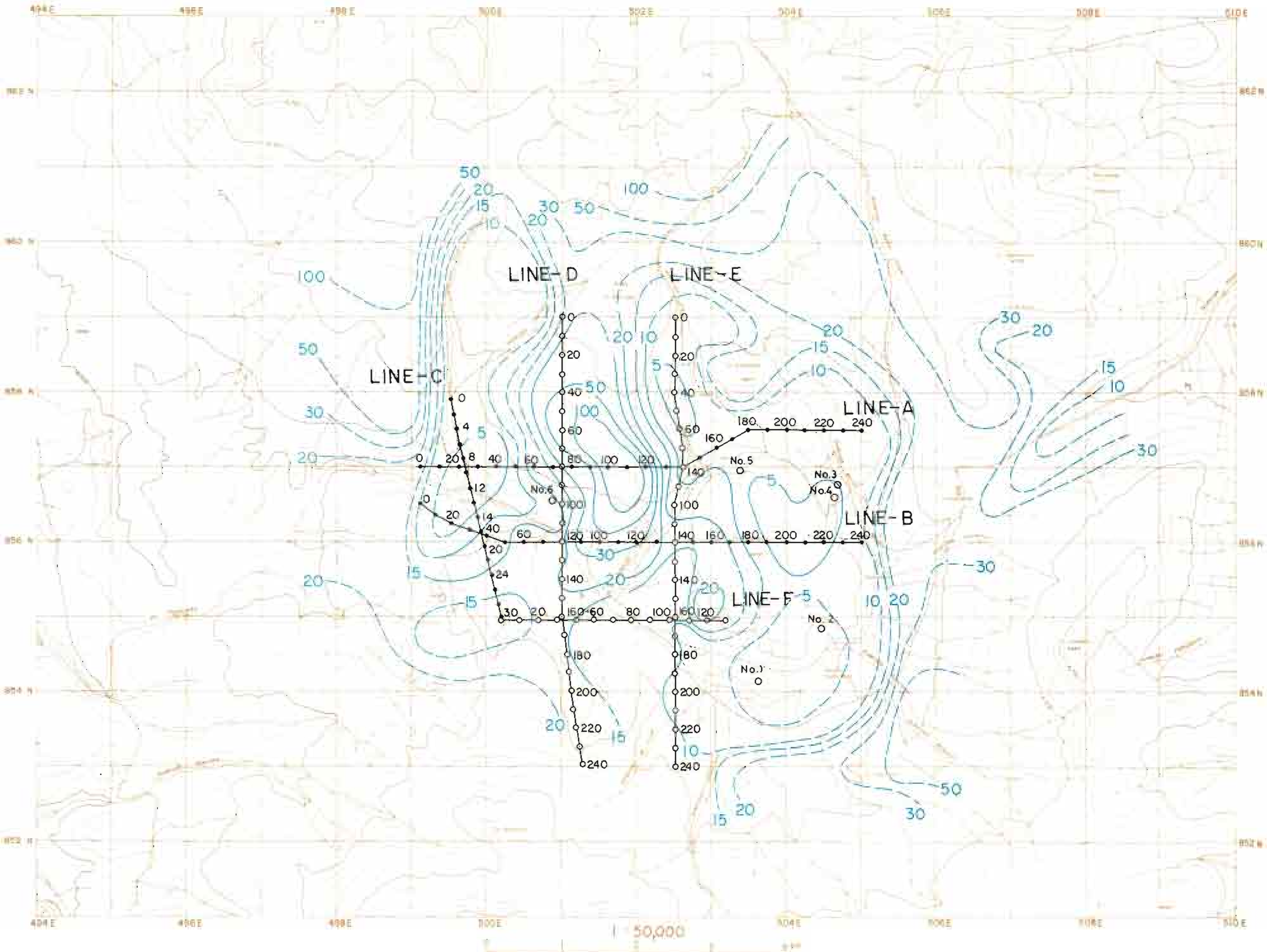

LEGEND

1978
1979
Exploratory W
Counter Line o
Apparent Resi
(Unit: Ω

Geothermal Power Development P
in Puchuldiza
the Republic of Chile

APPARENT RESISTIV
MAP

AB / 2 = 500m

1 : 50,000
0 1,000 2,0

Oct.~Dec, 1979 Fig. I-3-5

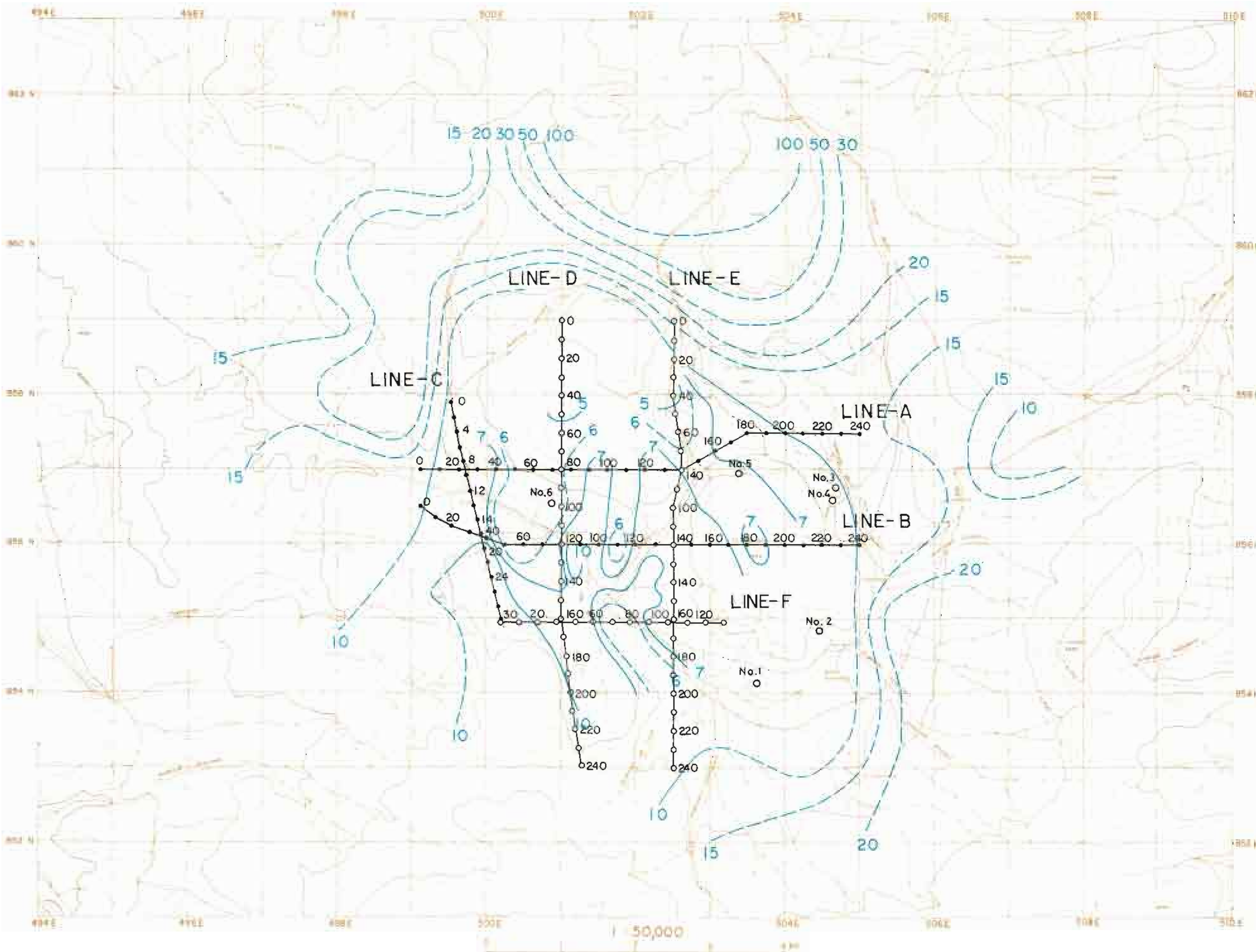

LEGEND

1978

1979

Exploratory We

Counter Line o
Apparent Resi
(Unit : Ω

Geothermal Power Development Proj
in Puchuldiza
the Republic of Chile

APPARENT RESISTIVI
MAP

AB / 2 = 1,000m

1 : 50,000

0 1,000 2,000

Oct.～Dec. 1979

Fig. I-3-5

Fig. II-2-2 DRILLING PROCESS OF WELL NO. 6

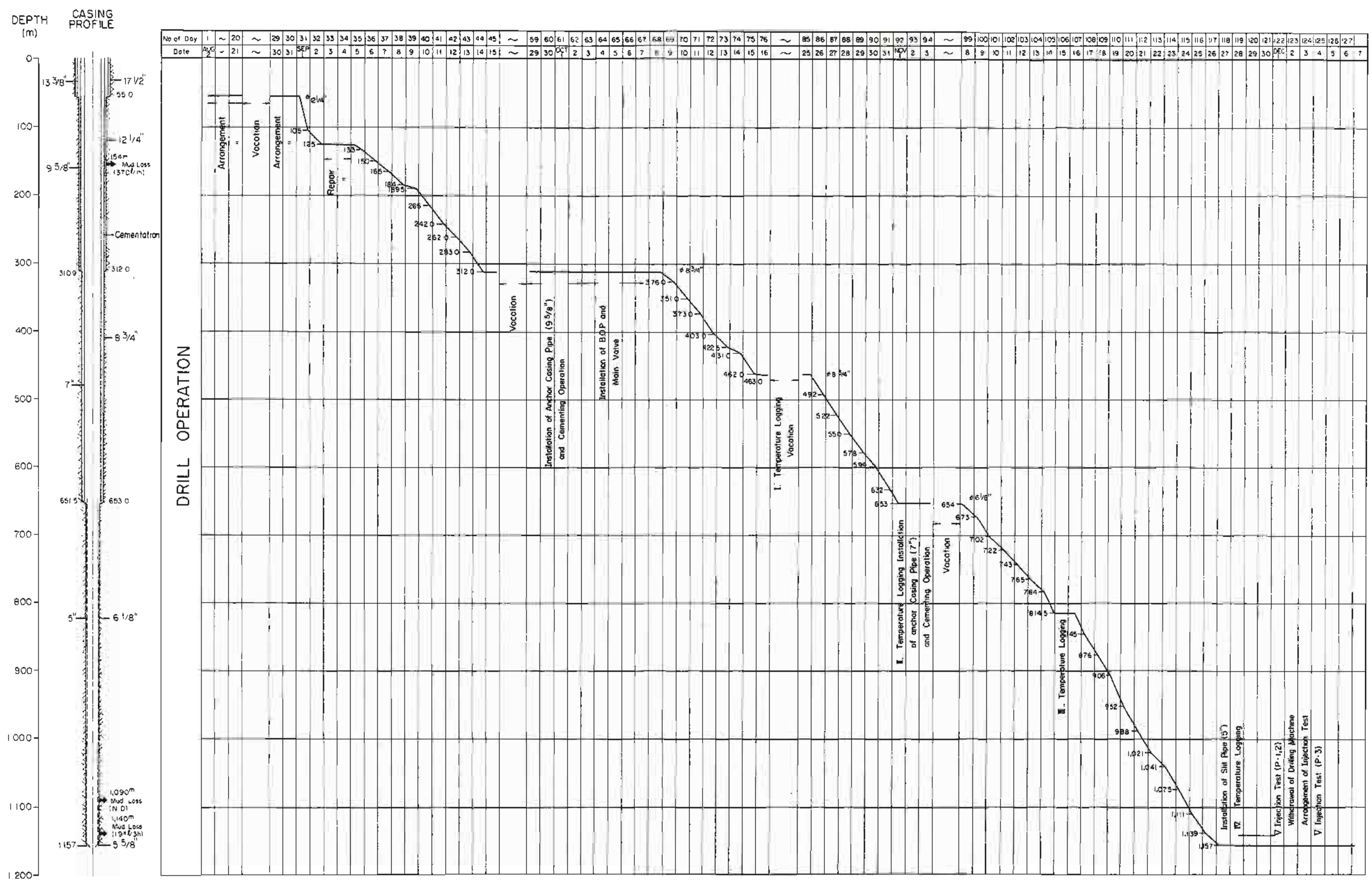

Fig. II–3–1 Geologic Column of Well No. 6, Puchuldiza

Depth (-m)	Column	Geologic Formation	Rock Type	Rock Description	Alteration
60		Pleistocene Volcanics (Qap)	Hornblende andesite lava and its pyroclastics	Porphyritic rocks characterized by large phenocryst of plagioclase and hornblende with porphyritic texture.	Alteration is not observed.
75 210 315 415		Puchuldiza Formation (Tpl)	Pyroxene andesite Lava intercalated with its pyroclastics	This andesite is black in colour and massive as a whole with few phenocrysts of plagioclase and pyroxene. (hyperthene and augite) This consist of tuff, lapilli tuff in the upper and tuff breccia in the lower part. Fragments included are mainly pyroxene andesite, which is essential material, and rarely rhyolitic or dacitic rock, which is thought to be derived from Utayane F. This andesite is essentially same to the upper. Its colour is brown to brownish grey, and sometimes flow-banding structure is observed.	Montmorillonite and few fine grain pyrite are recognized along the crack. The alteration develops mainly groundmass, rim of phenocryst and along the crack of phenocryst. Calcite is rarely filling the lower part is generally strong compared with upper part.
(500) 530		Condoriri Formation (Tct)	Dacitic pumiceous tuff or lapilli tuff	The formation is consisted of pumice, dacite breccia and clastic materials, and its sorting and grading are very poor.	The formation is wholly altered to pale green in colour. (montmorillonite)
662		Chojna Chaya Formation (Tch) ?	Tuff breccia	The formation is made up of many dacite breccia, a few andesite breccia and clastic sediment, and its sorting and grading are very poor.	The formation is wholly and strongly altered to green in colour (montmorillonite), and calcite veinlet and fine grain pyrite are rarely recognized.
750		Dyke (?)	Andesite	The dyke is characterized by very fine grained andesite with flow banding structure. Mafic minerals are very poor.	Deep green mineral is producting along crack, and mafic mineral is altered to green colour.
930		Utayane Formation (Tu)	Dacitic ignimbrite	Very strongly welded dacitic tuff characterized by banding structure including essential lense. Phenocryst is composed of plagioclase, quartz biotite and hornblende. The banding structure angle is about 40°. In some cases, this rock looks like homogenious andesite.	The formation, as a whole, is strongly altered, especially, groundmass and mafic minerals to montmorillonite, fine grained secondary quartz assemblage and mineral look like mixed layered minerals.
(1000) 1020 1060 1157		Churicollo Formation (Kch)	Pyroxene Andesite lava and its pyroclastics	Pyroclastic rock composed of andesite, dacite, fragment of plagioclase with small amount of quartz and mafic mineral and volcanic matrix. The Sarting is somewhat good but the grading is not recognized. Tuff breccia consist of andesite breccia, dacite and clastic sediment. Porphyritic andesite containing phenocryst of plagioclase, a few pyroxene. (Very strongly welded ignimbrite?)	This formation is strongly altered to deep green colour (chlorite), and sometimes fine calcite vein is recognized along the creek. Secondary epidote is observed in plagioclase phenocryst.

No.	Depth(m)	C.L.(%)	X-Ray	micro-scope	Resis-tivity	Remarks
1	151^{mts} ~ 153	(3)				
2	165 ~ 167	(5)				
3	186 ~ 192	(15)	○	○	○	
4	215 ~ 221	(27)	○	○		
5	243 ~ 247	(85)	○	○	○	
6	278 ~ 283	(20)			○	
7	315 ~ 320	(24)	○	○	○	
8	346 ~ 351	(35)				
9	368 ~ 373	(93)	○	○	○	
10	402 ~ 404	(40)	○	○	○	
11	427 ~ 431	(24)				
12	459.5 ~463	(96)			○	
13	489 ~ 492	(61)	○	○		
14	519 ~ 522	(90)			○	
15	550 ~ 552	(100)	○	○	○	
16	580 ~ 583	(87)	○	○	○	
17	611 ~ 614	(100)	○	○	○	
18	641 ~ 643	(100)	○	○		
19	671 ~ 673	(55)			○	
20	702 ~ 704	(100)	○	○	○	
21	733 ~ 735	(60)	○	○	○	
22	763 ~ 765	(45)	○	○	○	
23	782 ~ 784	(78)			○	
24	812 ~ 814.5	(100)	○	○	○	
25	843 ~ 845	(100)			○	
26	874 ~ 876	(100)			○	
27	904 ~ 908	(85)	○	○	○	
28	935 ~ 937	(100)	○	○	○	
29	965 ~ 967	(100)			○	
30	996 ~ 996.3	(83)	○	○		
31	1039 ~1041	(89)	○	○	○	
32	1075 ~1075.3	(67)			○	
33	1124 ~1126	(22)			○	
34	1154 ~1157	(82)	○	○	○	

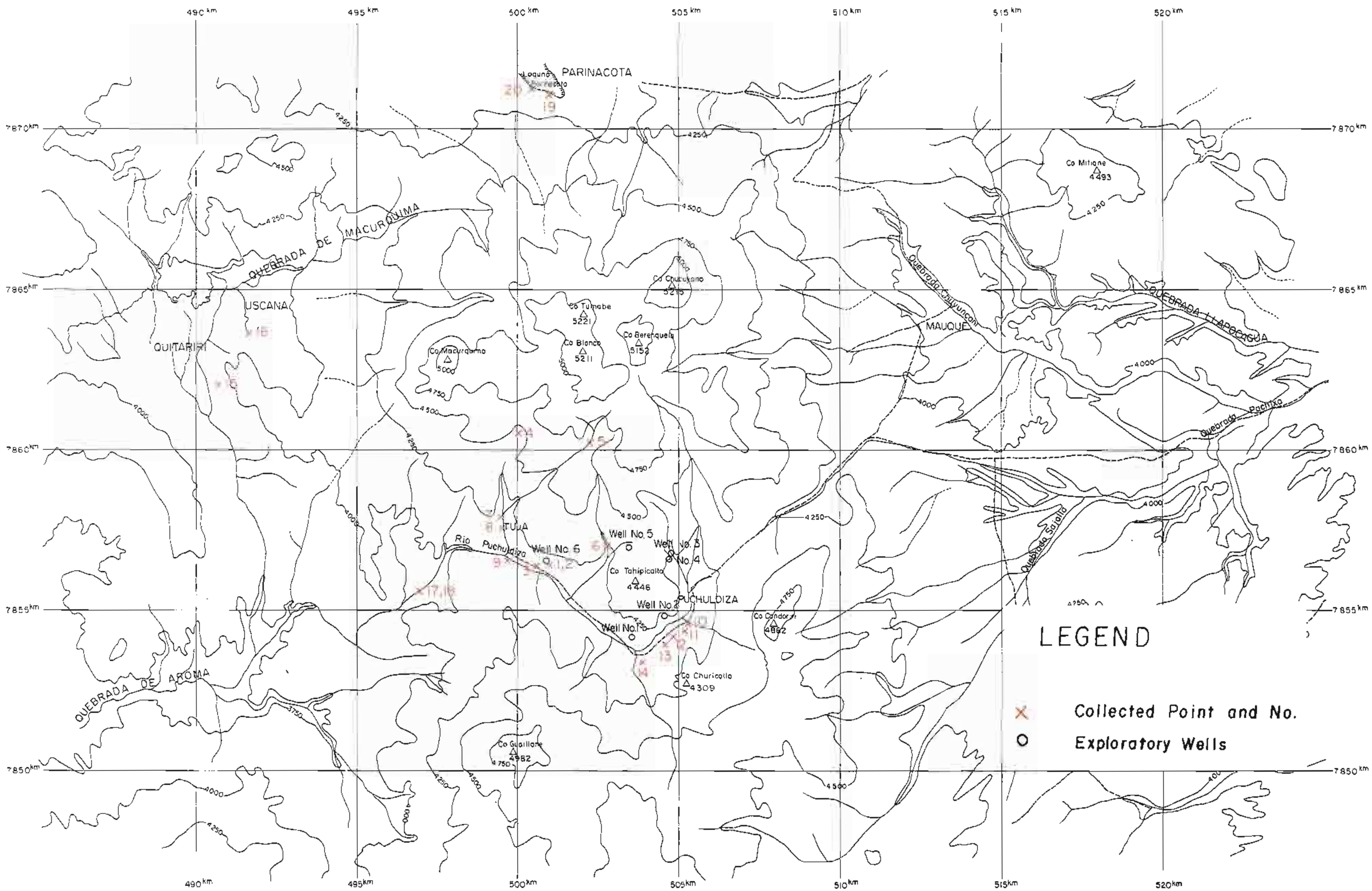

Fig. II-3-3 LOCATION OF COLLECTED SAMPLES

Fig. II-5-1 GENERALIZED COLUMNAR SECTION, WELL NO.6